

PVDF hollow fiber membrane modification for dye wastewater
treatment by ozonation membrane contacting process



A Thesis Submitted in Partial Fulfillment of the Requirements
for the Degree of Master of Science in Hazardous Substance and
Environmental Management
Inter-Department of Environmental Management
GRADUATE SCHOOL
Chulalongkorn University
Academic Year 2019
Copyright of Chulalongkorn University

การเพิ่มความไม่ชอบน้ำของเมมเบรนเส้นใยกลวง PVDF
ในการบำบัดน้ำเสียสี้อมด้วยกระบวนการเมมเบรนคอนแทคเตอร์
ร่วมกับกระบวนการโอโซนชั้น



วิทยานิพนธ์นี้เป็นส่วนหนึ่งของการศึกษาตามหลักสูตรปริญญาวิทยาศาสตรมหาบัณฑิต
สาขาวิชาการจัดการสารอันตรายและสิ่งแวดล้อม
สหสาขาวิชาการจัดการสิ่งแวดล้อม
บัณฑิตวิทยาลัย จุฬาลงกรณ์มหาวิทยาลัย
ปีการศึกษา 2562
ลิขสิทธิ์ของจุฬาลงกรณ์มหาวิทยาลัย

Thesis Title	PVDF hollow fiber membrane modification for dye wastewater treatment by ozonation membrane contacting process
By	Miss Hanh Le Thi My
Field of Study	Hazardous Substance and Environmental Management
Thesis Advisor	Dr. SERMPONG SAIRIAM
Thesis Co Advisor	Associate Professor Dr. ROONGKAN NUISIN

Accepted by the GRADUATE SCHOOL, Chulalongkorn University in Partial Fulfillment of the Requirement for the Master of Science

..... Dean of the GRADUATE SCHOOL
(Associate Professor Dr. THUMNOON NHUJAK)

THESIS COMMITTEE

.....	Chairman
(Assistant Professor Dr. CHANTRA TONGCUMPOU)	
.....	Thesis Advisor
(Dr. SERMPONG SAIRIAM)	
.....	Thesis Co-Advisor
(Associate Professor Dr. ROONGKAN NUISIN)	
.....	Examiner
(Dr. Jenyuk Lohwacharin)	
.....	Examiner
(Associate Professor Dr. MANASKORN RACHAKARAKIJ)	
.....	External Examiner
(Professor Dr. Tawan Sooknoi)	



จุฬาลงกรณ์มหาวิทยาลัย
CHULALONGKORN UNIVERSITY

อัน ลี ทิ มาช : การเพิ่มความไม่ชอบน้ำของเมมเบรนเส้นใยกลวง PVDF

ในการบำบัดน้ำเสียสี้อมด้วยกระบวนการเมมเบรนคอนแทคเตอร์ ร่วมกับกระบวนการโอโซนชั้น. (

PVDF hollow fiber membrane modification for dye wastewater treatment by ozonation membrane contacting process) อ.ที่ปรึกษาหลัก : ดร.เสริมพงษ์ สายเข็ม, อ.ที่ปรึกษาร่วม : รศ.

ดร.รุ่งกานต์ นุ้ยสินธุ์

น้ำเสียสี้อมและสารอินทรีย์จากน้ำทิ้งโรงงานสิ่งทอเป็นหนึ่งในมลพิษหลักในน้ำเสีย งานวิจัยนี้จึงได้ทำการศึกษาการบำบัดน้ำเสียสี้อมด้วยกระบวนการโอโซนเนชันโดยกระบวนการเมมเบรนคอนแทคเตอร์ ซึ่งมีการปรับสภาพผิวของ PVDF เมมเบรนแบบเส้นใยกลวงด้วยพลาสติกแบบหึ่งชนิดคู่ควบเหนียวน้ำ (PICP) และเชื่อมติดต่อด้วยสารกลุ่ม organosilane เพื่อเพิ่มคุณสมบัติความไม่ชอบน้ำ และไปประยุกต์ใช้บำบัดน้ำเสียสี้อมด้วยกระบวนการโอโซนเนชันในกระบวนการเมมเบรนคอนแทคเตอร์ เพื่อให้การปรับสภาพผิว PVDF เมมเบรน มีความเสถียร PVDF เมมเบรนที่ถูกกระตุ้นด้วยพลาสติกศึกษาอิทธิพลของพลาสติกสองชนิด (ก๊าซออกซิเจนและก๊าซอาร์กอน) สักย์ไฟฟ้าและความดัน จำนวนครั้งของพลาสติก หลังจากนั้นศึกษาอิทธิพลของสาร organosilane ที่แตกต่างกัน 4 ชนิด (methyltrichlorosilane (MTCS), trimethylchlorosilane (TMCS), 1H,1H,2H,2H-perfluorodecyltriethoxysilane (FAS-C8), and 1H, 1H, 2H, 2H-perfluorooctyltriethoxysilane (FAS-C6)) ความเข้มข้นของสาร organosilane และระยะเวลาในการเชื่อมติดสาร ผลการศึกษาพบว่า PVDF เมมเบรนที่ถูกกระตุ้นด้วยออกซิเจนพลาสติกมีประสิทธิภาพมากกว่าเมมเบรนที่กระตุ้นด้วยอาร์กอนพลาสติก เมมเบรนที่ถูกกระตุ้นด้วยพลาสติกเมื่อทำการเชื่อมติดกับสาร MTCS และ FAS-C8 พบว่าเพิ่มคุณสมบัติความไม่ชอบน้ำของเมมเบรน ในขณะที่คุณสมบัติความไม่ชอบน้ำของเมมเบรนที่กระตุ้นด้วยพลาสติกและเชื่อมติดด้วยสาร TMCS และ FAS-C6 ไม่เปลี่ยนแปลง ซึ่งการปรับสภาพผิวเมมเบรนยืนยันได้จากกราฟตำแหน่งหมู่ฟังก์ชัน และสารประกอบของซิลิกอนในการวิเคราะห์ด้วยเครื่อง FTIR และ EDX และความขรุขระของผิวเมมเบรนลดลง หลังจากกระตุ้นเมมเบรนด้วยออกซิเจนพลาสติกภายใต้สภาวะ 10 kV/0.3 mbar/จำนวน 2 ครั้ง และการเชื่อมติดด้วยสาร MTCS เป็นเวลา 4 ชั่วโมง และ FAS-C8 เป็นเวลา 6 ชั่วโมง พบว่ามุมสัมผัสของน้ำเพิ่มขึ้นจาก 74.7° เป็น 125.3° และ 112.7.4° ตามลำดับ PVDF เมมเบรนที่ปรับสภาพผิวมีค่าฟลักซ์โอโซนสูงกว่าเมมเบรนที่ไม่มีการปรับสภาพ เมมเบรน PVDF-FAS-C8 ให้ฟลักซ์โอโซนและการกำจัดสี้อมดีกว่าเมมเบรน PVDF-MTCS และผลการบำบัดน้ำเสียสี้อม Direct Blue 71 (DB 71) และ สี้อม Reactive Red 239 (RR 239) ด้วยเมมเบรน PVDF-FAS-C8 สามารถลดความเข้มข้นข้างสมบูรณ์หลังจาก 90 นาที ส่วนการลดลง COD ของสี้อม DB 71 และสี้อม RR 239 ด้วยเมมเบรนที่ปรับสภาพด้วย PVDF-FAS-C8 มีค่าเท่ากับร้อยละ 62.5 และ ร้อยละ 67.5 ตามลำดับ การใช้เมมเบรนที่มีการปรับสภาพในกระบวนการเมมเบรนคอนแทคเตอร์เพื่อการบำบัดน้ำเสียสี้อมพบว่ามีค่าใช้จ่ายเวลาน้อยกว่าเมมเบรนที่ไม่มีการปรับสภาพ การศึกษาครั้งนี้แสดงให้เห็นว่าเมมเบรนที่มีการปรับสภาพผิวเพื่อเพิ่มคุณสมบัติความไม่ชอบน้ำมีศักยภาพในการเพิ่มคุณสมบัติความไม่ชอบน้ำและสามารถนำไปใช้ในกระบวนการเมมเบรนคอนแทคเตอร์ได้

สาขาวิชา การจัดการสารอันตรายและสิ่งแวดล้อม

ปีการศึกษา 2562

ลายมือชื่อ นิสิต

ลายมือชื่อ อ.ที่ปรึกษาหลัก

ลายมือชื่อ อ.ที่ปรึกษาร่วม

6087613820 : MAJOR HAZARDOUS SUBSTANCE AND ENVIRONMENTAL
MANAGEMENT

KEYWORD: PVDF hollow fiber membrane; hydrophobicity; organosilanes; plasma activation;
ozonation membrane contactor

Hanh Le Thi My : PVDF hollow fiber membrane modification for dye wastewater
treatment by ozonation membrane contacting process. Advisor: Dr. SERMPONG
SAIRIAM Co-advisor: Assoc. Prof. Dr. ROONGKAN NUISIN

One of the main pollutions from textile wastewater is the dyeing wastewater containing color and organic matters. Among the treatment methods of dye wastewater, ozonation membrane contactor was used as the concept of this research. PVDF membranes were developed by pulse inductively coupled plasma (PICP) and grafted by organosilanes for hydrophobicity enhancement applied for dye wastewater treatment by ozonation membrane contactor. To obtain a stable grafting, the surface of PVDF hollow fiber membrane was activated by the plasma operating condition including two different plasma gases (oxygen and argon), applied voltage and pressure, plasma treatment shot, followed by grafting with four different organosilanes (methyltrichlorosilane (MTCS), trimethylchlorosilane (TMCS), 1H,1H,2H,2H-perfluorodecyltriethoxysilane (FAS-C8), and 1H, 1H, 2H, 2H-perfluorooctyltriethoxysilane (FAS-C6), organosilane concentration and different grafting time. The results found that oxygen plasma activation of PVDF membrane was more effective compared to argon plasma. The hydrophobic membrane modified by MTCS and FAS-C8 was increased, while the plasma-activated membranes grafted by TMCS and FAS-C6 did not change. The success of membrane modification was confirmed by the presence of silicon functional group and composition in FTIR and EDX results and the decrease of surface roughness. After activated by oxygen plasma under 10kV/0.3 mbar/2 shots followed by grafting with MTCS for 4h and FAS-C8 for 6h, the water contact angle was greatly increased from 74.7° to 125.3° and 112.7.4°, respectively. The ozone flux of modified membranes was higher and more stable than that of the original PVDF membrane. In addition, PVDF-FAS-C8 membrane gave the highest results in terms of ozone flux and dye removal. Direct Blue 71 (DB 71) and Reactive Red 239 (RR 239) decolorization by PVDF-FAS-C8 membrane were almost complete decolorization. After 90 mins, the COD removals of DB 71 and RR 239 by PVDF-FAS-C8 were 62.5% and 67.5%, respectively. The energy consumption of modified membrane in membrane contactor for dye wastewater was lower than that of original membrane. This study demonstrated that the modified membrane has a potential interest in improving hydrophobicity and membrane contactor applications.

จุฬาลงกรณ์มหาวิทยาลัย
CHULALONGKORN UNIVERSITY

Field of Study: Hazardous Substance and
Environmental Management

Academic Year: 2019

Student's Signature

Advisor's Signature

Co-advisor's Signature

ACKNOWLEDGEMENTS

I would like to express my great appreciation to my advisor Dr. Sermpong Sairiam and my Co-advisor Associate Prof. Roongkan Nuisin for their patient guidance, efficient suggestion, and encouragement throughout my thesis time. I am also thankful to the committee members for their valuable advice and for examining my research. I would like to thank the Department of Environmental Science, Chulalongkorn University and Department of Chemical Engineering, Faculty of Engineering, King Mongkut's University of Technology Thonburi for experimental facilities provided, and Department of Physics, Chulalongkorn University for plasma machine supported. I would like to thank the Hazardous Substance Management program (HSM), Chulalongkorn University, Thailand Research Fund (TRF) and Commission of Higher Education, and the Research program of industrial waste management-policies and practice for financial support. Great appreciation goes to the ASEAN Scholarship Program offered by the Chulalongkorn University and to all the program officers. Last but not least, I would like to say thank to officers and friends at HSM for their help and encouragement.



Hanh Le Thi My

TABLE OF CONTENTS

	Page
.....	iii
ABSTRACT (THAI)	iii
.....	iv
ABSTRACT (ENGLISH).....	iv
ACKNOWLEDGEMENTS.....	v
TABLE OF CONTENTS.....	vi
LIST OF TABLES.....	ix
LIST OF FIGURES.....	x
CHAPTER 1 INTRODUCTION.....	1
1.1 Statement.....	1
1.2 Hypotheses.....	4
1.3 Objectives.....	4
1.4 Scope of study.....	5
CHAPTER 2 BACKGROUND AND LITERATURE REVIEWS.....	6
2.1 Dye wastewater.....	6
2.1.1 Environmental effects and health – related issues of dye wastewater.....	6
2.1.2 Dye characteristics.....	7
2.2 Current dye wastewater treatment methods.....	8
2.3 Gas-liquid membrane contactor processes.....	10
2.3.1 Principle of gas-liquid membrane contactor.....	11
2.3.2 Membrane materials for ozonation contactor.....	13
2.4 Hydrophobic surface modification of existing PVDF hollow fiber membrane	14
2.4.1 Current hydrophobic surface modification for PVDF membrane.....	15
2.4.2 Plasma activation.....	17
2.4.3 Pulse inductively coupled plasma (PICP).....	18

2.4.4	The parameters effect to membrane surface modification	19
2.5	Ozonation membrane contactor process.....	19
2.5.1	Ozonation reaction	19
2.5.2	The parameters effect the ozonation membrane contactor process on wastewater treatment.....	20
2.6	Membrane characterization	21
2.6.1	Contact angle measurement.....	21
2.6.2	Fourier-transform infrared spectroscopy (FT-IR)	22
2.6.3	Scanning electron microscope (SEM) and Energy Dispersive X-ray (EDX) analysis	22
2.6.4	Surface roughness.....	22
CHAPTER 3	METHODOLOGY	23
3.1	Materials	23
3.2	Membrane hydrophobic modification	24
3.2.1	Plasma activation.....	24
3.2.2	Membrane grafting	25
3.2.3	Membrane characterization	26
3.3	Application on dye wastewater treatment	27
3.3.1	The long-term ozone fluxes of membranes	28
3.3.2	Decolorization of dye wastewater by ozonation using modified membranes.....	29
3.4	Energy consumption of ozonation membrane contactor process	30
3.4.1	Energy consumed of pump.....	30
3.4.2	Energy consumption during ozone generation.....	31
CHAPTER 4	RESULTS AND DISCUSSION.....	32
4.1	Effect of plasma operation parameters on membrane modification.....	32
4.1.1	Effect of plasma gases	32
4.1.2	Effect of plasma operating conditions.....	37
4.1.3	Effect of plasma treatment shot.....	41
4.2	Hydrophobic modification by grafting with organosilanes.....	44

4.2.1 Effect of grafting organosilanes concentration	44
4.2.2 Effect of grafting time and organosilanes	46
4.3 Long term ozone flux of original membrane and modified membranes	60
4.4 Dye wastewater treatment by ozonation membrane contactor	62
4.4.1 Comparison of decolorization performance of modified and original membranes.....	62
4.4.2 Effect of ozone concentrations	64
4.4.3 Effect of dye concentration	66
4.4.4 Effect of different dyes	68
4.5 Comparison of hydrophobicity enhancement of PVDF membrane by plasma- activated methods and application in membrane contactors	74
4.6 Proposal of dye wastewater treatment plan using ozonation membrane contactor process	76
4.7 Energy consumption analysis of ozonation membrane contactor process	76
CHAPTER 5 CONCLUSIONS AND RECOMMENDATIONS	79
5.1 Hydrophobic membrane modification by PICP and follow by grafting with organosilanes	79
5.2 Application for dye wastewater treatment by ozonation membrane contactor .	80
5.3 Recommendation	80
REFERENCES	82
APPENDIXES	88
VITA	90

LIST OF TABLES

	Page
Table 2.1 Chemical structure and related information of Direct Blue 71 and Reactive Red 239	8
Table 2.2 Commercial membranes commonly used for membrane contactors [12, 40]	14
Table 3.1 Details of membranes and modules employed in ozonation membrane contactor system.....	27
Table 4.1 Changes of the chemical composition of membrane surface under different plasma gases.....	37
Table 4.2 Changes of the chemical composition of membrane surface under different plasma operating conditions	41
Table 4.3 Changes of the chemical composition of membrane surface	53
Table 4.4 Surface roughness parameters of original and modified membranes	58
Table 4.5 Chemical composition of membranes under optimized modification condition	59
Table 4.6 Decolorization rate of DB 71 at different ozonation concentration by using different membranes	66
Table 4.7 Comparison of different plasma-based modification methods for enhancing PVDF membrane hydrophobicity	75
Table 4.8 Energy consumption for ozonation membrane contactor with different dye concentrations using original and modified membranes	78

LIST OF FIGURES

	Page
Figure 2.1 Operation mode of membrane contactor in microporous membrane: (a) non-wetting patterns, (b) overall wetting mode and (c) partial-wetting mode. C_i : gas concentration in each resistance i.e. gas, liquid and membrane resistances	11
Figure 2.2 Mass transfer regions and resistance-in-series in non-wetted membrane contactor.....	13
Figure 2.3 Reaction between ceramic membrane with Fluoroalkylsilane	15
Figure 2.4 Reaction mechanisms between methyltrichlorosilane and the PVA/cellulose nanofibrils (CNFs) membrane surface	16
Figure 2.5 The mechanism of inert gases plasma activation	18
Figure 2.6 Reactions of ozone and dissolved solids	20
Figure 3.1 Research framework.....	23
Figure 3.2 The structure of organosilanes.....	24
Figure 3.3 Schematic diagram of pulsed inductively coupled plasma (PICP) system [23].....	25
Figure 3.4 Experimental setup for ozone flux measurement of ozonation membrane contactor (liquid velocity: 0.46 m/s, gas velocity: 2 m/s, 100 mg/l DB 71).....	28
Figure 3.5 Schematic diagram of ozonation membrane contactor device for dye solution treatment.....	29
Figure 4.1 The WCA of grafted membranes activated by different plasma gases and different plasma applied voltage under operating pressure at 0.25 mbar, followed by grafting with 0.02M MTCS for 2h.....	34
Figure 4.2 Schematic reaction mechanism of plasma treatment on PVDF membrane	34
Figure 4.3 SEM images of a) original membrane, b) modified membrane activated by O_2 , and c) modified membrane activated by Ar (operating condition of 8 kV and 0.25 mbar followed by grafting with MTCS for 2h)	35
Figure 4.4 FTIR spectra of PVDF membrane a) original membrane; b) modified membrane activated by O_2 , and c) modified membrane activated by Ar (operating condition of 8 kV and 0.25 mbar followed by grafting with MTCS for 2h)	36

Figure 4.5 WCA of the modified membranes activated by oxygen plasma gas under different plasma operating conditions followed by grafting with 0.2 M MTCS for 2h	38
Figure 4.6 SEM images of modified membranes under operating condition of (a, e) 8kV/0.30 mbar, (b, f) 10kV/0.30 mbar, (c,g) 8kV/0.25 mbar ,(d,h) 10kV/0.25 mbar, at plasma treatment time of 1 shot followed by grafted with 0.02M MTCS	40
Figure 4.7 The WCAs of modified membranes activated by oxygen plasma gas at 10 kV/0.3 mbar for different plasma treatment times and grafted by 0.02M of different solutions for 2h	42
Figure 4.8 SEM images of activated membranes (a-c) and grafted membranes (d-f), at plasma treatment time of 1 shot (a, d), 2 shots (b, e), and 3 shots (c, f) at activation condition of 10 kV/0.3 mbar followed by grafted with 0.02M MTCS for 2h	43
Figure 4.9 PVDF membrane modification by methods of plasma activation followed by organosilane direct grafting	44
Figure 4.10 WCA of modified membrane at different organosilane concentrations after activated by O ₂ plasma gas, under applied voltage of 10 kV/0.30 mbar/2 shots	45
Figure 4.11 SEM images of modified membrane grafted by different organosilanes and concentrations: a) 0.005M FAS-C8, b) 0.01M FAS-C8, c) 0.02M FAS-C8, d) 0.005M MTCS, e) 0.01M MTCS, and f) 0.02M MTCS.....	46
Figure 4.12 WCA of modified membranes after activated by 1 shot of O ₂ plasma under 8 kV/0.25 mbar followed by grafting with 0.02M organosilane.	48
Figure 4.13 Reaction mechanisms between methyltrichlorosilane and the activated PVDF membrane surface	49
Figure 4.14 Outer surface of membranes grafted by different conditions activated by O ₂ /8 kV/0.25 mbar/1 shot: a) original membrane, b) activated membranes, c) 0.02M TMCS-2h, d) 0.02M FAS-C6- 2h, e) 0.02M FAS-C8- 2h, f) 0.02M MTCS -0.5h , g) 0.02M MTCS-2h, and h) 0.02M MTCS- 4h.....	50
Figure 4.15 FTIR spectra of activated membrane under oxygen plasma activation at 8kV/0.25 mbar/1 shot followed by grafting with different organosilanes: a) original PVDF membrane, b) 0.02M FAS-C8-2h, c) 0.02M FAS-C6-2h, d) 0.02M TMCS, 2h, and e) 0.02M MTCS-2h.....	51
Figure 4.16 FTIR spectra of activated membrane under oxygen plasma activation at 8kV/0.25 mbar/1 shot followed by grafting with 0.02M MTCS at different grafting time a) activated membrane, b) 0.5h, c) 2h and d) 4h	52

Figure 4.17 WCA of modified membranes after activated by 1 shot of O ₂ plasma under 10 kV/ 0.30 mbar followed by grafting with 0.02M organosilane	54
Figure 4.18 Outer surface of modified membrane grafted by different organosilanes and grafting time activated by O ₂ /10 kV/0.30 mbar/2 shots: a) FAS-C8-2h, b) FAS-C8-4h, c) FAS-C8-6h, d) MTCS-2h, e) MTCS-4h and f) MTCS-6h	55
Figure 4.19 AFM 3D images and cross-section profiles along the marked directions of a) original PVDF membrane and modified membranes: b) MTCS-4h, c) MTCS-6h, d) FAS-C8-4h and e) FAS-C8-6h.....	57
Figure 4.20 Cross section of modified membrane grafted by different organosilanes and grafting time activated by O ₂ /10 kV/0.30 mbar/2 shots: a) original membrane, b) FAS-C8-6h, c) MTCS-4h.....	58
Figure 4.21 Membrane grafted by organosilanes (a) MTCS and (b) FAS-C8	59
Figure 4.22 Long term ozone flux of original membrane and modified membranes using 100 mg/l DB 71 (liquid velocity: 0.46 m/s, gas velocity: 2 m/s, and ozone concentration: 40 mg/l).....	61
Figure 4.23 Dye wastewater treatment by membrane contacting process with ozone: a) DB 71 removal, b) ozone consumption of DB 71, c) RR 239 removal, and d) ozone consumption of RR 239, (liquid velocity: 0.46 m/s, ozone concentration: 40 mg/l).	63
Figure 4.24 Effect of ozone concentration on DB 71 decolorization by ozonation membrane contactor of a) original PVDF, b) PVDF-MTCS, c) PVDF-FAS-C8 membranes (liquid velocity: 0.46m/s, dye concentration: 100 mg/l)	65
Figure 4.25 Effect of dye concentrations on dye decolorization: a) DB 71 removal, b) ozone consumption of DB 71, c) RR 239 removal, and d) ozone consumption of RR 239, (liquid velocity: 0.46 m/s, ozone concentration: 40 mg/l).....	68
Figure 4.26 Effect of different dyes on dye decolorization by ozonation membrane contactor: a) COD removal and decolorization and b) pH changes of RR 239 and DB 71 using PVDF-FAS-C8 membrane contactor (dye concentration: 100 mg/l, ozone concentration: 40 mg/l, liquid velocity: 0.46 m/s).....	70
Figure 4.27 Spectral changes in the UV–vis absorption spectra of dyes during membrane ozonation process using PVDF-FAS-C8 membrane: a) DB 71 and b) RR 239.....	72
Figure 4.28 The pathway of RR 239 degradation by ozone conducted by Dias <i>et al.</i> , (2019) [3]	73
Figure 4.29 Flow diagram for proposed dye wastewater treatment plant.....	76

CHAPTER 1

INTRODUCTION

1.1 Statement

Textile industry is one of the most important, oldest, largest, and most global industries in the world. With the escalating demand for textile products, textile plants are growing rapidly and causing a major worldwide environmental problem [1]. In particular, textile industries are developing quickly in developing countries, with the poor wastewater treatment system, which poses a worldwide threat to the ecology and public health. Furthermore, the textile industry is considered one of the worst pollution sources because it consumes a large amount of water and chemicals, which damage the environment when they are discharged. According to the research, 10-25% of textile dyes are lost during the dyeing process and 2-20% are directly discharged as aqueous effluents in different environmental components [2]. The textile industry generates large volumes of effluent, which is caused by the loss of dye during the dyeing process. In which, azo dyes account for more than 50% of total dyes used, in particular, Reactive Red 239 (RR 239), Reactive Black 5 and Direct Blue 71 (DB 71) are commonly dyes used in the textile industry for dyeing of cotton and polyester fabrics [3, 4]. Azo dyes are very difficult to degrade due to their stable and their molecular structure with at least one azo bond ($-N=N-$) linked aromatic rings [5]. Once the dye effluent reaches the water ecosystems, dye color attenuates the light interrupting penetration photosynthetic activity, and dye contaminants could deplete dissolved oxygen affecting aquatic life [3]. Besides, the breaking down of azo linkages forms amines, which are classified as toxic and carcinogenic [5]. Because of their characteristics and their toxicity, dye removal becomes environmentally important.

There are several studies efforted to find effective treatments to remove azo dyes and their colors. The conventional methods that are used for dye wastewater treatment are physical methods, for example, coagulation-flocculation and adsorption and biological methods such as anaerobic and aerobic methods. These methods can usually reduce biological oxygen demand (BOD) and chemical oxygen demand (COD) in textile wastewater but they did not work on dye color removal [6].

Advanced oxidation processes (AOPs) are considered as an effective method for decolorizing wastewater due to the strong power for breaking organic compound structure [7]. Among these methods, the ozonation process has been paid great attention due to its high treatment effective and its environmentally friendly. In particular, the pollutants in wastewater including color, odor, and microorganisms are directly destroyed by oxidation, without creating toxic by-products or significant residues [6, 8]. Ozonation process is suitable for decolorization because of its property to break the conjugated double bonds that are common in the dye chromophores [7]. To diffuse ozone into water, conventionally, bubble columns were used, however, ozone mass transfer reactor has been addressed many disadvantages; for example, flooding, uploading, emulsion, and foaming [8].

Gas-liquid membrane contactor has been used to solve these problems. This method can enhance the solubility of ozone in water due to its high contacting area [9]. Gas-liquid membrane contactors are made of hydrophobic microporous membranes which prevents liquid entering the pore and enables gas phase to come over. Hollow fiber-based membrane modules have been widely used for making membrane contactors due to a large membrane surface area per unit volume [10]. The performance of the gas – liquid membrane contactor is largely affected by the properties of the membranes which are porosity, hydrophobicity, and thickness [11].

The typical kinds of membrane that are used for operating in membrane contactor are polypropylene (PP), polytetrafluoroethylene (PTFE), and polyvinylidene fluoride (PVDF) [11]. The hydrophobicity of membrane is measured by water contact angle (WCA). Based on the WCA, the hydrophobicity is in the order of PTFE > PVDF > PP [12]. Besides, since ozone is very active, the materials should have a strong resistance when oxidized by ozone oxidation. Santos *et al.* (2015) indicated that PTFE and PVDF membranes showed high resistance to ozone oxidation while PP membranes were destroyed [13]. Therefore, PTFE and PVDF membranes have been widely used for ozonation membrane contactor. However, PTFE membrane is much more expensive compared to PVDF membrane due to the complexity in solvent selection of fabrication process [14]. Meanwhile, PVDF membrane has received much attention due to its high hydrophobic properties, thermal stability and excellent chemical resistance ability [15, 16]. Although PVDF membranes are highly

hydrophobic, the wetting problem could occur after long-time operation, which can reduce the mass transfer efficiency. To prevent membrane wetting of PVDF membrane, there are several studies have been focused on improving the hydrophobicity of membrane.

Direct grafting reaction using organosilane compound has been successful used for enhancing the hydrophobicity of ceramic membranes. Fluoroalkylsilane (FAS) and chloroalkylsilane (CAS) are two groups of organosilane that have been successfully applied for membrane hydrophobicity enhancement [14, 16-18]. The principle of this method is that the reactive silanol species of organosilane reacts with abundant hydroxyl groups (-OH) presented on the ceramic membrane, then changed membrane surface to hydrophobic membrane [18]. There are no -OH groups on PVDF membrane, therefore, introducing -OH groups onto membrane surface is necessary.

Chemical activation and plasma activation are two common methods that have been used to introduce -OH group on membrane surface. Yang *et al.* (2011) studied on fluorination of PVDF membrane by both chemical activation (sodium hydroxide, NaOH) and plasma activation (atmospheric plasma) followed by grafted with 1H,1H,2H,2H-perfluorodecyl acrylate solution. The results showed that both chemical and physical activation methods could enhance the hydrophobicity of membrane surface. However, plasma activation method had the less effect to membrane characteristics than chemical activation method [14]. Hashim *et al.* (2011) indicated that NaOH solution effect on the decrease in mechanical strength and crystallinity of PVDF hollow fiber membranes, even in the low concentration and was aggravated with the extended treatment time [19]. Furthermore, Rabuni *et al.* (2015) indicated that the stability of PVDF membrane was affected even at NaOH concentration of 0.01M [20]. Therefore, plasma modification method could be an alternative activation.

Plasma treatment method has been used to activate the membrane surface by using oxidative and inert plasma gases. In particular, oxygen plasma is very effective in hydrophilic modification because it can direct introduce -OH functional groups, whereas, inert plasma such as helium (He) and Argon (Ar) plasma can introduce ion and active radical on the membrane surface [21]. For example, radio frequency (RF)

generated plasma has been reported to successfully introduce -OH group onto PVDF membranes using different plasma gases [14, 22]. Pulse inductively coupled plasma (PICP) is a high energy system that could be used for membrane modification since the desired effect can be achieved within a short treatment period. In addition, PICP is a flexible system that plasma energy can be controlled through varying the applied voltage and operating gas pressure [23]. Since the design of PICP is much simpler than inductively coupled RF reactor plasma, the pulse treatment is more practical. Therefore, a study on the effects of plasma energy on membrane surfaces using PICP is of interest.

This study aims to enhance the hydrophobicity of existing PVDF hollow fiber membranes and apply modified membranes to treat dye solutions using ozonation membrane contactor process. PVDF hollow fiber membranes were modified by plasma activation using PICP and direct grafting using organosilanes. Reactive Red 239 (RR 239) and Direct Blue 71 (DB 71) as typical examples of mono- and tri-azo dye pollutants in dye wastewater were selected for decolorization study.

1.2 Hypotheses

- Membrane hydrophobicity of existing PVDF membranes can be improved by membrane modification with plasma activation by PICP followed by grafting with organosilanes.
- Ozonation membrane contactor process using modified PVDF membrane can improve the decolorization performance of dye wastewater treatment compared to original membranes.

1.3 Objectives

The main objective of this work is to improve ozonation membrane contactor process on the dye wastewater treatment by enhancing the hydrophobicity of existing PVDF. In particular:

- To enhance the hydrophobicity of existing PVDF hollow fiber membrane surface by using different PICP activation and organosilane grafting conditions.
- To determine the decolorization performance of ozonation membrane contactor process on the dye wastewater treatment by membrane contactor using original PVDF membrane and modified PVDF membranes.

1.4 Scope of study

This research focuses on enhancing the hydrophobicity of existing PVDF membranes by surface modification with PICP activation and direct grafting using organosilane, then apply modified membranes for ozonation membrane contactor process on decolorization of dye wastewater. The PICP activation conditions such as plasma gases, plasma shots and plasma operating condition and grafting conditions such as organosilane types, organosilane concentration and grafting time was investigated. After modifying, PVDF membranes were used in ozonation membrane contactors for investigating the color removals of dye wastewater. Long-term ozone fluxes of original membrane and modified membranes were studied. The parameters such as effect of ozone dose, effect of dyes and membranes were investigated. Besides, chemical oxidation demand (COD) and dye concentration were discussed the dye wastewater treatment efficiency.

CHAPTER 2

BACKGROUND AND LITERATURE REVIEWS

2.1 Dye wastewater

2.1.1 *Environmental effects and health – related issues of dye wastewater*

The environmental issues which cause by residual dye content or residual color in treated textile effluents are always a concern for each textile operator. The dye wastewater is a mixing of various chemicals in both organic and inorganic compound with wastewaters from the production processes, which leads to change in both biological and chemical parameters of the receiving water bodies, then causes several impacts to people health [1].

(a) Environmental effects

Due to the complexing of chemical mixed, dye wastewater is very harmful to the environment if released without proper treatment. Wastewater with high concentrations of textile stops the reoxygenation capacity of the receiving water and cutoff sunlight, thereby upsetting biological activity in aquatic life and the photosynthesis process of aquatic plants or algae [2]. The direct consequences of dye wastewater discharging to the environment are aesthetic issues, damage flora and fauna of ecosystem, groundwater pollution, depletion of DO of receiving water body; and the indirect consequences are eutrophication, affect to on aquatic life, and cause of various human illnesses.

The quality indicators that regulators and researchers are looking for polluting effect or toxicity of textile wastewater are the high salt content, high total solids (TS), high total dissolved solids (TDS), high total suspended solids (TSS), low BOD, high COD, strong color, and other potentially hazardous or dangerous organic compounds included into each textile processing technological steps [2].

(b) Health-related issues

Dyes are synthetic nature and structure mainly aromatic, most of them are non-biodegradable, having carcinogenic action or causing allergies, dermatitis, or skin

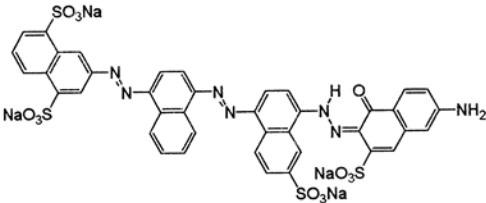
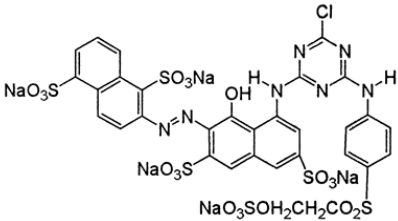
irritation. In addition, both dyes chemical and its by-products after long-time presence in water show both acute and chronic toxicity. Due to the adsorption of azo dyes and their breakdown products (toxic amines) through the gastrointestinal tract, skin, and lungs, dyes wastewater has a high potential health risk, especially the formation of hemoglobin adducts and disturbance of blood formation [1]. In addition, several azo dyes cause damage of DNA that can lead to the genesis of malignant tumors; for example, Direct Black 38 azo dye and its breakdown derivatives inducing cancer in humans and animals [2].

2.1.2 Dye characteristics

Azo dyes are compounds with the presence of at least one azo group ($-N=N-$) double bonds linked to phenyl and naphthyl radicals, and are widely used in textile, printing, cosmetics, pharmaceutical, food, and many other industries [5]. Approximately half of all known dyes are azo dyes; in which, their by-products are more toxic than themselves and can remain for decades in the aquatic environment [24]. Besides, large quantities of azo dye remain in dye effluent after finishing dyeing processes. Azo dyes and their pigments are versatile. They are the most common synthetic colorants released into the environment [5]. When these azo dyes released to the water bodies, their by-product can form aromatic amines, which may be more toxic than the dye molecules themselves and is considered hazardous by the Occupational Safety and Health Administration Hazard Communication Standard [25]. Hence, it is necessary to find out the effective method to treat dye wastewater.

DB 71 and RR 239 are widely azo dyes used, DB 71 is a tri-azo compound with three azo double bond and RR 239 is a mono-azo compound with one azo double bond, which make them difficult to degrade. The structures and some related information of these dyes are shown in Table 2.1:

Table 2.1 Chemical structure and related information of Direct Blue 71 and Reactive Red 239

Dye	Direct Blue 71 (DB71)	Reactive Red 239 (RR239)
Trade name	Sirius Blue SBRR	Remazol Brilliant Red 3BS
Structure		
λ_{\max} (nm)	594	542
Molecular weight (g/mol)	1029.87	1136.32
Solubility	10 g/L (60°C), 20 g/L (97°C)	180 g/l (50°C)
C.I name	C.I.Direct Blue 71, C.I.34140	C.I.Reactive Red 239
IUPAC name	tetrasodium;3-[[4-[[4-[(6-amino-1-hydroxy-3-sulfonatophthalen-2-yl)diazenyl]-6-sulfonatophthalen-1-yl]diazenyl]naphthalen-1-yl]diazenyl]naphthalene-1,5-disulfonate	2-phenylamino]-1,3,5-triazin-2-yl] amino)-1-oxo-3,6-disulfo-1,2-dihydronaphthalen-2-ylidene]hydrazin-1-yl] naphthalene-1,5-disulfonic acid

λ_{\max} : Wavelength of maximum absorbance; references: [26, 27]

CHULALONGKORN UNIVERSITY

2.2 Current dye wastewater treatment methods

Many processes have been applied for dye wastewater treatment, which are categorized into three groups: biological, physical, and chemical processes. There were many kinds of microorganisms that had been used for textile wastewater treatment. Ghasemi *et al.* (2010) applied *Phanerochaete chrysosporium* RP 78 to treat seven kinds of azo dye, 100% decolorization was achieved after 24h of reaction [28]. Jin *et al.* (2009) indicated that *Escherichia coli* JM109 could remove 80 % of DB 71 in 12h [4]. This method is considered as a cost-competitive and environmentally friendly due to no use of chemicals and non-product at the end of the process. Nevertheless, this method took longer time than others. Besides, many non-

biodegradable components in textile wastewater could not be degraded by microorganisms [29]. Therefore, physical and chemical processes have been more commonly used for textile wastewater handling.

Most physical methods used for dye removal are separation process and the main disadvantage of these processes is the disposal of dye-containing sludge as in coagulation process and dye sorbed adsorbents. Recently, filtration processes such as ultrafiltration (UF), nanofiltration (NF) and reverse osmosis (RO) have been used for water recovery and reuse. These methods also have been used for dyes removal. Membrane-based processes are able to separate hydrolyzed dyestuff and dyeing auxiliaries out of wastewater, thereby reducing coloration and COD content [30]. Nevertheless, there are many disadvantages of this method that have been noticed, such as its cost of initial investment, possible fouling of membrane and the generation of another waste containing water insoluble dyes and starch which need further treatment [31]. In contrast, complex dye compounds undergo a series of degradation in chemical degradation methods [32].

Oxidation processes are the usually used for degradation of dyes by chemical means due to its easiness of application [31]. Ozonation is a powerful process, which is widely considered as environmentally friendly applications. Ozonation is relatively effective in reducing coloration of various dye origins and toxic effects of textile effluents; the main environmental concern related to textile wastewater effluent discharge. Günes *et al.* (2012) worked on RR 239 solution treatment (500 mg/l), after 90 min of ozonation time, 80% of color removal was observed [27]. Dias *et al.* (2019) found that full RR 239 color removal was achieved in 10 min and the removal of COD reached 62% in 20 min of ozonation at ozone dose of 20 mg/l (50 mg/l of RR 239) [3]. One major benefit of the ozonation is that the by-product of ozonation process is not harmful to the environment since it is made from oxygen and decomposes back to oxygen [6, 33]. Turhan *et al.* (2009) studied on DB 71 removal using ozonation process; after 27 min of ozonation, decolorization was completed and there was no toxicity in breakdown product of effluent [26]. Besides, ozone can be used in its gaseous state and consequently does not raise the volume of the wastewater and does not result in sludge generation [31]. Conventionally, ozone is diffused into water by using bubbles, stirred tank reactors, packed towers, or tube reactors, which

are practical and economic for ozone mass transfer [34]. However, these reactors had been faced with some problems, for example, non-reacted areas due to the largeness of reactors, flooding, emulsion, unloading, and foaming [6, 34]. In addition, due to the short half-life of ozone in water, the constant ozonation is necessary, thus, it causes the high cost of these processes. To solve these problems, bubble-less membrane contactor can be an excellent alternative.

The gas-liquid membrane contactor is used to separate gas and liquid by using hydrophobic membrane. The separating mechanism of membrane contactor is that the gas diffuses through the membrane and then dissolves into the liquid. Therefore, the disadvantages that occur in traditional contactors could be avoided. In addition, the mass transfer process of membrane contactor is bubble-less; the high volumetric mass transfer efficiency can be reached and the specific surface area is rather large, especially in a hollow fiber membrane contactor [34]. Ozonation membrane contactor have been used for textile wastewater treatment. Ciardelli *et al.* (2003) used ceramic ($\alpha\text{-Al}_2\text{O}_3$) hollow fiber membranes contactor to decolorize dye wastewater color. After 2h operating time, the amount of dissolved ozone reduced was 50 mg/l while the decolorization performance was only 38% [35]. Atchariyawut *et al.* (2009) applied PVDF hollow fiber ozonation membrane contactor to treat Reactive Red 120 dye wastewater, and found that the dye color was removed roughly 68% after the 4h [8]. Bamperng *et al.* (2010) investigated the decolorization performance of Acid Blue 113 by using PVDF and PTFE membranes. The results showed that the decolorization and the reduction of COD depends on the membrane hydrophobicity. After 1h, the decolorization of Acid Blue 113 reached 97% by using PVDF ozonation contactor [6].

2.3 Gas-liquid membrane contactor processes

Membrane contactors are a system where porous membranes are used to carry out mass transfer between phases. Gas-liquid membrane contactor is a device that achieves gas-liquid mass transfer without dispersion of one phase within another [36]. There were several important advantages of membrane contactor had been noticed, including absence of emulsions, no flooding at high flow rates, no unloading at low

flow rates, no density difference between fluids required, and surprisingly high interfacial area [11]. In addition, membrane contactor has high surface area per volume, which offers 30 times more area than what achieved in gas absorbers and 500 times what obtained in liquid/liquid extraction columns [37].

Flat-sheet membrane and hollow fiber membrane are two types of membranes which are used to make membrane contactor. With high membrane packing, the hollow fiber membrane has higher productivity per unit volume of the membrane module compared to typical flat-sheet membranes. Use of flat-sheet membrane modules is more complicated due to the requirements for spacers and supports, while hollow fiber membranes are self-supporting[10]. Therefore, hollow fiber membranes have been used widely for membrane contactor, especially for gas-liquid membrane contactor [10].

2.3.1 Principle of gas-liquid membrane contactor

In this process, the hydrophobic porous membranes are employed as a barrier to separate gas and liquid phases [8]. There are three operation modes of membrane contactor as shown in Figure 2.1: (a) non-wetting patterns, (b) partial-wetting mode and (c) overall wetting mode. Among these operation modes, non-wetting mode of operation, which its pores are filled by gas phase, is highly preferred, as it leads to minimal diffusion resistance in membrane pores [11].

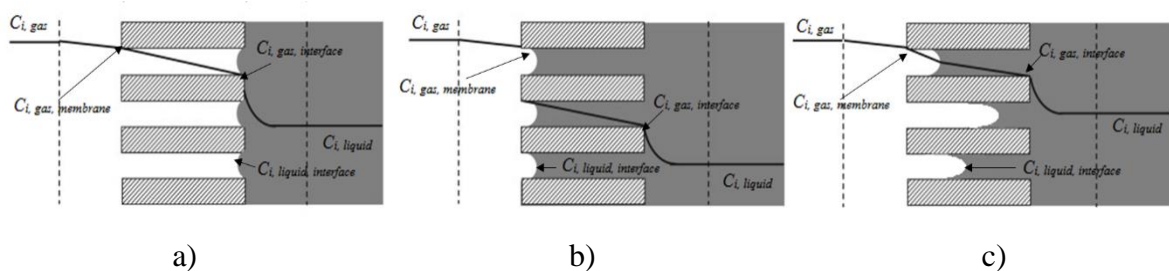


Figure 2.1 Operation mode of membrane contactor in microporous membrane: (a) non-wetting patterns, (b) overall wetting mode and (c) partial-wetting mode. C_i : gas concentration in each resistance i.e. gas, liquid and membrane resistances

The mass-transfer in non-wetted gas-liquid membrane contactor is shown in Figure 2.2. There are three resistances in series that the feed gas has encounter, which are resistance of gas phase boundary layer ($1/k_g$), membrane resistance ($1/k_m$) and resistance of liquid phase boundary layer ($1/k_l$). In the gas -liquid membrane contactor processes, the gas is transported from the bulk of gas phase to the interface between gas phase and membranes; then be transported through the membrane pores; and in the end of the process, the dissolution of a gas component into a liquid (with or without the reaction) [6, 8]. The overall mass transfer resistance ($1/K_{ol}$) (m/s) can be analyze by Equation (1) [6, 11]:

$$\frac{1}{K_{ol}} = \frac{1}{EK_l} + \frac{d_o}{Hk_m d_{ln}} + \frac{d_o}{Hk_g d_i} \quad (1)$$

where, K_{ol} is the overall mass transfer coefficient based liquid phase (m/s)

k_g, k_m, k_l are the individual mass transfer coefficients (m/s) of the gas phase, membrane and liquid phase, respectively

d_i, d_o, d_{ln} are the inner, outer and logarithmic mean diameters (m) of the fibers, respectively

E is the enhancement factor which is included to account for the effect of the reaction

H is Henry's constant (mg/l in gas)/(mg/l in liquid)

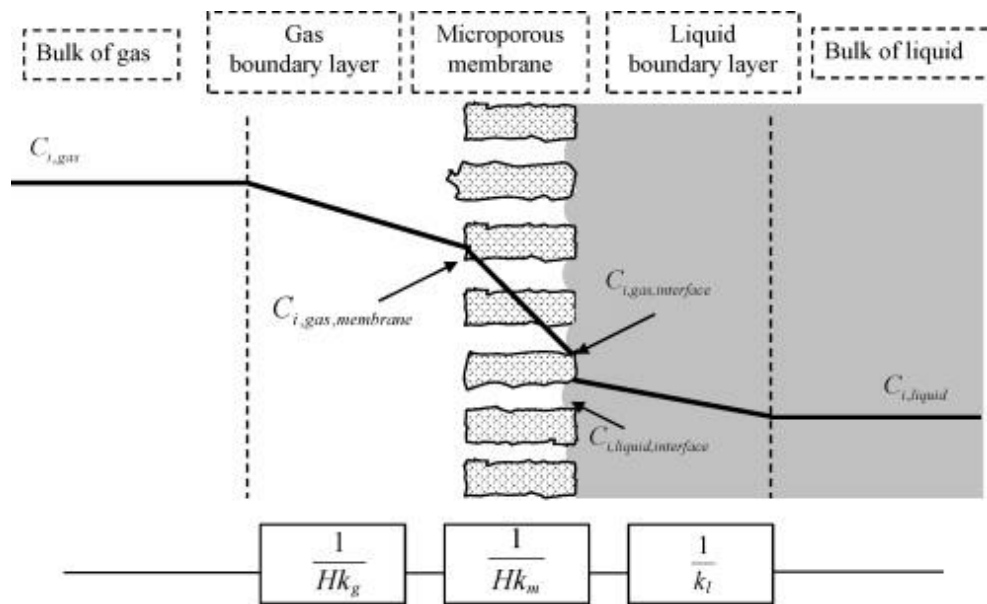


Figure 2.2 Mass transfer regions and resistance-in-series in non-wetted membrane contactor.

Membranes resistance become more significant when membrane pores wetted by liquid absorbents reducing gas transfer efficiency after long-term operation [11]. To keep the membrane contactor be non-wetting operation mode, the membrane materials which are used for making the membrane contactors must be hydrophobic membranes to prevent the membrane wetting occurred.

2.3.2 Membrane materials for ozonation contactor

The definition of a hydrophobic surface is when its static water contact angle (WCA) $\theta > 90^\circ$ but hydrophilic surface is $\theta < 90^\circ$ [38]. The hydrophobic membranes used to make membrane contactors usually are polypropylene (PP), polyethylene (PE), polyvinylidene fluoride (PVDF), and polytetrafluoroethylene (PTFE). The hydrophobicity order of these types of membranes is PTFE > PVDF > PP [12]. In addition, the ozone resistance was in the following order: PTFE > PVDF > PE [39]. The chemical structures and some membrane properties are summarized in Table 2.2:

Table 2.2 Commercial membranes commonly used for membrane contactors [12, 40]

Types of membrane	Chemical structure	Contact angle (°)	Melting point (°C)
PP	$\left[\begin{array}{cc} \text{H} & \text{CH}_3 \\ & \\ -\text{C} & - & \text{C}- \\ & \\ \text{H} & \text{H} \end{array} \right]_n$	≥ 95	160
PVDF	$\left[\begin{array}{cc} \text{H} & \text{F} \\ & \\ -\text{C} & - & \text{C}- \\ & \\ \text{H} & \text{F} \end{array} \right]_n$	≥ 65	177
PTFE	$\left[\begin{array}{cc} \text{F} & \text{F} \\ & \\ -\text{C} & - & \text{C}- \\ & \\ \text{F} & \text{F} \end{array} \right]_n$	≥ 105	327

However, the price of PTFE hollow fiber membrane is much more expensive compared to others, which is about 32 times higher than that of PVDF membrane. The phase inversion process of PTFE production limited the fabrication of this membrane type due to the complexity in solvent selection; thus, its cost is expensive [14]. On the contrary, PVDF had received great attention because of its outstanding properties such as high mechanical strength, thermal stability, chemical resistance, and high hydrophobicity, compared to other commercialized polymeric materials [41]. Therefore, PVDF membrane has become more popular membrane used. However, after long-term operating, membrane wetting could occur.

2.4 Hydrophobic surface modification of existing PVDF hollow fiber membrane

There are many methods that have been used for membrane hydrophobic modification, such as (1) the improvement of membrane preparation process, (2) the introduction of perfluorinated polymers, and (3) the surface hydrophobic modification of existing PVDF membranes. The methods that have been paid more attention is surface modification processes.

2.4.1 Current hydrophobic surface modification for PVDF membrane

Surface modification is a technique which is used to enhance the required performance of a membrane by adding a small amount of a functional group onto the surface or by changing the surface characteristics by means of physical or chemical methods.

There were several studies that have successfully enhanced the hydrophobicity of ceramic membrane by direct grafting using organosilane compound. Organosilane refers to a molecule which has one Si atom connected with four functional groups, SiX_4 . Generally, X are $-\text{Cl}$, $-\text{OCH}_2\text{CH}_3$, $-\text{OCH}_3$, and the reactivity of these groups decreases in order of $\text{Si-NR}_2 > \text{Si-Cl} > \text{Si-OCCH}_3 > \text{Si-OCH}_3 > \text{Si-OCH}_2\text{CH}_3$ [42]. Fluoroalkylsilane (FAS) and chloroalkylsilane (CAS) are two groups of organosilane that have been applied for membrane hydrophobicity enhancement [14, 16-18]. During grafting, the organosilane with reactive silanol species reacts with $-\text{OH}$ groups presented on the ceramic membrane to increase membrane hydrophobicity, as shown in Figure 2.3 [18, 43].

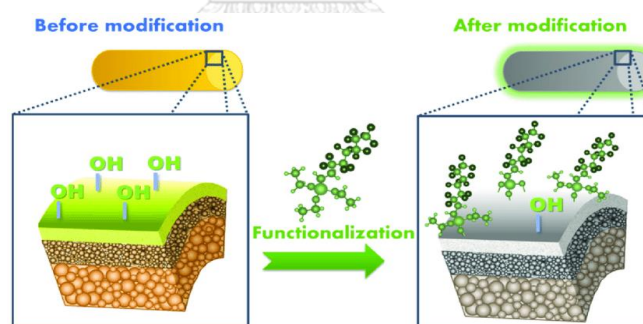


Figure 2.3 Reaction between ceramic membrane with Fluoroalkylsilane

Besides, CAS groups can react with moisture in the air, creating a two-way reaction of the CAS compounds: horizontal reaction with $-\text{OH}$ groups on membrane surface and vertical reaction with moisture [44].

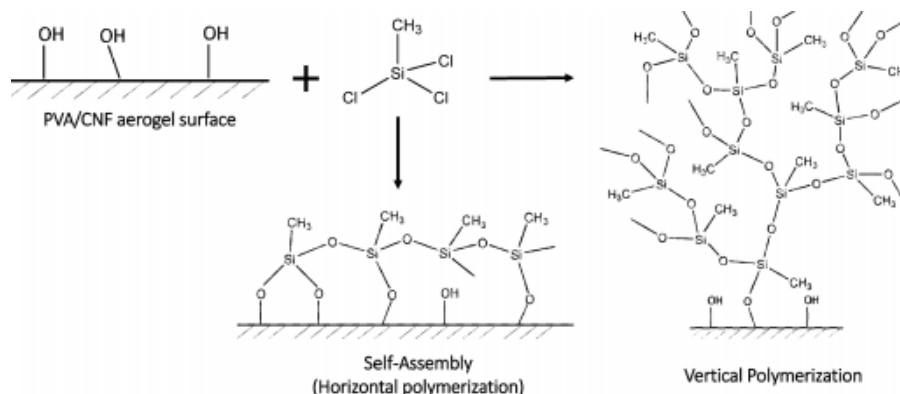


Figure 2.4 Reaction mechanisms between methyltrichlorosilane and the PVA/cellulose nanofibrils (CNFs) membrane surface

However, PVDF membranes have no hydroxyl group. Therefore, to enhance the hydrophobicity of PVDF membrane by this method, -OH groups should be introduced onto membrane surface using physical activation and chemical activation methods. For chemical activation, PVDF membrane is activated by a strong alkaline active group; then, the organosilane are grafted onto a membrane surface. For plasma activation, there are many kinds of plasma can introduce OH groups on membrane surface, such as He, H₂O, O₂, air and Ar gases. Yang *et al.* (2011) studied on performance improvement of distillation process with modified PVDF membrane by chemical and plasma activation methods. For chemical method, PVDF membrane was hydroxylated by lithium hydroxide solution and successive reduction with an organic sodium borohydride solution followed by cross-linking with a perfluoro-compound of perfluoropolyether containing ethoxysilane terminal groups. For the plasma activation method, the PVDF membrane surface was firstly activated by RF plasma to introduce free radicals; then, the activated membrane was polymerized by 1H,1H,2H,2H-perfluorodecyl acrylate solution, which is a hydrophobic monomer. The results showed that the WCA of modified membranes activated by the chemical is higher than that of plasma-activated membranes, which increased from 88° to 115° and 105°, respectively. In addition, comparing to unmodified PVDF hollow-fiber membrane, both modified membranes showed greater hydrophobicity and mechanical strength and smaller maximum pore sizes [14]. However, the use of alkaline for activation affects the membrane physical characteristics. Liu *et al.* (2010) found that the

membrane pore size decreased by increasing alkaline treatment time. The pore size reduction may occur due to the microstructural shrinkage of the membrane by alkaline treatment [45]. In addition, Hashim *et al.* (2011) indicated that the mechanical strength of the membranes was further reduced with an increase in concentration and temperature of NaOH solutions [19]. Therefore, plasma activation method is considered as an alternative since this method is less damage for membrane structure.

Cold plasma such as radio frequency (RF) has been successful used to modify PVDF membrane surface. Zheng *et al.* (2009) modified PVDF flat membrane surface by using O₂ plasma activation and grafted by methyltrichlorosilane (MTCS) vapor. The result showed that the WCA of membranes dropped from 88° to 81° after 10 mins of RF plasma activation, then increased to 134° after grafted by chemical vapor. However, the chemical vapor method is very expensive due to a large number of chemicals required for the vapor grafting process (MTCS solution 33%) [16]. Xu *et al.* (2015) indicated that the WCA of flat membrane could increase from 70.1° to 121° after activated by RF Argon (Ar) plasma for 120 s followed by grafted with N-octyltriethoxysilane 12% for 2h [22].

2.4.2 Plasma activation

Plasma treatment methods are considered as a less-harmful technique for membrane surface, compared to chemical treatment method [15]. During this process, electrons and ions from the plasma-phase react with the membrane surface, without affecting the bulk of membrane [46]. The purpose of plasma activation is to introduce the functional group or ion and active radicals on the membrane surface, making the grafting step more effective. Several types of plasma gases can be used to introduce -OH group onto membrane surface, including inert gases such as He and Ar and oxidative gases such as O₂, atmospheric, H₂O, etc.

(a) Inert plasma gases

Inert plasma gases such as Ar and He are not able to directly introduce new functional groups onto the surface of membrane but could increase surface hydrophilicity by reaction of the plasma activated surfaces upon exposure to ambient

air. After exposed to the air, peroxy ($\text{ROO}\cdot$), hydroperoxy ($\cdot\text{OOH}$) and hydroxyl species are generated on membrane surface, as presented in Figure 2.5 [21, 47].

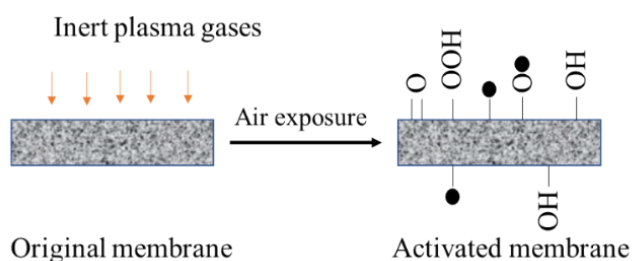


Figure 2.5 The mechanism of inert gases plasma activation

(b) Oxidative plasma gases

O_2 , H_2O and air gases are mainly used to introduce polar functionalities to the membranes. These oxidative plasma gases would increase the hydrophilicity of membrane surface by adding the hydrophilic functional groups. Similar to inert plasma gases, during oxidative plasma activation, electron, ion, radical, and UV radiation can react with the membrane surface. In addition, these radicals formed on the membrane surface can react directly with these gases or with the created fragments in the plasma phase; then, the OH group would be introduced onto membrane surface [21].

2.4.3 Pulse inductively coupled plasma (PICP)

Pulse inductively coupled plasma (PICP) is one of the high energy plasma systems which could be used to modify PVDF membrane surface due to the fact that the surface treatment by PICP does not require lengthy treatment period to achieve desired effects [23]. Since the design of PICP is much simpler than typical inductively coupled RF reactor plasma, the pulse treatment is more practical. Besides, PICP plasma temperature can be controlled by operating pressure and applied voltage, suitable for investigating the optimize plasma energy for membrane modification. There are some advantages of PICP had been noticed such as minimizes the thermal

load of samples and achieve desired effects within a short treatment period. PICP had successful used for enhancing the hydrophilicity of gelatin films [23]. To the best of our knowledge, PICP plasma has never been used for PVDF membrane activation.

2.4.4 The parameters effect to membrane surface modification

(a) Plasma treatment time and plasma energy

Plasma treatment time and plasma temperature affect the membrane water contact angle and membrane pore size of membrane. The abundant of OH groups of membrane surface also affects the reaction with organosilane solution [22, 48]. Furthermore, the membrane pore size also increases with the increase of plasma treatment time. The increasing of membrane pore size results in the increase of mass flux performance. However, wetting problem could be occurred with the large membrane pore size.

(b) Grafting concentration and grafting time

Organosilane solution concentration also affects the hydrophobicity enhancement of membrane surface. Zheng *et al.* (2009) indicated that the WCA of membranes modified by vapor grafting process increased with the increase of MTCS concentration until reaching a plateau. Besides, the functional groups of each organosilane affect the reaction time by their reaction rate [17]. Therefore, grafting concentration and grafting time are relatively crucial in achieving maximum reaction between silanol and OH during the grafting process.

2.5 Ozonation membrane contactor process

2.5.1 Ozonation reaction

In water, ozone is characterized by driving the oxidation in two mechanisms: direct reaction with dissolved molecular ozone (O_3) and indirect reaction with the radical species such as hydroxyl ($\bullet OH$), and hydroperoxyl ($\bullet OOH$) (Figure 2.6). The parameters such as pH and temperature of the media and ozone dose affect the combination of two above pathways, affecting the treatment efficiency [49].

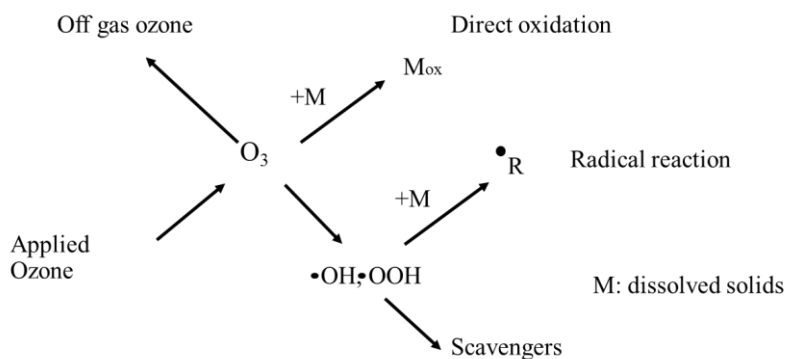


Figure 2.6 Reactions of ozone and dissolved solids

2.5.2 The parameters effect the ozonation membrane contactor process on wastewater treatment

(a) Ozone dosage

Ozone dosage is one of the most important factors that affect the dye removal efficiency. The optimize of applied ozone dose making the process reach the maximum decolorization efficiency [49]. Sevimli *et al.* (2002) indicated that the decolorization performance increased with the increasing of ozone dose, in particular, ozone utilization ratios of dye bath wastewater were 64% and 39% for the applied ozone doses of 24.1 mg/l and 87.2 mg/l, respectively [50].

(b) Dye concentration

The study on effect of dye concentration is essential since the it contributes to the color and organic load of dye wastewater. Gao *et al.* (2012) studied the feasibility of ozonation for different dye concentration, from 50 – 800 mg/l. The results showed that the dye removal efficiency decreased with the increase of dye concentration. In additions, the ozone consumption increased with the increase of initial dye concentration [51].

(c) pH

Ozone molecules attack selected specific parts of organic molecules such as double bonds or the aromatic system of direct reactive dyes under acidic pH conditions. In contrast, hydroxide radicals from ozone depletion react unspecific to

organic compounds under alkaline pH [49]. For instance, Kusvuran *et al.* showed that an increase of pH from 3 to 10 results in increasing of the removal percentages from 50% to 83.3% after 4 min ozonation of Reactive Blue 5 [52].

(d) Wetting characteristics of membrane

Membrane pore size, membrane porosities, and membrane hydrophobicity affect the membrane wetting, which poses an effect on ozone mass transfer efficiency. Ciardelli *et al.* (2003) found that the ozone mass transfer value was higher with the higher membrane pore size [35]. However, membrane wetting could occur quickly with the high membrane pore size and high porosities [11]. In contrast, high membrane hydrophobicity could prevent membrane wetting. Bamperng *et al.* (2010) indicated that PTFE membrane, which has higher WCA and lower porosities compared to PVDF membranes, gave higher stable and ozone flux than PVDF membranes [6].

2.6 Membrane characterization

2.6.1 Contact angle measurement

Water contact angle is considered as a typical method to determine the hydrophobicity of membrane. Conventionally, WCA is measured by the angle where liquid–vapor interface meets a solid surface. For hollow fiber membrane, WCA is determined by tensiometer, in which the Wilhelmy method is used [53]. The WCA is calculated by Equation (2):

$$\cos\theta = \frac{F - F_b}{L\sigma} \quad (2)$$

where, θ is water contact angle, F is the total force felt by the fiber at any submersion position, and F_b is the buoyant component of the force on the fiber at any submersion position. F_b is due to the fiber displacing liquid as it is submerged and removed, L is wetted length and σ is surface tension.

2.6.2 *Fourier-transform infrared spectroscopy (FT-IR)*

Each functional group has a specific vibration characteristic in the infrared spectrum, which can be determined by FTIR. This method is generally used to determine the membrane material and to confirm the chemical reaction of membrane modification [18].

2.6.3 *Scanning electron microscope (SEM) and Energy Dispersive X-ray (EDX) analysis*

The surface morphology of the outer surface and cross section of the PVDF membrane before and after each modification step is observed by using SEM which determines the surface morphology and pore structure of the membrane. It is important to investigate the effectiveness of modification process by using the SEM image of original membranes and modified membranes. Energy dispersive X-ray (EDX) connected with SEM examines the surface chemistry of the PVDF membranes. The spectrum includes detailed peaks that provide the elemental analysis or the surface composition of the membrane surface. Some very light elements such as H and He cannot be detected by this method because solid-state X-ray detector has a relatively poor energy resolution and sensitivity to elements present in low abundances [18]. This method can be useful in determining the correct methods of membrane modification process.

2.6.4 *Surface roughness*

Surface roughness is determined using atomic force microscopy (AFM). AFM provides 3D profile of surface roughness, including height parameters, spacing and hybrid parameters. Average surface roughness (R_a) that is the mean of the absolute height of the surface profile (Z) at all positions (x) of the sample is the most widely used in the height parameter. Besides, distinguish between peaks and valleys is also important information to fully characterize a surface [54]. Surface roughness is one of the key factors affecting the membrane hydrophobicity in terms of water contact angle. There are some studies reported that the surface roughness of membrane grafted with chloroalkylsilane and fluoroalkylsilane decreased with the increase of water contact angle [16, 17].

CHAPTER 3

METHODOLOGY

This work was conducted with two main parts: membrane hydrophobic modification and dye wastewater treatment using modified membranes as ozonation membrane contactor, as shown in Figure 3.1. In the first experiment, PVDF membranes surface was activated by plasma treatment, then grafted by organosilanes to enhance the hydrophobicity. The treatment conditions such as plasma gas, plasma exposure time, plasma operating conditions, organosilanes, grafting solution concentration and grafting time were investigated. After being treated by each modifying step, membrane samples were analyzed the chemical and physical changed. Finally, the original and modified membrane were applied for dye wastewater treatment by ozonation membrane contactor.

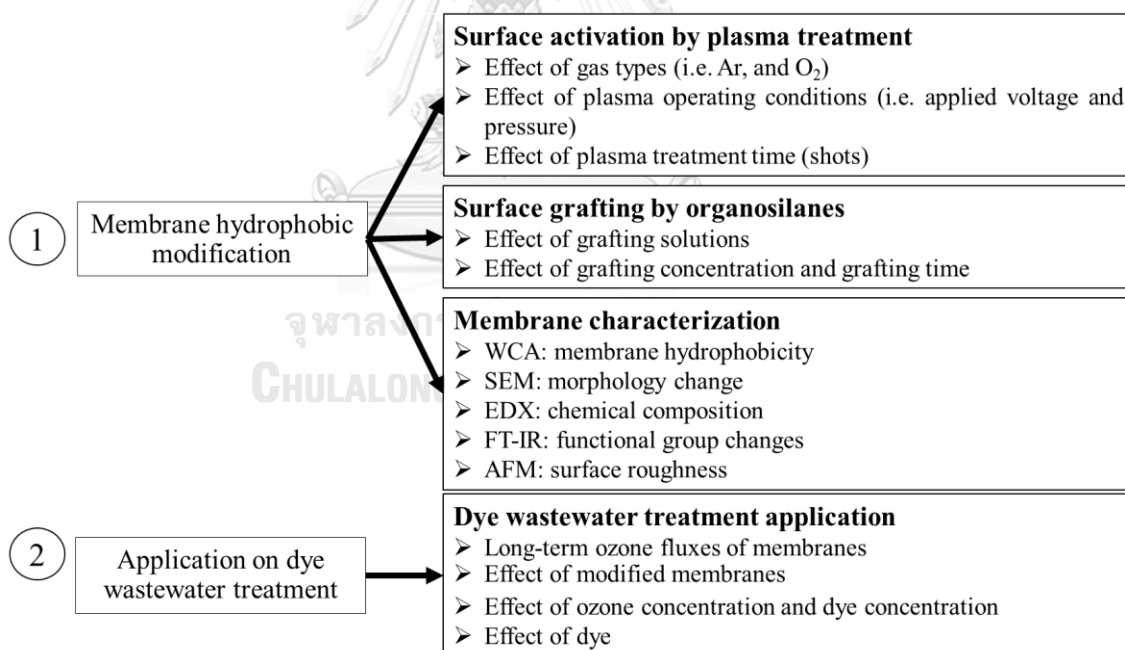


Figure 3.1 Research framework

3.1 Materials

PVDF membranes were purchased from Altrateck. Toluene and hexane were obtained from Qrec. Methyltrichloroalkylsilane (MTCS), trimethylchloroalkylsilane

(TMCS), 1H,1H,2H,2H-perfluorodecyltriethoxysilane (FAS-C8), and 1H, 1H, 2H, 2H-perfluorooctyltriethoxysilane (FAS-C6) were acquired from Aldrich. The different organosilanes used were described in Figure 3.2. Direct Blue 71 (DB 71) and Reactive Red 239 (RR 239) was manufactured and kindly provided by DyStar Thai Ltd. The properties of DB 71 and RR 239 are shown in Table 2.1. Oxygen (O₂) and Argon (Ar) gases were of analytical grade.

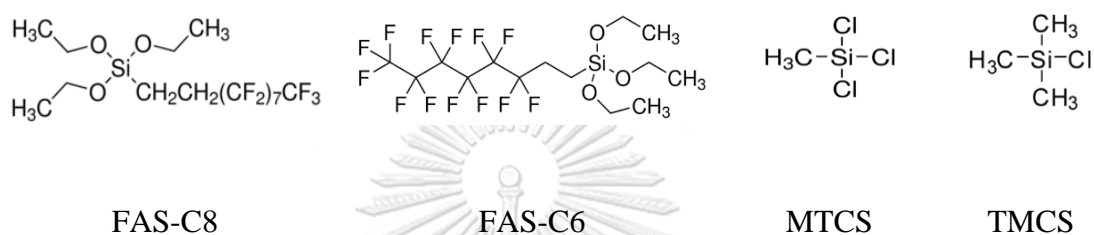


Figure 3.2 The structure of organosilanes

3.2 Membrane hydrophobic modification

In this study, PVDF membrane modification involved a two-step processes: (1) surface activation by exposing membrane to a pulsed inductively coupled plasma (PICP) for a few plasma shots and (2) direct grafting by immersing membranes into organosilanes within a given time period as followed.

3.2.1 Plasma activation

PVDF hollow fiber membranes were placed in a sample holder inside the cylindrical quartz tube of the PICP system as presented in Figure 3.3. Plasma activation was conducted using PICP driven by charging an applied voltage under an operating pressure using two 30 μF capacitor banks with a charging potential of 20 kV. The operating pressure was controlled by pressure gauge and applied voltage was controlled by capacitor controller. Gas was fed from the tank into the plasma chamber. Subsequently, a current is discharged through a steel coil around the quartz tube that produces the internal plasma through the ionization of gas inside the chamber.

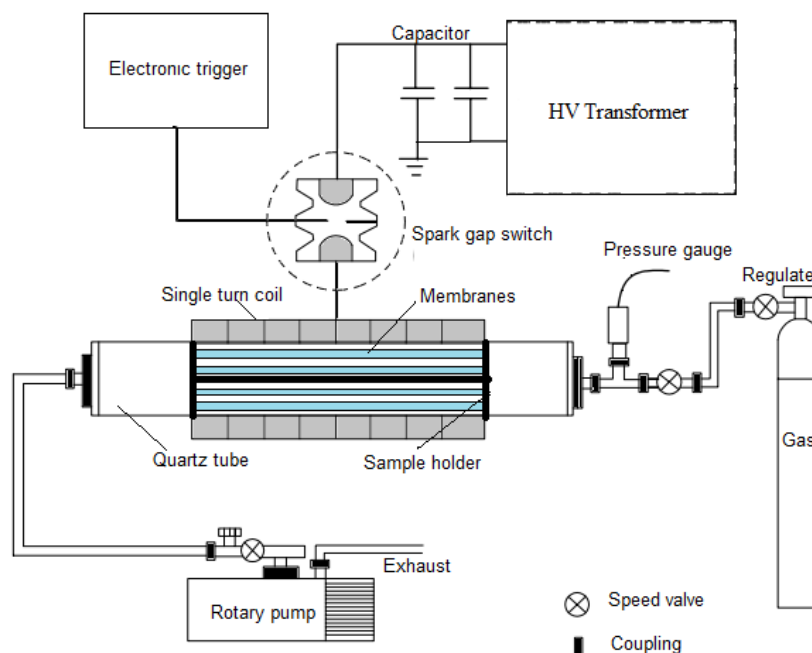


Figure 3.3 Schematic diagram of pulsed inductively coupled plasma (PICP) system [23]

Oxygen (O_2) and argon (Ar) plasma gases were used to activate the membrane surface. Different plasma operating conditions including operating pressure (0.25-0.35 mbar), applied voltage (8-10 kV), and plasma treatment shot (1-3 shots) were investigated.

3.2.2 Membrane grafting

After membrane activation, the activated membranes were immersed into different organosilanes in closed plastic containers. Four different organosilanes namely FAS-C8, FAS-C6, MTCS, and TMCS were selected to study. MTCS and TMCS were prepared by dissolving in toluene, but FAS-C6 and FAS-C8 were prepared by dissolving in hexane [17]. Grafting conditions such as grafting time and grafting concentration were investigated. The solution concentration was ranged from 0.005M – 0.020M and the grafting time was studied from 0.5h-6h. Then, the grafted membranes were rinsed either pure hexane or pure toluene for three times to remove any unreacted chemicals from the membranes and were dried at 60°C in an oven

(Model 700, Memmert) for 2h. Modified membranes were kept at room temperature for characterization.

3.2.3 Membrane characterization

a) Water contact angle:

After modification, the modified membrane samples were analyzed for water contact angle (WCA) using a tensiometer (DCAT 11, Dataphysics, Germany). The advancing contact angle was determined three cycles by SCAT software (version 2.4.8.48) and at least six sample readings of each membrane were reported.

b) Membrane morphology and chemical compositions

Membrane morphology and chemical compositions of membranes were investigated via scanning electron microscopy (SEM) (JEOL, JSM-IT500HR) coupled with a dispersive energy X-ray (EDX) at an accelerating voltage of 15.0 kV for both unmodified and modified membranes. The membrane surface was coated with gold under a vacuum condition to avoid electrostatic charging.

c) Surface roughness

Roughness and morphology of membrane were further analyzed by using atomic force microscopy (AFM, SPA 400, SEIKO). The membrane surface was imaged with a scan size of $10 \times 10 \mu\text{m}$. The surface roughness of the membrane was recorded in terms of the mean roughness (R_a). The surface profile such as peak height (Z), peak diameter and distance between peaks were calculated from the cross-section profiles along the marked directions of membranes by Gwyddion software.

d) Chemical functional groups

Fourier-transform infrared (FTIR) spectroscopy was used to investigate any changes in chemical functional group. The surface infrared spectra were recorded using an IR Prestige-21 FTIR spectrophotometer (SHIMADZU) at a resolution of 4 cm^{-1} in attenuated total reflection (ATR) mode. The inverted surface spectra of the membranes were recorded between wavenumber 500 cm^{-1} and 4000 cm^{-1} .

e) Membrane porosity

Membrane porosity (ϵ) was calculate using gravimetric method [55]. Membranes were cut to the same size and transferred into beakers with pure water. After immersing in water for 48h, samples were taken out and dried for 4h under 60°C. The weights of water contained in the membrane pores were recorded by using the analytical weight (MS204S). The porosity of hollow fiber membranes was calculated as Equation (3):

$$\epsilon = \frac{(W_b - W_a)/\rho_w}{(W_b - W_a)/\rho_w + W_a/\rho_p} \quad (3)$$

where: W_b and W_a are weights of membrane before and after drying, respectively. ρ_w is density of water (1 g/cm³), ρ_p is theoretical density of PVDF (1.78 g/cm³).

3.3 Application on dye wastewater treatment

After obtaining the optimized modification conditions, original PVDF hollow fiber membranes and modified membranes were studied in ozonation membrane contactor for DB 71 and RR 239 decolorization. The ozone flux and dye decolorization of ozonation membrane contactor using original membrane and modified membranes were compared. The specifications of membrane and module were shown in Table 3.1.

Table 3.1 Details of membranes and modules employed in ozonation membrane contactor system

Fiber outer diameter (mm)	1.13
Fiber inert diameter (mm)	0.8
Number of fibers	25
Module outer diameter (mm)	10
Module inter diameter (mm)	8
Effective module length (mm)	250
Effective area (m ²)	0.01571

3.3.1 The long-term ozone fluxes of membranes

The aim of this experiment is investigation of the ozone flux in original PVDF membrane and modified PVDF membranes by time, in order to evaluate the effective stability of membrane modification at fixed ozone concentration, gas velocity and liquid velocity. The outlet ozone gas concentration was measured every 1h by ozone analyzer (OLD/DL-5, Canada). Ozone gas and dye solution were operated under counter-current mode as illustrated in Figure 3.4. In this process, ozone gas was produced by the ozone generator using pure oxygen with industrial grade. Ozone was fed to the top of the membrane module through the shell side of the membrane by oriented vertically at a velocity of 2 m/s, measured by a gas flow meter (Bios defender 510). Meanwhile, dye wastewater was pumped from the feed tank to the bottom of the module through the lumen side of the hollow fibers by a peristaltic pump (L/S® Easy-load® II, Masterflex) at the liquid velocity of 0.46 m/s.

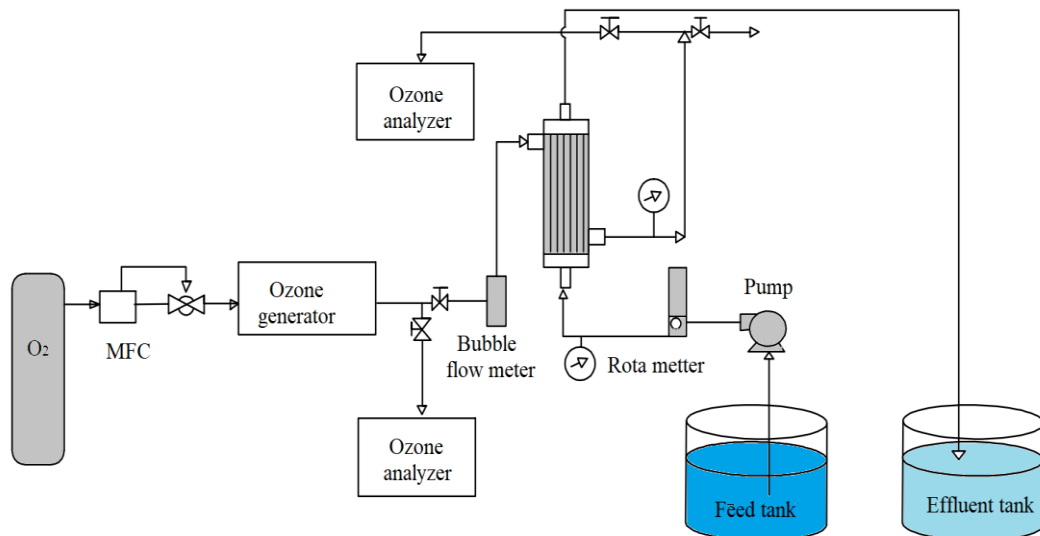


Figure 3.4 Experimental setup for ozone flux measurement of ozonation membrane contactor (liquid velocity: 0.46 m/s, gas velocity: 2 m/s, 100 mg/l DB 71)

The ozone flux ($\text{g}/\text{m}^2\text{s}$) can be determined by Equation 4:

$$J_{\text{O}_3} = \frac{Q_{\text{O}_3} \times (C_{\text{O}_3, \text{in}} - C_{\text{O}_3, \text{out}})}{A} \quad (4)$$

where, Q_{O_3} is the ozone flow rate (m^3/s), $C_{O_3,in}$ is the inlet ozone gas concentration (g/m^3), $C_{O_3,out}$ is the outlet ozone gas concentration (g/m^3) and A is the effective area of the membrane (m^2).

3.3.2 Decolorization of dye wastewater by ozonation using modified membranes

This experiment aims to investigate the dye wastewater treatment performance at different dyes and membranes by ozonation membrane contactor. The modified membranes under different modification conditions were selected to study as membrane in membrane contactor. The experimental setup was similar to that in the experiment of ozone flux measurement, excepted the outlet dye wastewater was recycled back to feed tank as shown in Figure 3.5. RR 239 and DB 71 azo dyes were selected to investigate the effect of dyes on treatment performance. The ozone concentration from 30-60 mg/l and dye solution concentration from 50-200 mg/l were investigated. Treated wastewater was sampled from sampling port to analyze COD and dye concentration at different time.

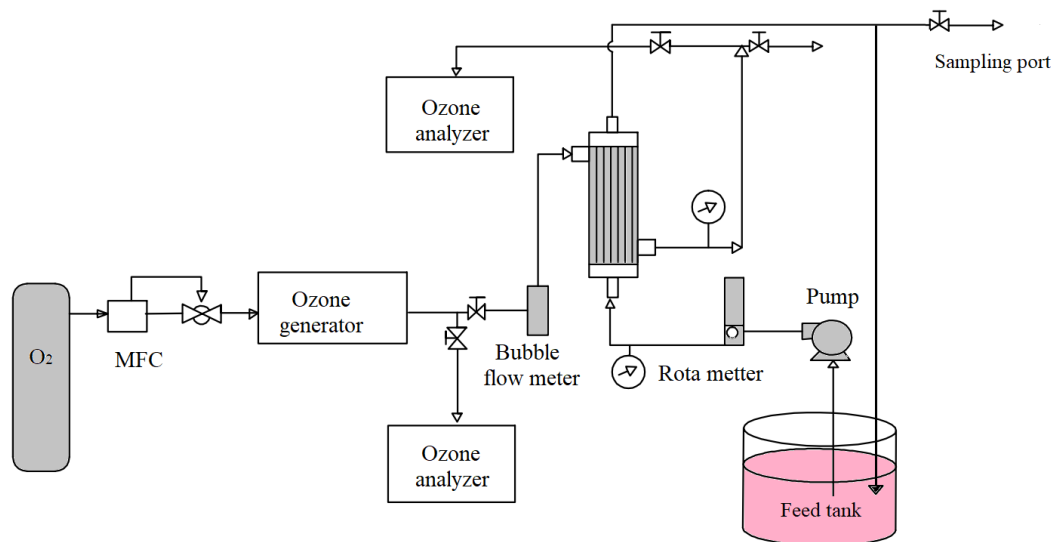


Figure 3.5 Schematic diagram of ozonation membrane contactor device for dye solution treatment

Dye concentration was measured by UV-spectrophotometer (UV-VIS, PerkinElmer) and COD was analyzed by closed reflux titrimetric method. The treatment efficiency was calculated by the Equation (5):

$$\text{Removal efficiency (\%)} = \frac{C_0 - C}{C_0} \times 100 \quad (5)$$

where, C_0 and C are the dye concentration (mg/l) before and after treatment for time (mins).

The decolorization of dyes by ozone ozidation is pseudo-first order with respect to both ozone and dye [56]. The dye ozonation kinetic was measured according to Equation (6):

$$C = C_0 \times e^{-k_{app}t} \quad (6)$$

Therefore, the pseudo-first-order trend was observed by plotting $\ln(C_0/C)$ versus reaction time following Equation (7):

$$\ln \frac{C_0}{C_t} = k_{app}t \quad (7)$$

where C_0 and C_t are initial and treated dye concentrations (mg/l) at reaction time t (min), and k is apparent rate constant (min^{-1}).

3.4 Energy consumption of ozonation membrane contactor process

To evaluate the energy consumed of the process, the energy demand to treat 1 m^3 of dye wastewater which consisted of pump and ozone generator energies was calculated as followed:

3.4.1 Energy consumed of pump

The role of the peristaltic pump is to feed water into membrane module and to recirculate water to the feed tank. The energy demand for peristaltic pump (E_p) was determined by Equation (8):

$$E_p = P \times T \quad (8)$$

where P is power required (kW), T is the time required to treat 1 m^3 of water (h). This was assumed that the requirement for discharged wastewater is 10 mg/l, T was determined by Equation (9):

$$T = \frac{-\ln \frac{C}{C_0} \times 1000}{k_{app} \times V \times 60} \quad (9)$$

where k is apparent constant rate (min^{-1}), and V is solution volume (L).

The power required for the pump was determined by Equation (10) [57]:

$$P = \frac{q \times \rho \times g \times \Sigma h}{\eta} = \frac{q \times \Delta P}{\eta} \quad (10)$$

where q is liquid flow rate (m^3/s), ρ is the density of feed water under room temperature (kg/m^3), g is the gravitation ($9.8 \text{ m}/\text{s}^2$). The total water head ($\Sigma h = \Sigma \Delta P / \rho g$) of the system was determined from pressure drop (ΔP). η is the efficiency of pump which was assumed to be 75%. The pressure drop was calculated based on Darcy-Weisbach [57] as followed Equations (11-13):

$$\Delta P = \frac{f \rho v^2 L}{2d} \quad (11)$$

$$f R_e = 64 \quad (12)$$

$$R_e = \frac{d v \rho}{\mu} \quad (13)$$

where f is Darcy friction factor, v is the liquid velocity ($0.46 \text{ m}/\text{s}$), L is the length of pipe in different sections (m), d is the diameter of pipe or membrane channels (m). The ΔP was calculated at different sections of system such as pipe and membrane channel using online pressure drop calculator (Pressure Drop Online-Calculator, Software-Factory H. Schmitz).

3.4.2 Energy consumption during ozone generation

The energy demand (kWh) during operational period was calculated following Equation (14) [57, 58]:

$$E_{EO}(\text{O}_3) = \frac{-\ln \frac{C}{C_0} \times r \times [\text{O}_3] \times Q_{\text{O}_3}}{k_{\text{app}} \times V \times 1000} \quad (14)$$

where r is energy requirement for ozone production ($10 \text{ kWh}/\text{kg}$ ozone), $[\text{O}_3]$ is ozone concentration used in the process ($\text{mg O}_3/\text{l}$), and Q_{O_3} is the flow rate of ozone (l/min), k is apparent constant rate (min^{-1}), and V is dye volume (L).

CHAPTER 4

RESULTS AND DISCUSSION

4.1 Effect of plasma operation parameters on membrane modification

In order to enhance the hydrophobicity, the PVDF membrane was modified by PICP activation followed by grafting with organosilanes. To optimize the plasma operation parameters on membrane hydrophobicity enhancement, the plasma gas type, plasma operating condition, and plasma treatment time were varied, while the grafting condition was kept constant at organosilane concentration of 0.02M and grafting time of 2h. Water contact angle (WCA), membrane morphology, surface roughness, membrane porosity and membrane chemical structure changed were analyzed.

4.1.1 Effect of plasma gases

In order to investigate the effect of different plasma gases on membrane activation, argon (Ar) and oxygen (O₂) gas were studied. The applied voltage was ranged from 8 kV to 10 kV, and the operating pressure was kept constant at 0.25 mbar. The changing in WCA of the modified membrane with and without plasma activation were compared as shown in Figure 4.1. In which, after grafted with 0.02M MTCS for 2h, all modified membranes activated by PICP gave a higher WCA compared to that of modified membranes without plasma activation (control sample). Under the operating condition of applied voltage at 10 kV and operating pressure at 0.25 mbar followed by grafting with 0.02M MTCS for 2h, WCA of the modified membranes was increased from 74.7° (original) to 98.1° and 114.8° by Ar and O₂ plasma activation, respectively, while the WCA of the control sample (without grafting) was 89.0°. The increase in WCA implied that the hydrophobicity of membrane was increased. It was due to the formation of radicals and functional groups on the membrane surface by plasma treatment. The introduction of functional groups by plasma gas is demonstrated as in Figure 4.2 [47, 59]. In the plasma process, gases are ionized to energetic ions, photons, and electrons that interact with the

polymer, resulting in the changes of chemical and physical of the membrane surface [59]. Metastable argon and metastable oxygen are the most important active species presented in plasma, which its energy has sufficiently high to promote the C-F bond scission [47, 59]. After that, functional groups could be formed on membrane surface. These functional groups react with organosilane which enhance the membrane hydrophobicity.

On the other hand, plasma gases play an important role in membrane modification efficiency. For all conditions, the WCA of the 0.02M MTCS grafted membrane activated by O₂ plasma was higher than that of membranes activated by Ar plasma. For activation condition of 8 kV/0.25 mbar, the WCA of 0.02M MTCS grafted membrane activated by O₂ was 119.4°, while that of grafted membrane activated by Ar was much lower (92.0°). Similarly, under the operating condition of 10 kV/0.25 mbar, the WCA of 0.02M MTCS grafted membrane treated by O₂ was higher than that of membrane treated by Ar, which was 105.9° and 98.1°, respectively. This was because O₂ plasma directly introduced -OH groups, while Ar plasma introduced ions and active radicals onto the membrane surface [21]. Therefore, more reactions between -OH groups and MTCS occur on membranes activated by O₂ plasma as their surfaces have more -OH groups than membranes activated by Ar plasma. Kaynak *et al.* (2013) also reported that at the same operating condition, membrane treated by O₂ plasma gave lower WCA than membrane treated by Ar plasma which was decreased from 84.6° to 68.4° and 63.2° by Ar and O₂ plasma treatment, respectively. In addition, the WCA of membranes depends on surface morphology and chemical composition on membrane surface [60].

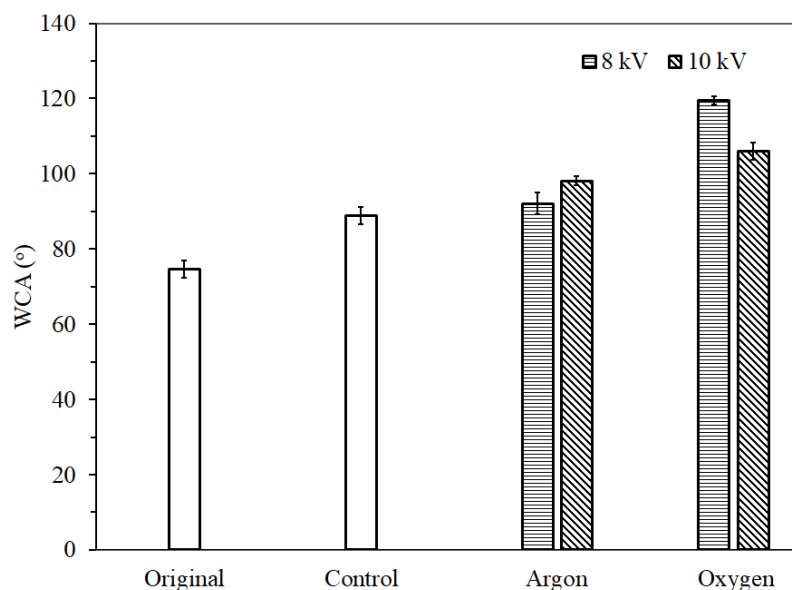


Figure 4.1 The WCA of grafted membranes activated by different plasma gases and different plasma applied voltage under operating pressure at 0.25 mbar, followed by grafting with 0.02M MTCS for 2h



Figure 4.2 Schematic reaction mechanism of plasma treatment on PVDF membrane

The difference of membrane surface treated by plasma gases were confirmed by SEM images (Figure 4.3). It could be observed that there were some particles on the surface of grafted membrane. At the same operating conditions, the particles on surface of O_2 activated membrane followed by grafting with 0.02M MTCS were bigger than those formed on membrane activated by Ar plasma. These particles were

corresponding to the Si-O-Si hydrophobic network presented on the membrane surface, as confirmed by the FTIR and EDX as shown in Figure 4.4 and Table 4.1.

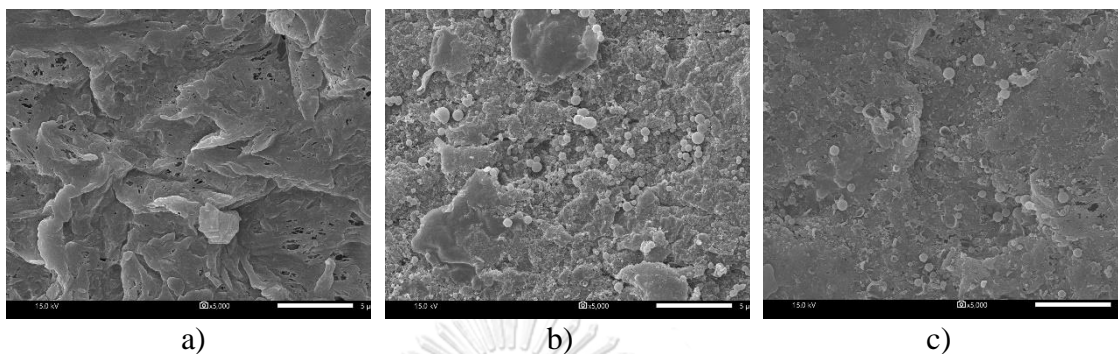


Figure 4.3 SEM images of a) original membrane, b) modified membrane activated by O₂, and c) modified membrane activated by Ar (operating condition of 8 kV and 0.25 mbar followed by grafting with MTCS for 2h)

The changes of the chemical components induced by the introduction of functional groups and MTCS on the PVDF surfaces were confirmed by FTIR analysis as shown in Figure 4.4. The featured functional groups of PVDF membranes were presented in FTIR spectra, in which, stretching bands of CF₂ appeared at wave number of 1067 cm⁻¹ and 1274 cm⁻¹ [61], and the stretching bands of CH₂ appeared at 1402 cm⁻¹ and 2890-3100 cm⁻¹. While Ar activated membrane followed by grafting with 0.02M MTCS did not significantly changed compared to original PVDF membrane, there were three new peaks found in the spectra of grafted membrane activated by O₂ plasma. The introduction of MTCS was confirmed by the presence of peaks at around 783 cm⁻¹, 1034 cm⁻¹, and 1141 cm⁻¹, which are attributed to the Si-O-Si vibrations in the methylsilicone network [62, 63].

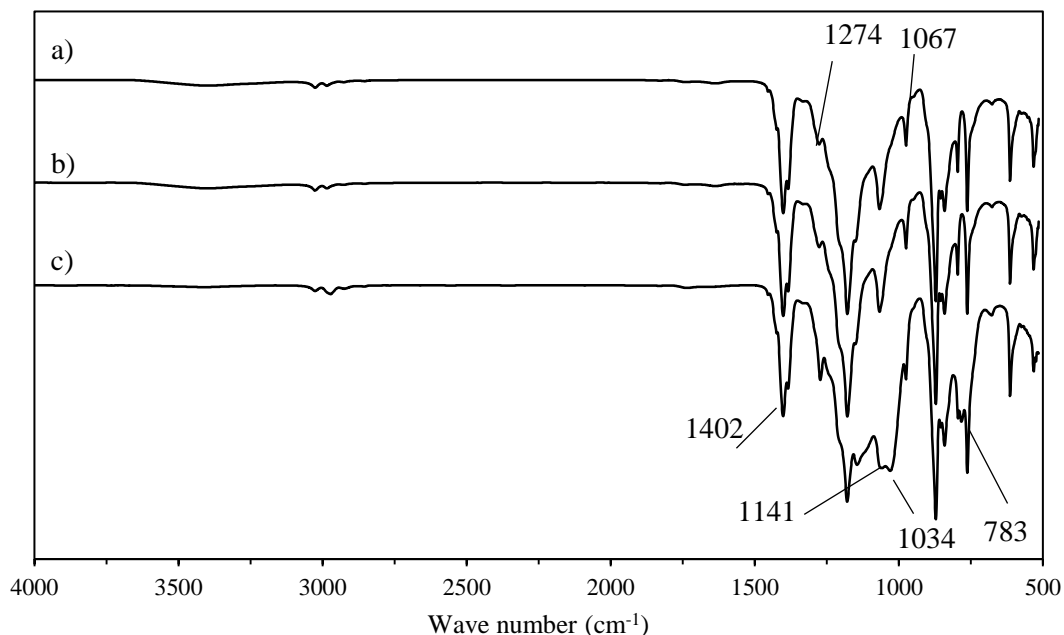


Figure 4.4 FTIR spectra of PVDF membrane a) original membrane; b) modified membrane activated by O₂, and c) modified membrane activated by Ar (operating condition of 8 kV and 0.25 mbar followed by grafting with MTCS for 2h)

Carbon (C), fluorine (F), oxygen (O), and silicon (Si) contents were analyzed at different membranes after plasma activation by different plasma gases and after grafted by MTCS as presented in Table 4.1. The results indicated that the O₂ activated membrane followed by grafted with MTCS showed the presence of O, while the original PVDF membrane and Ar activated membrane showed the presence of only C and F. The active plasma gas such as O₂ directly introduced -OH groups to membrane surface, whereas, inert plasma gas such as Ar only can generate the active radicals on to membrane surface, then, form the -OH groups after exposure to the air [21]. Due to the high abundance of -OH groups on the membrane surface, the Si content of grafted membranes activated by O₂ plasma was higher than that of membranes activated by Ar plasma. The presences of Si and O element proved that membranes were successfully modified by PICP system followed by grafted with MTCS.

Table 4.1 Changes of the chemical composition of membrane surface under different plasma gases

Membranes		Element composition (%)			
		C	F	O	Si
Original PVDF membrane		53.4	46.6	-	-
Modified membranes					
Ar plasma	Activated	54.6	45.3	-	-
	Grafted	53.3	42.6	3.1	0.8
O ₂ plasma	Activated	51.8	46.2	2.0	-
	Grafted	53.3	28.5	12.3	5.9

This experiment proved that the different plasma gases posed the different effects on membrane modification. In addition, the plasma activation followed by grafting with MTCS could enhance the hydrophobicity of membrane surface, expressed by WCA. Besides, O₂ plasma gave more effect on membrane hydrophilicity enhancement than that of Ar plasma due to the introduction of functional groups process. After grafted by MTCS, the membrane activated by O₂ plasma gave higher results in terms of WCA and Si content than membrane activated by Ar plasma, therefore, O₂ plasma activation was chosen for further experiments.

4.1.2 Effect of plasma operating conditions

According to the obtained results of WCA, O₂ plasma activation was selected to investigate the effect of PICP operating conditions. The operating plasma conditions were studied, including applied voltage (8-10 kV) and operating pressure (0.25-0.30 mbar). The results found that the WCA of the activated membranes were not significant changed, excepted 8 kV/0.30 mbar and 10 kV/0.25 mbar. After grafting with 0.02M MTCS for 2h, WCA of grafted membranes were not significant different (119.4°-122.4°). Meanwhile, WCA of grafted membranes activated under operating conditions of 8 kV/0.30 mbar and 10 kV/0.25 mbar were much lower which was 106.2° and 105.9°, respectively, as shown in Figure 4.5. This result was likely because of the effect of plasma energy on the membrane surface. The plasma energy

decreased with the increase of operating pressure but increased with applied voltage [64]. Based on that, the plasma energy of the operating condition of 8 kV/0.30 mbar was lowest while that of 10 kV/0.25 mbar was highest. It could be seen that at lower plasma energy (8 kV/0.30 mbar) and higher plasma energy (10kV/0.25 mbar), the effectiveness of membrane modification was lower.

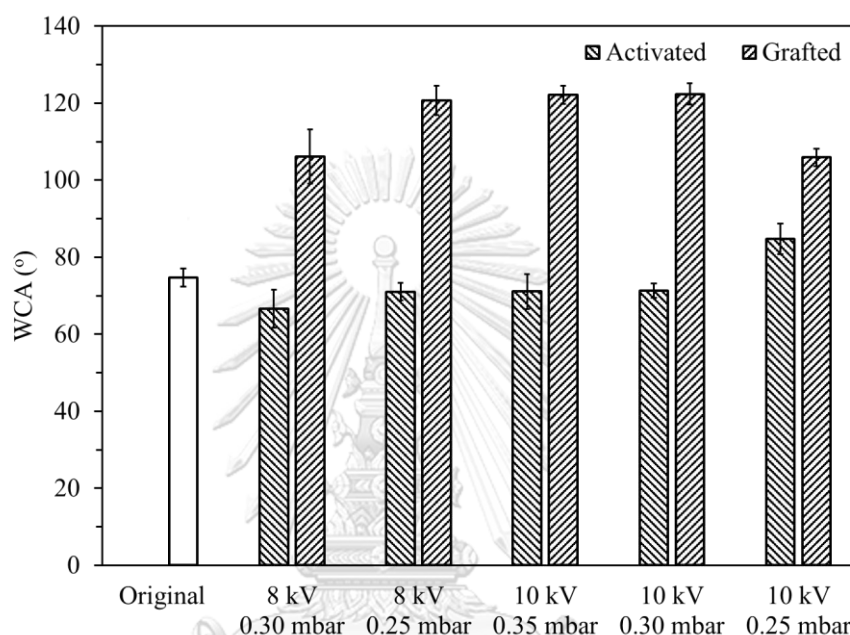


Figure 4.5 WCA of the modified membranes activated by oxygen plasma gas under different plasma operating conditions followed by grafting with 0.2 M MTCS for 2h

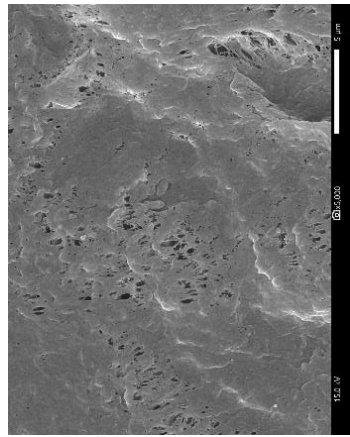
SEM analysis was employed to characterize the surface morphology of membranes. Figure 4.6 (a-d) showed that the membrane surface did not significantly change after activated by O₂ plasma; excepted under the condition of 10 kV/0.25 mbar, the membrane surface was melted and there was some small holes presence. It was reported that both etching process and introduction of functional groups process might happen on membrane surface during plasma activation [65]. In this work, etching process might play more important role under the operating condition of 10 kV/0.25 bar.

The changing of membrane surfaces under different operating condition after grafted with 0.02M MTCS for 2h were shown in Figure 4.6 (d-f). After grafting

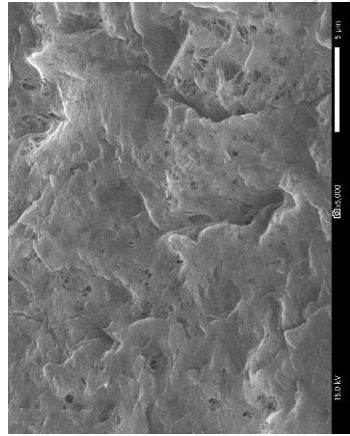
process, the differences in morphology of membrane surface by different plasma operating conditions were noticeable. There were some particles on the surface of the grafted membrane. In addition, the sizes of particles presented on grafted membrane activated by 8 kV/0.30 mbar were small, while those of grafted membrane activated by 8 kV/0.25 mbar and 10 kV/0.30 mbar were more prominent and could be observed easily. Due to the high plasma energy, the particles on modified membrane under 10 kV/0.25 mbar was presented unevenly and was smaller compared to other conditions.

The contents of O and Si of MTCS grafted membranes activated by 8kV/0.30 mbar (4.7%, and 2.0%, respectively) and by 10 kV/0.25 mbar (2.3% and 0.2%, respectively) were less than other conditions (Table 4.2). This result was probably because of the effect of plasma energy on membrane surface. At low plasma temperature (8 kV/0.30 mbar), the plasma energy was having lower effective on functional group introduction. At high plasma energy (10 kV/0.25 mbar), the etching process was probably better than introducing functional group process [65]. Besides, higher O content on membrane surface resulted in the higher Si content. It can be seen that the amount of Si and O presented on modified membrane surface increased with the increasing of WCA. The Si content presented on grafted membrane activated by 8 kV/0.25 mbar, and 10 kV/0.30 mbar were highest, which were 5.9% and 3.1%, respectively.

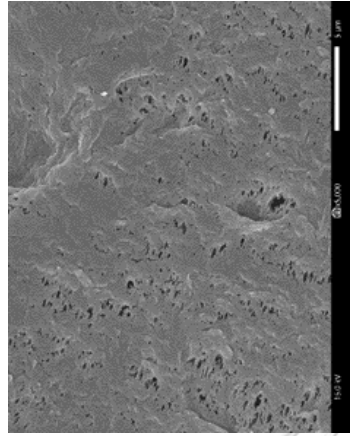
Activated membranes



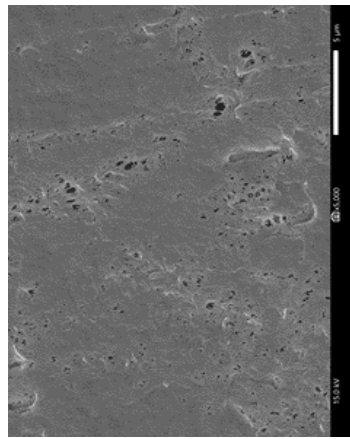
a)



b)

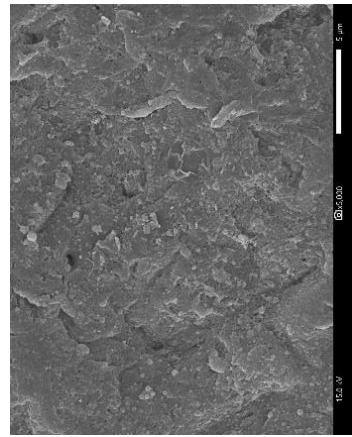


c)

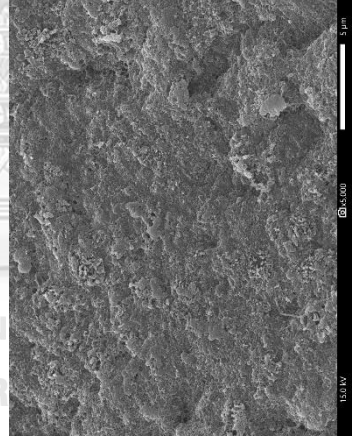


d)

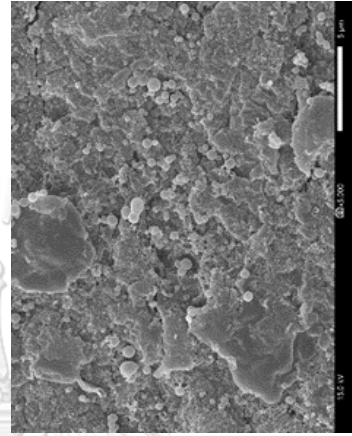
Grafted membranes



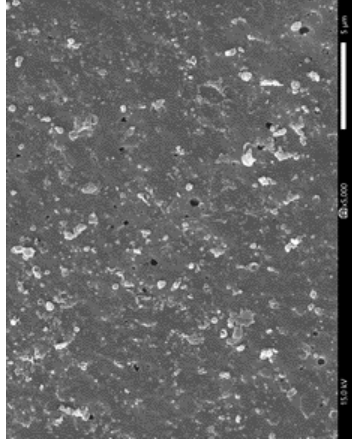
e)



f)



g)



h)

Figure 4.6 SEM images of modified membranes under operating condition of (a, e) 8kV/0.30 mbar, (b, f) 10kV/0.30 mbar, (c,g) 8kV/0.25 mbar, (d,h) 10kV/0.25 mbar, at plasma treatment time of 1 shot followed by grafted with 0.02M MTCS

Table 4.2 Changes of the chemical composition of membrane surface under different plasma operating conditions

Plasma operating conditions			Elemental composition (%)			
Voltage (kV)	Pressure (mbar)	Time (shot)	C	F	O	Si
-	-	-	53.4	46.6	-	-
8	0.25	1	53.3	28.5	12.3	5.9
8	0.30	1	52.1	41.2	4.7	2.0
10	0.25	1	50.2	47.3	2.3	0.2
10	0.30	1	49.9	40.5	6.5	3.1
10	0.30	2	49.4	30.3	14.0	6.3

Note: Activated by O₂ plasma gas followed by grafting with 0.02M MTCS for 2h

The results showed that the membrane modification process was influenced by plasma energy, at the high plasma energy, membrane surface was destroyed. In this work, both plasma operating condition of 8 kV/0.25 mbar and 10 kV/0.30 mbar showed the highest results in terms of WCA and Si and O composition. However, the breaking down voltage of this PICP system for oxygen gas was 8 kV at which plasma discharged was not stable. Therefore, the condition of 10 kV/0.30 mbar was chosen for the next experiment.

4.1.3 Effect of plasma treatment shot

To investigate the effect of plasma treatment time, the O₂ activated membranes at the applied voltage of 10 kV/0.30 mbar for 1 to 3 shots followed by grafting with 0.02M MTCS for 2h were studied. Figure 4.7 shows the effect of varying plasma treatment shot on membrane WCA. Without MTCS grafting, the WCA of membranes reduced slightly from 74.7° (original) to 71.1° after 1 plasma shot, and then reduced to 60.1° after 2 shots. This could be primarily attributed to the introduction of increasing numbers of -OH groups on the membrane surface. However, the WCA of the membranes increased from 60.1° to 74.8° when increasing the treatment time from 2 shots to 3 shots. This was possibly because the membrane

characteristics changed after exposure to plasma gas for a longer duration. As mentioned above, both etching process and functional groups introduction process may occur in plasma activation. The etching process showed the more important role when the plasma treatment time is more than 2 shots.

After activated by O₂ plasma, activated membranes were immersed into 0.02M MTCS and 0.02M FAS-C8 for 2h. The results showed that the WCA of membranes was increased from 122.4° to 124.6° and from 97.1° to 106.9° for membranes grafted by MTCS and FAS-C8, respectively when the plasma treatment time increases from 1 shot to 2 shots. This was the result of the increasing of -OH groups when the plasma treatment shot increase. Nevertheless, the WCA of grafted membranes was declined when the plasma treatment increases to 3 shots which might because of morphological changed of membranes.

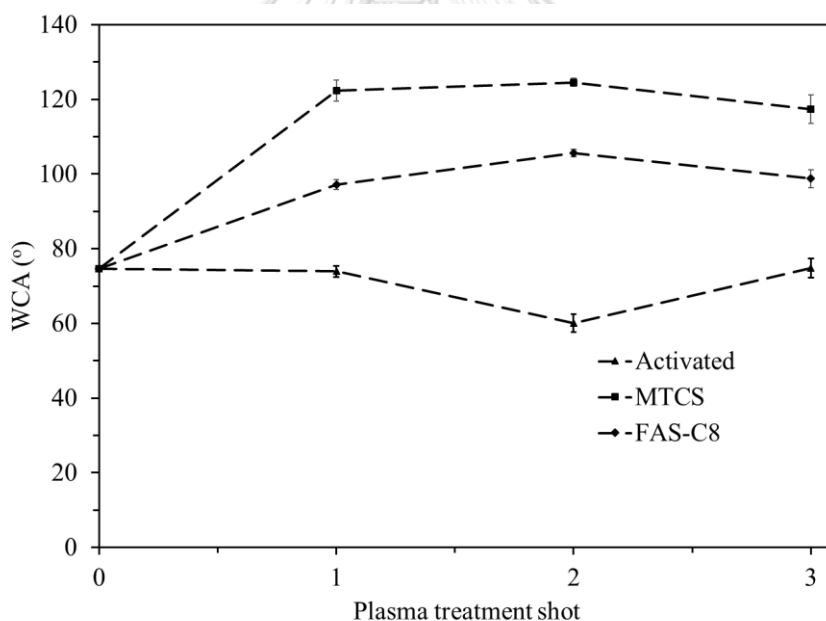


Figure 4.7 The WCAs of modified membranes activated by oxygen plasma gas at 10 kV/0.3 mbar for different plasma treatment times and grafted by 0.02M of different solutions for 2h

Morphological changes of membranes after activated by plasma at different plasma treatment shot are shown in Figure 4.8 (a-c). It could be seen that the membrane surface did not change after activated by plasma treatment time of 1 shot

and 2 shots. However, the membrane surface was destroyed by the presence of holes under the plasma treatment time of 3 shots, as shown in Figure 4.8c. As a result, the hydrophobic particles presented on membrane activated for 3 shots was smaller compared to other conditions. Besides, particles on the surface of membrane activated for 2 shots were distributed evenly on membrane surface and were bigger compared to those on membrane activated for 1 shot.

The EDX results indicated that F content of membrane activated by 2 shots was lower than that of membrane activated by 1 shot which was 30.3 % and 40.5 %, respectively, as reported in Table 4.2. It was possibly due to the high membrane defluorination of the treatment time of 2 shots compared to the treatment time of 1 shot. As a result, the O and Si content on membrane treated by 2 shots was higher. It was implied that the treatment time of 2 shots was suitable for the activation of PVDF membrane surface. When the plasma treatment shot exceeds 2 times, the etching process would dominate, resulting in membrane destroying.

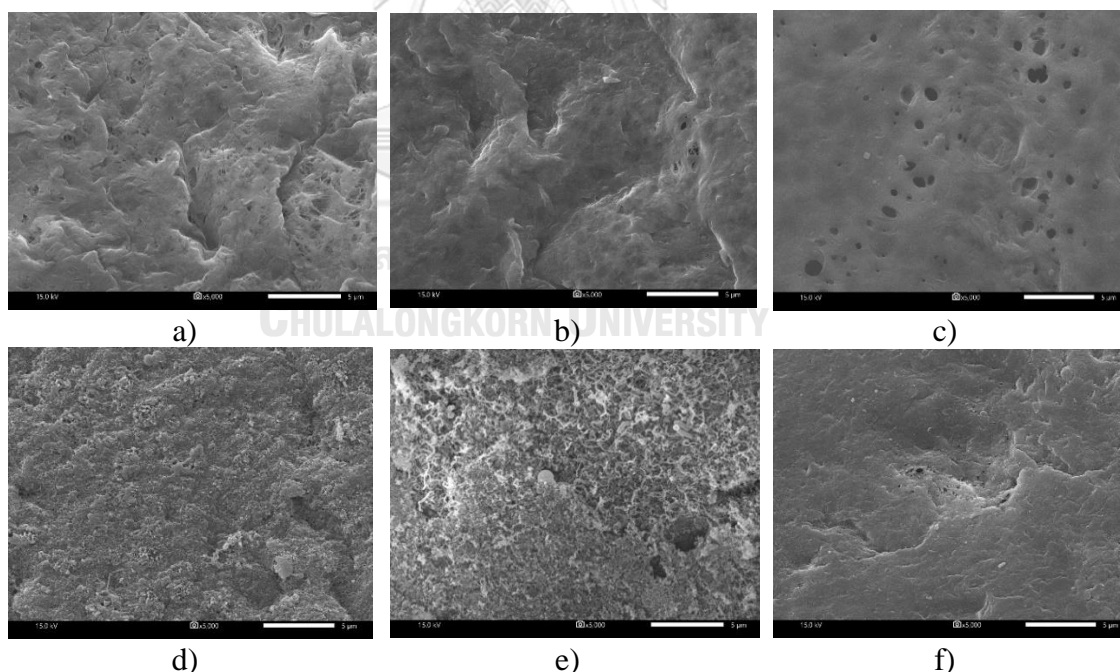


Figure 4.8 SEM images of activated membranes (a-c) and grafted membranes (d-f), at plasma treatment time of 1 shot (a, d), 2 shots (b, e), and 3 shots (c, f) at activation condition of 10 kV/0.3 mbar followed by grafted with 0.02M MTCS for 2h

4.2 Hydrophobic modification by grafting with organosilanes

In the grafting process, the reactive silanol species of organosilane could replace the hydroxyl group presence on membrane surface and in the atmospheric moisture [16, 63] as shown in Figure 4.9.

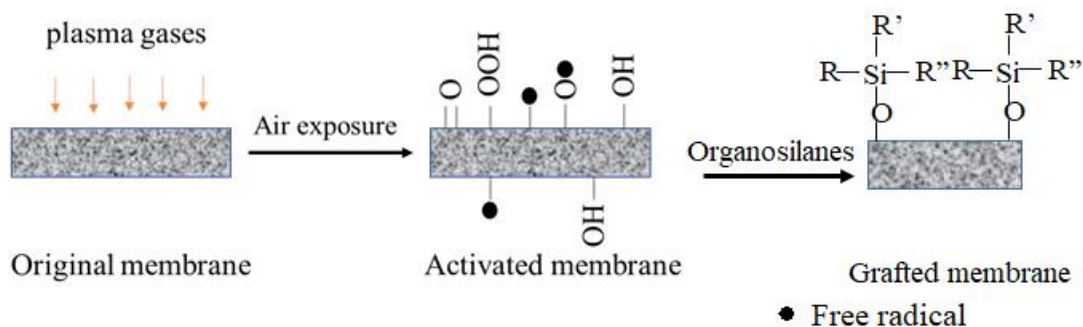


Figure 4.9 PVDF membrane modification by methods of plasma activation followed by organosilane direct grafting

Beside the plasma activation condition, the grafting condition also effect to the membrane hydrophobicity enhancement. In order to optimize the membrane grafting parameters, after activated by oxygen plasma gas, membranes were immersed into organosilanes at different concentrations and different grafting time.

4.2.1 Effect of grafting organosilanes concentration

To investigate the effect of grafting solution concentration, membrane was activated by O_2 plasma then immersed into organosilanes at different organosilane concentrations. The plasma operating condition was kept constant at 10 kV and 0.30 mbar and plasma treatment time of 2 shot, followed by grafting with 0.005-0.02 M of MTCS and FAS-C8.

The results showed that the WCA of modified membranes was increased with the increase of organosilane concentration as illustrated in Figure 4.10. For example, when increasing the organosilane concentration from 0.01M to 0.02M, the WCA of membrane grafted by MTCS and FAS-C8 increased from 102.3° to 124.6° and from 89.2° to 106.9° , respectively. This was because when the concentration of

organosilane increased, the -OH groups present on the membrane surface and in the moisture could easily be reacted with organosilanes, hence, enhancing the membrane hydrophobicity [16].

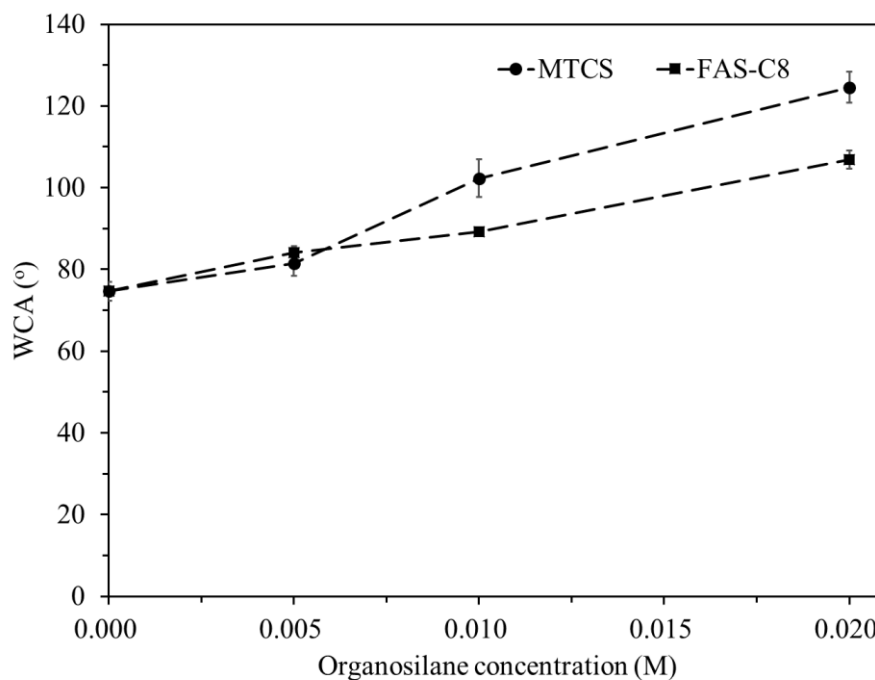


Figure 4.10 WCA of modified membrane at different organosilane concentrations after activated by O₂ plasma gas, under applied voltage of 10 kV/0.30 mbar/2 shots

The results showed that the outer surface of membranes grafted by FAS-C8 was smooth, while particles were found on the surface of membrane grafted by MTCS. The size and number of particles on membrane grafted by MTCS increased with the increasing of solution concentration, as shown in Figure 4.11.

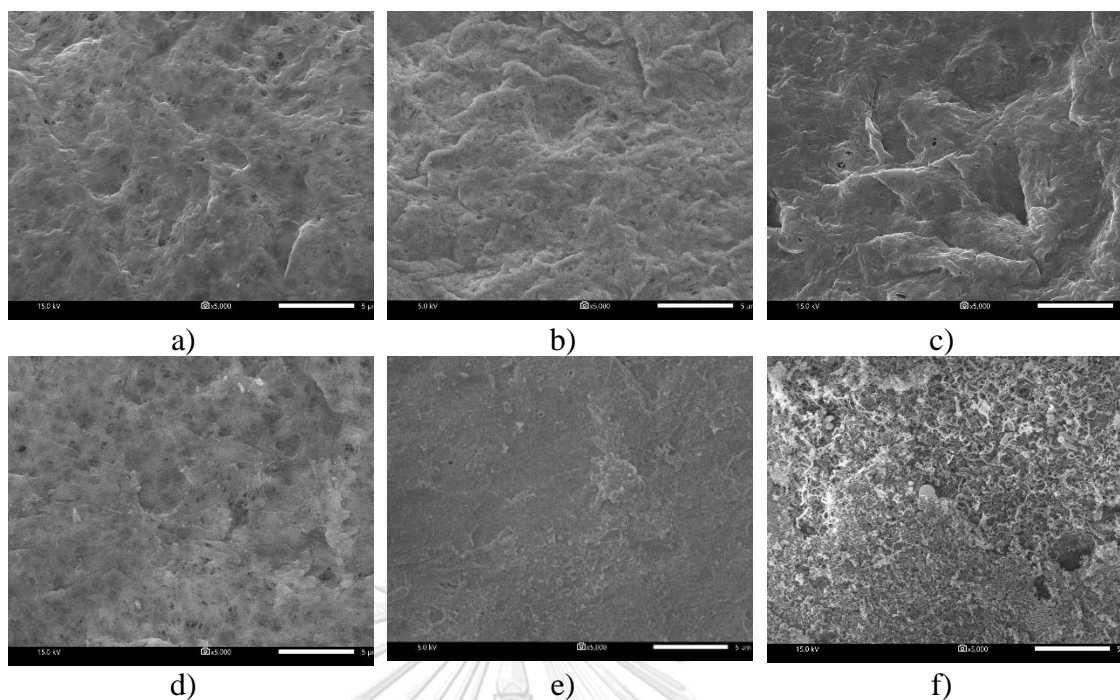


Figure 4.11 SEM images of modified membrane grafted by different organosilanes and concentrations: a) 0.005M FAS-C8, b) 0.01M FAS-C8, c) 0.02M FAS-C8, d) 0.005M MTCS, e) 0.01M MTCS, and f) 0.02M MTCS

It was clear that the grafting efficiency increased with the increasing of organosilane concentration. The concentration of 0.02 M was chosen for further experiments.

4.2.2 *Effect of grafting time and organosilanes*

Figure 4.12 shows the WCA of modified membranes with different grafting organosilanes. MTCS, TMCS, FAS-C6, and FAS-C8 were studied for membrane grafting at fixed organosilane concentration of 0.02M. The plasma activation condition was kept constant by O₂ plasma gas at 8kV/0.25 mbar, and plasma treatment time of 1 shot. The results revealed that the WCA of grafted membranes was increased with the increasing of grafting time. This was because the grafted organosilane increased with the grafting time, leading to an increase in the WCA [16]. However, the WCA of membrane grafted by TMCS and FAS-C6 did not have any significant changes. In addition, it could be also observed that increasing in WCA of membrane grafted by fluoroalkylsilane (FAS-C6 and FAS-C8) was slower than that of

chloroalkylsilane (MTCS and TMCS). After grafted for 0.5h, the WCA of membrane grafted by MTCS increased from 71.0° (activated membrane) to 114.8° after 2h of grafting time. For the membrane treated by FAS-C8 for 0.5h, WCA increased to 91.6° after 2h of grafting time and reached 104.9° after 4h. Kujawa and Wojciech (2016) indicated that the hydrophobicity of membrane depends on chemical and geometrical of membrane surface [66]. The differences of the WCA of membrane grafted by organosilanes is possibly due to the reactivity of silanol species that was reacted with -OH group. Perera *et al.* (2016) indicated that the reactivity of functional groups connected with Si atoms in organosilane compound decreases in the order of Si-NR₂ > Si-Cl > Si-OCCH₃ > Si-OCH₃ > Si-OCH₂CH₃ [42]. Functional groups of MTCS which can react with -OH groups are Cl, while that of FAS-C8 and FAS-C6 are -OCH₃, as shown in Figure 3.2, resulting in the lower WCA of FAS-C8 and FAS-C6. The higher reactivity of MTCS with -Cl was related to the low bounding dissociation energy of Si-Cl, at 60.28 kcal/mol, while that of Si-OCH₃ was 108.0 kcal/mol [67]. In addition, Kujawa *et al.* (2019) indicated that membrane grafted by nonfluorinated compound contained -Cl showed the higher WCA and surface roughness compared to fluorinated compound [67].



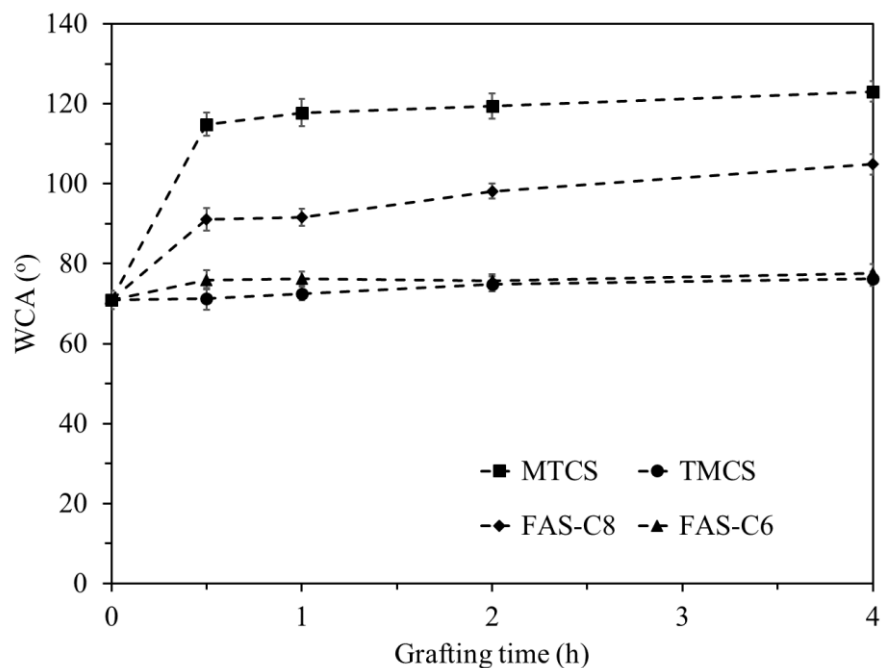


Figure 4.12 WCA of modified membranes after activated by 1 shot of O₂ plasma under 8 kV/0.25 mbar followed by grafting with 0.02M organosilane.

The organosilanes were reacted with -OH groups presented on membrane surface and in the moisture of the air by the active functional groups. MTCS and FAS-C8 have three functional sites available for bonding molecules with -OH groups on membrane surfaces, while TMCS has only one (Figure 3.1) [17]. Therefore, the WCA of membrane grafted by TMCS was lower than that of membrane grafted by MTCS and FAS-C8. In addition, the WCA of membrane grafted by TMCS and FAS-C6 was not changed much, revealing that the membrane grafting was not successful by these organosilanes.

Figure 4.14 shows the SEM results of membrane surface after modifying with different grafting conditions. After activated by O₂ plasma under 8 kV/0.25 mbar and plasma treatment time of 1 shot, the membrane surface was not significantly changed compared to original PVDF membrane, as presented in the Figure 4.14 (a-b). Besides, membrane surface had considerable changes after grafted by organosilanes. It could be observed that the surfaces of membrane grafted by TMCS, FAS-C6 and FAS-C8 for 2h did not change much (Figure 4.14 c-e), while MTCS formed the particles on

the membrane surface. The particles were also found on the modified membranes by MTCS as shown in Figure 4.14 f-h. The differences in the morphology changed of organosilanes were probably because of the intermolecular activity. It was reported that MTCS is much more reactive with itself, resulting in the observable spherical particles found on membrane surfaces [17].

The particles formed were due to the horizontal reaction between MTCS chemical and the -OH groups presented on membrane surface and vertical reaction between MTCS with the moisture of the air, then form the methylsilicon hydrophobic network on membrane surface [44] as illustrated by Figure 4.13.

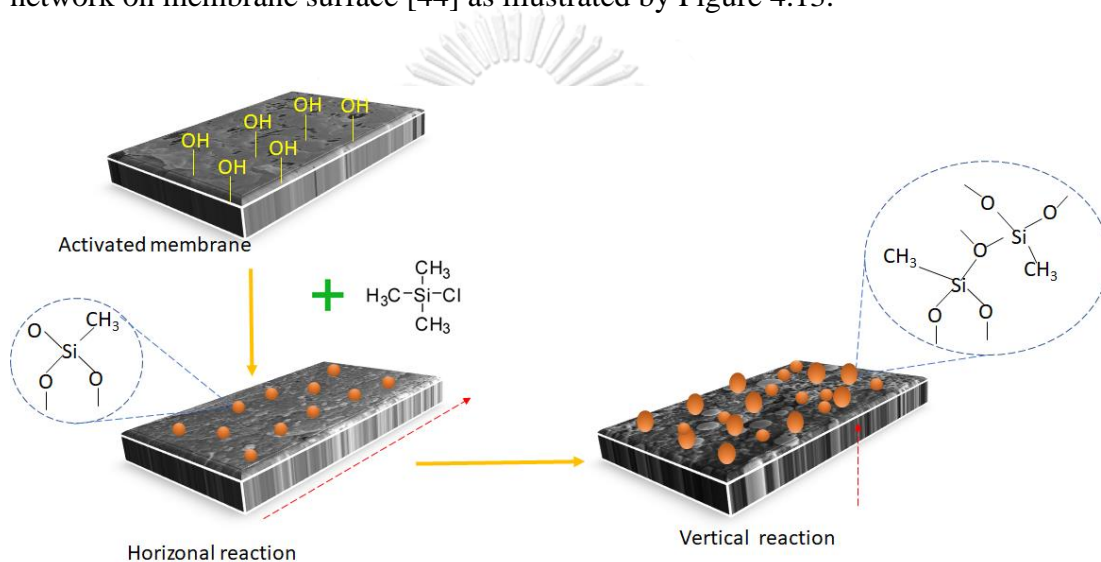


Figure 4.13 Reaction mechanisms between methyltrichlorosilane and the activated PVDF membrane surface

It could be easily observed that the numbers and sizes of particles were increased with the grafting time. This was due to the increase in vertical reaction of methylsilicon network on membrane surface over time [44].

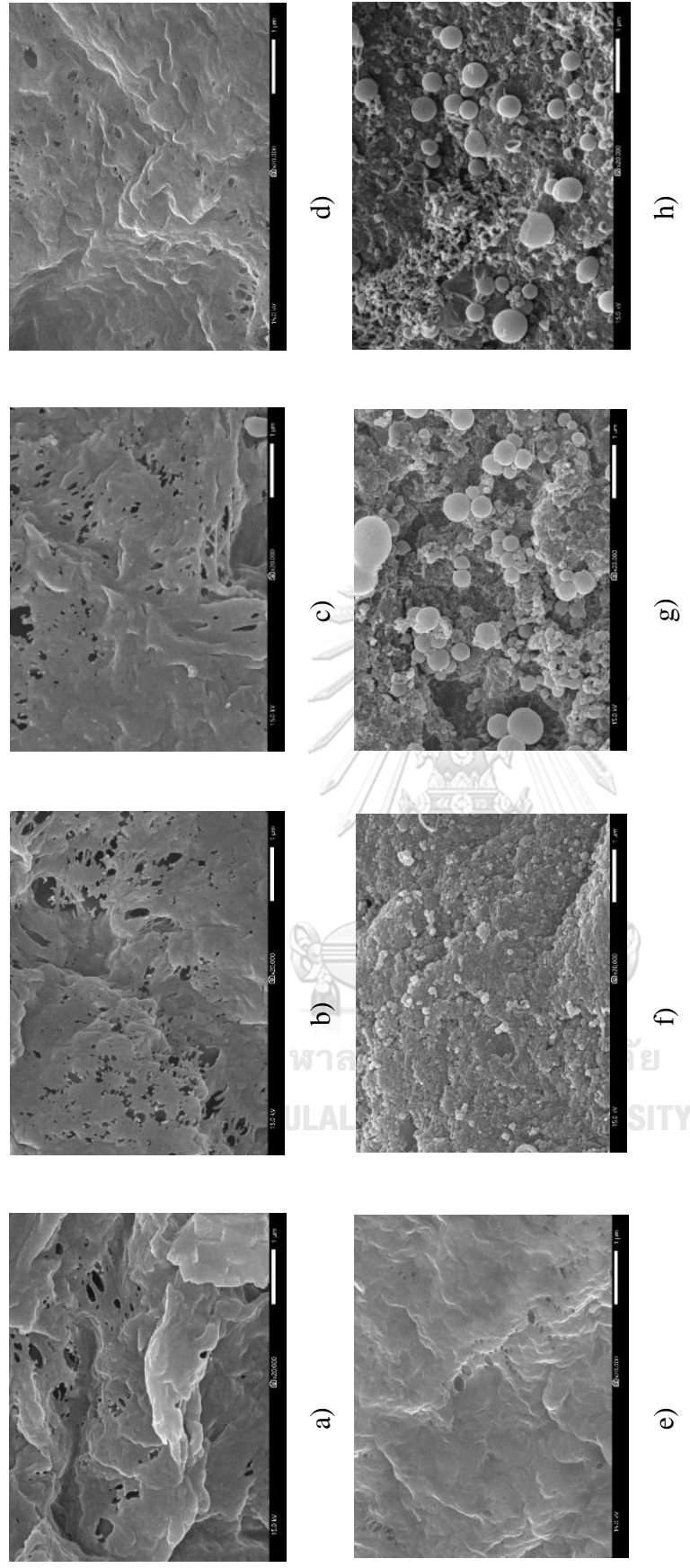


Figure 4.14 Outer surface of membranes grafted by different conditions activated by $O_2/8$ kV/0.25 mbar/1 shot: a) original membrane, b) activated membranes, c) 0.02M TMCS-2h, d) 0.02M FAS-C6- 2h, e) 0.02M FAS-C8- 2h, f) 0.02M MTCS -0.5h , g) 0.02M MTCS-2h, and h) 0.02M MTCS- 4h

Figure 4.15 presents the FTIR results of modified membrane grafted by different organosilanes. The results showed that the spectra of membrane grafted by FAS-C6 and TMCS was not changed compared to original membrane, while the peaks contributed to Si-O-Si appeared on membrane grafted by MTCS (783, 1034, 1141 cm^{-1}) and FAS-C8 (707 cm^{-1} and 660 cm^{-1}) [68]. It was implied that membrane was successfully grafted by MTCS and FAS-C8.

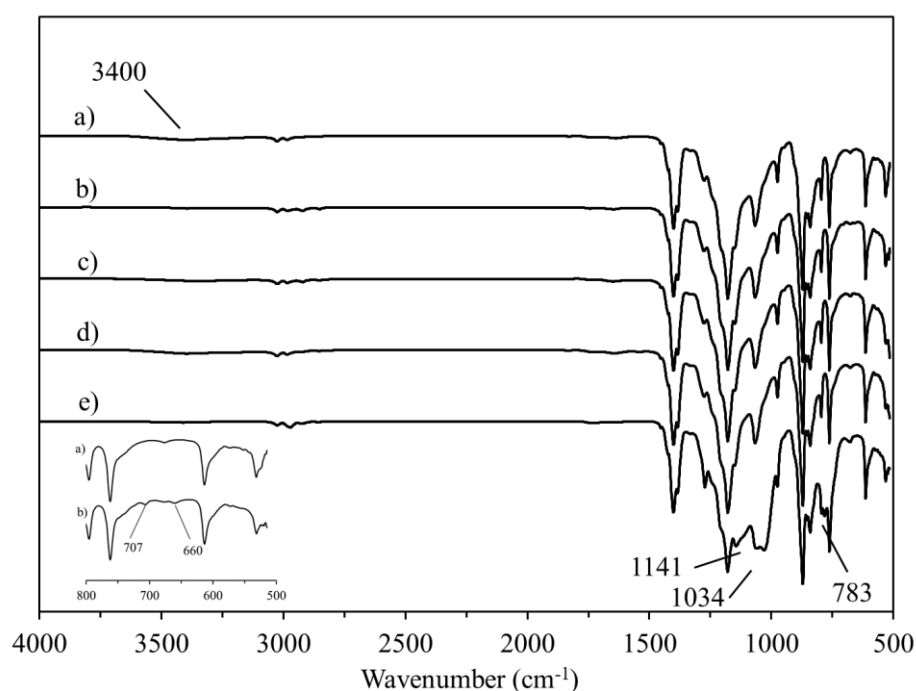


Figure 4.15 FTIR spectra of activated membrane under oxygen plasma activation at 8kV/0.25 mbar/1 shot followed by grafting with different organosilanes: a) original PVDF membrane, b) 0.02M FAS-C8-2h, c) 0.02M FAS-C6-2h, d) 0.02M TMCS, 2h, and e) 0.02M MTCS-2h.

Figure 4.16 illustrates the FTIR results of membrane grafted by different grafting time. The peak at wavenumber 3400 cm^{-1} was attributed to -OH groups, which was smaller when the grafting time increases due to the more completely react between -OH groups and organosilane. As aforementioned, the peaks at wavenumber 783 cm^{-1} , 1034 cm^{-1} , 1141 cm^{-1} were attributed to Si-O-Si network. These peaks were

found in the FTIR spectra of membrane grafted by MTCS for 0.5h and were deepened when the grafting time was increased with grafting time.

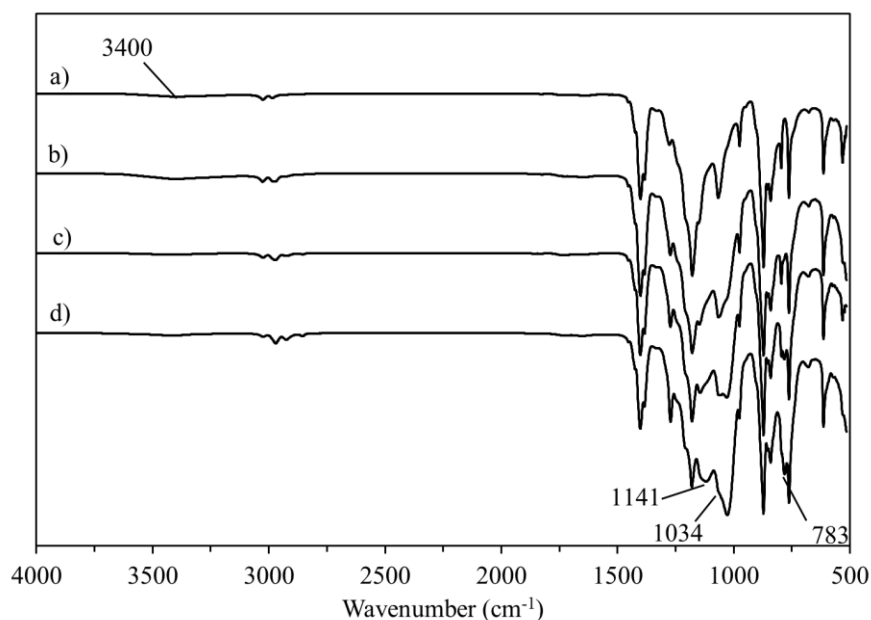


Figure 4.16 FTIR spectra of activated membrane under oxygen plasma activation at 8kV/0.25 mbar/1 shot followed by grafting with 0.02M MTCS at different grafting time a) activated membrane, b) 0.5h, c) 2h and d) 4h

The formation of the hydrophobic network was further confirmed by EDX characterization as shown in Table 4.3. For the original membrane surface, there was only the presence of C and F. After activated by O₂ plasma at the applied voltage of 8 kV, a small amount of O was added due to the introducing of -OH groups on membrane surface. After grafted by organosilanes, Si and O were presented on membrane grafted by MTCS and FAS-C8. The Si and O which found on the surface of membrane grafted by MTCS and FAS-C8 proved that methylsilicon network were successfully formed. In addition, the Si and O contents on membrane grafted by MTCS was higher than that of membrane grafted by FAS-C8. In contrast, there was no Si presence on membrane surfaces grafted by TMCS and FAS-C6.

Table 4.3 Changes of the chemical composition of membrane surface

Atomic concentration (%)	PVDF membranes					
	Original	Activated	Grafted by organosilanes			
			TMCS	MTCS	FAS-C6	FAS-C8
C	53.4	51.7	53.0	53.3	51.6	51.9
F	46.6	46.2	47.0	28.5	47.6	47.5
O	-	2.1	-	12.3	0.8	0.5
Si	-	-	-	5.9	-	0.1

Note: Modification condition: 1 shot of O₂ plasma gas at applied voltage of 8 kV followed by 2h grafting time.

According to the results, it could be concluded that PVDF membranes were successfully modified by O₂ plasma activation followed by grafted with organosilanes. The O₂ plasma treatment for 2 shots followed by grafting with 0.02M MTCS gave the highest results of WCA. For different organosilanes, the results found that MTCS and FAS-C8 were effective in membrane modification process. The optimized condition of plasma activation process (10 kV/0.30 mbar/2 shots) and the optimized condition of grafting process (0.02M) was taken to study further grafting time as illustrated in Figure 4.17. FAS-C8 and MTCS then were selected to modified membrane. For 0.5h of grafting time, the WCA of membrane grafted by MTCS and FAS-C8 were not significantly different, which were 103.8° and 102.6°, respectively. After grafted for 2h, WCA of membrane grafted by MTCS increased rapidly to 124.6° and then was constant, while that of membrane grafted by FAS-C8 was slightly increased to 105.7°. Then, WCA of membrane grafted by FAS-C8 increased from 106.9° to 112.4° when grafting time increased from 4h to 6h. This was because of the reactivity of silanol species in each organosilane as aforementioned.

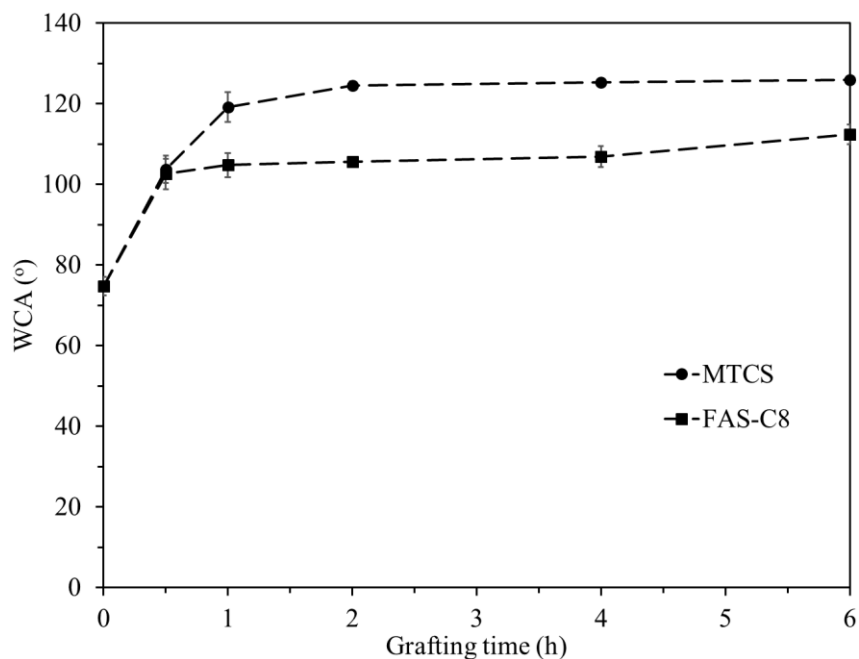


Figure 4.17 WCA of modified membranes after activated by 1 shot of O₂ plasma under 10 kV/ 0.30 mbar followed by grafting with 0.02M organosilane

The morphologies of membranes at different organosilane concentrations were shown in Figure 4.18. For the surface of membrane grafted by FAS-C8, the particles appeared on the membrane grafted for 6h (Figure 4.18c). In contrast, the particles were formed on the surface of membrane grafted by MTCS. The presence of spherical particles on the membrane surface was because the organosilanes react with itself as aforementioned. There was no difference on membrane grafted by MTCS for 4h and 6h (Figure 4.18 e and f).

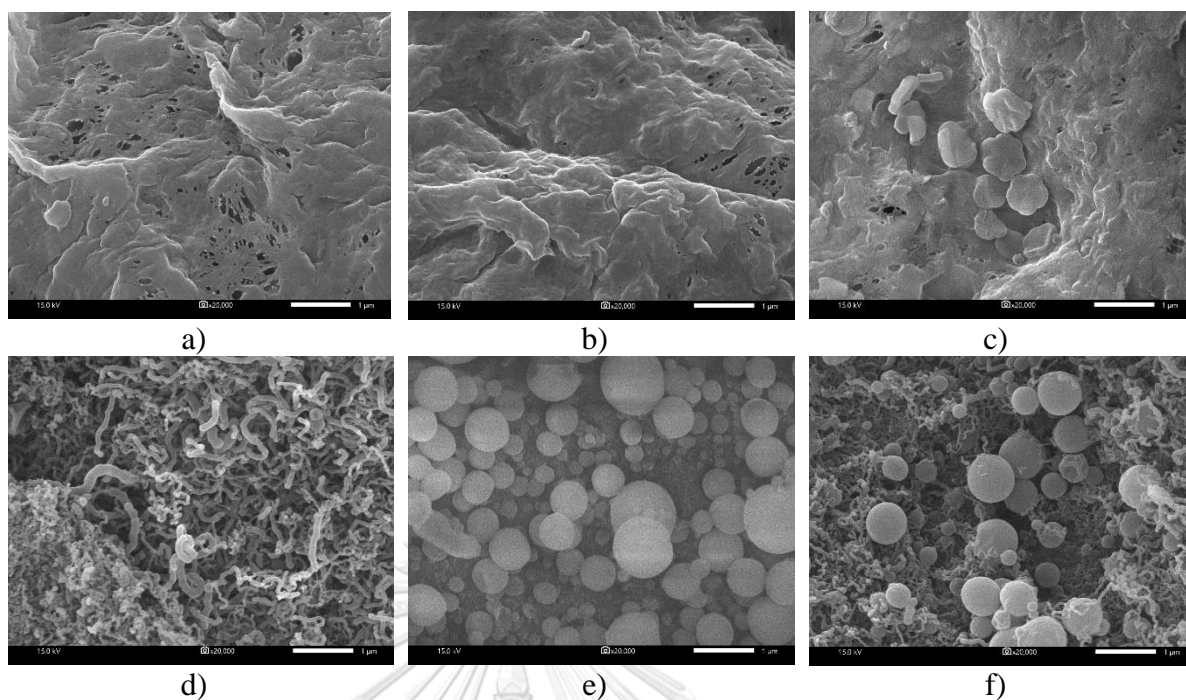


Figure 4.18 Outer surface of modified membrane grafted by different organosilanes and grafting time activated by $O_2/10$ kV/ 0.30 mbar/ 2 shots: a) FAS-C8-2h, b) FAS-C8-4h, c) FAS-C8-6h, d) MTCS-2h, e) MTCS-4h and f) MTCS-6h

The surface roughness of membranes was discussed in terms of the mean roughness (R_a) and the surface profile such as peak height (Z), peak diameter and distance between peaks. As shown in Table 4.4, the surface roughness decreased after hydrophilization. R_a value was decreased from 251.1 nm (original) to 118.0 and 87.2 nm of membrane grafted by MTCS and FAS-C8 for 6h, respectively. This observation agreed well with studies of Zheng *et al.* (2009) [16] and Sethunga *et al.* (2018) [61]. Sethunga *et al.* (2018) reported that after activated by NaOH followed by grafting with Fluorolink S10, the roughness of PVDF membrane was reduced from 0.52 nm to 0.026 nm [61]. AFM 3D images and cross-section profiles along the marked directions of the original PVDF membrane and modified membranes are shown in Figure 4.19. It could be seen that original membrane surface was formed by smooth surface and many regular microreliefs while there are nanoparticles and high peak layers covered on modified membranes. The profile of peaks showed that the distance between peaks of original membrane was $6.93 \mu\text{m}$ while that of membrane treated by MTCS and FAS-C8 for 4h was much lower at $0.82 \mu\text{m}$ and $2.97 \mu\text{m}$, respectively.

After grafted for 6h, that distance between peaks of membranes grafted by MTCS and FAS-C8 were reduced to 0.77 μm and 1.73 μm , respectively. The height of peaks of original membrane was 899 nm, while that of membranes grafted by MTCS for 6h was 384 nm compared to 55.8 nm of membrane grafted by FAS-C8. Zheng *et al.* (2009) indicated that original membranes with the high distinction between peaks and high height between valley and peak were easier to be wet [16]. Yusefi *et al.* (2016) found that the differences in R_a of the original membrane and grafted membrane were because the roughness depends on Z value, which corresponding to the distance between valley and nodules [69]. Since organosilanes created hydrophobic layers on membrane surfaces by the interaction between vertical and horizontal polymerization of silanol, Z value of modified membranes was smaller, thus, R_a was lower [70]. As can be seen in Figure 4.19, membrane pores were filled by hydrophobic layers, reducing the deep of valleys. It was implied that hydrophobic layers were formed on membrane, resulting in the reduction of roughness. The surface roughness was decreased by treatment time for both membranes grafted by MTCS and FAS-C8, as a result of the formation of hydrophobic layers on membrane surface.

In case of modified membrane, the surface roughness of modified membrane grafted by MTCS were higher than that of membrane grafted by FAS-C8, leading to increase WCA. Kujawa and Wojciech (2016) indicated that fluorinated compounds such as FAS-C8 create monolayer on the membrane, while nonfluorinated molecules such as MTCS formed disordered and multilayer structure [66]. This is the reason for the higher in R_a of membrane grafted by MTCS compared to membrane grafted by FAS-C8. In addition, MTCS is much more reactive with itself, resulting in taking place bulk vertical polymerization which causes higher surface roughness and higher WCA [16]. With denser and shaper nanoscale peaks on membrane surface, the roughness of membrane grafted by MTCS was higher, related to higher membrane hydrophobicity [16]. Furthermore, it could be seen that the cross-section profile of peaks on membrane grafted by MTCS for 4h and 6h was not changed much, while that of membrane grafted by FAS-C8 showed a significant change.

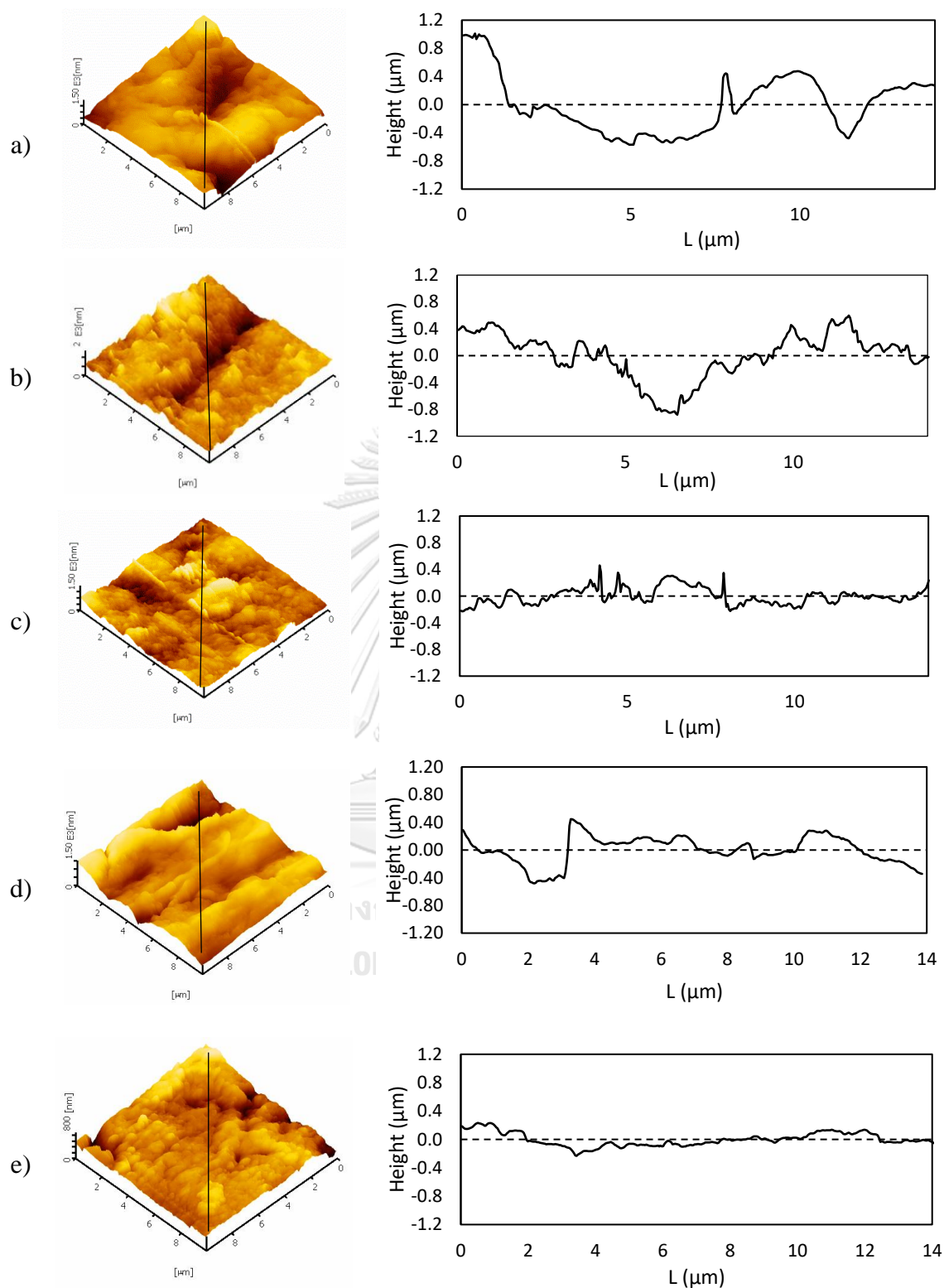


Figure 4.19 AFM 3D images and cross-section profiles along the marked directions of a) original PVDF membrane and modified membranes: b) MTCS-4h, c) MTCS-6h, d) FAS-C8-4h and e) FAS-C8-6h

Table 4.4 Surface roughness parameters of original and modified membranes

Parameters	WCA (°)	R _a (nm)	Diameter of peak (μm)	Distance between peaks (μm)	Peak height (nm)
Original	74.7	271.1	6.37	6.93	899
MTCS-4h	125.3	242.0	0.77	0.82	284
MTCS-6h	126.0	118.0	0.68	0.77	247
FAS-C8-4h	106.9	110.7	1.27	2.97	168
FAS-C8-6h	112.4	87.2	0.84	1.23	56

According to the WCA, SEM and surface roughness results, two modification conditions were selected as the optimized conditions which were membrane grafted by 0.02M MTCS for 4h (PVDF-MTCS) and membrane grafted by 0.02M FAS-C8 for 6h (PVDF-FAS-C8) at activation conditions of O₂ plasma at 10 kV/0.30 mbar/2 shots. Besides, the particles were found in the cross-section of PVDF-MTCS membrane (Figure 4.20 c)

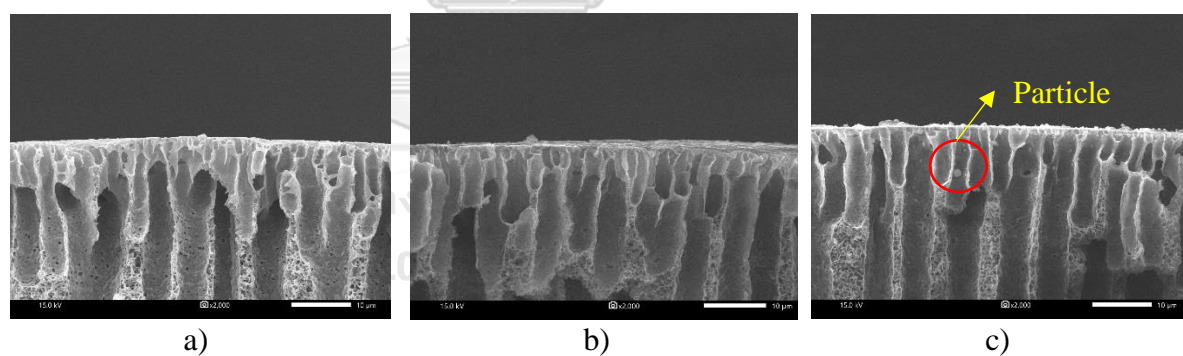


Figure 4.20 Cross section of modified membrane grafted by different organosilanes and grafting time activated by O₂/10 kV/0.30 mbar/2 shots: a) original membrane, b) FAS-C8-6h, c) MTCS-4h

The chemical composition results of optimized modification condition are shown in Table 4.5. It could be seen that after treated by O₂ plasma under 10 kV/0.30 mbar/2 shots, the F content of membrane dropped from 46.6% to 37.5%, which was the result of defluorination process. After grafted by organosilanes, the F content on

surface of PVDF-MTCS membrane was decreased to 28.1%, while that number of PVDF-FAS-C8 increased to 41%. This could be explained by the different in chemical structure of each organosilane (Figure 3.2). The formation of membrane surface after grafting by MTCS was Si-O-Si structure link with -CH₃ functional group, while that of membrane grafted by FAS-C8 was the linkage between Si-O-Si and the F long chain as presented in Figure 4.21 [44, 71].

Table 4.5 Chemical composition of membranes under optimized modification condition

Elements	Original PVDF membrane	Activated membrane	PVDF-MTCS	PVDF-FAS-C8
C	53.4	62.2	43.9	58.1
F	46.6	37.5	28.1	41.0
O	-	0.3	22.1	0.8
Si	-	-	5.9	0.1

Note: activated by O₂ plasma gas at 10 kV/0.3 mbar/2 shots

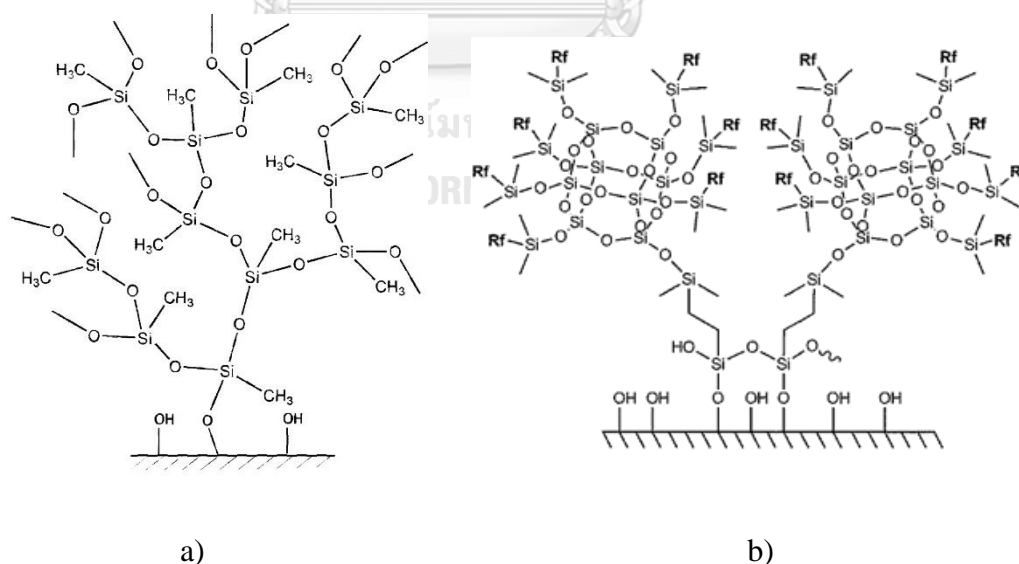


Figure 4.21 Membrane grafted by organosilanes (a) MTCS and (b) FAS-C8

The membrane porosity of original PVDF membrane and modified membranes were also measured. After modification, the porosity of membrane reduced from 83.5% (original membrane) to 66.1% and 78.9% of PVDF-MTCS and PVDF-FAS-C8, respectively. This was probably because membrane pores were blocked by organosilane layers as shown in Figure 4.19. This result was similar to the study of Sethunga *et al.* (2018) that after modified by NaOH followed by grafted with Fluorolink S10, the membrane porosity was decreased from 82% to 79% when the WCA increased from 84.5° to 111.7° [61]. Marek (2007) indicated that with the higher membrane porosity, the membrane wettability was higher [72]. It was implied that PVDF-MTCS gave the higher hydrophobicity compared to PVDF-FAS-C8 and original PVDF membranes.

4.3 Long term ozone flux of original membrane and modified membranes

The long-term ozone fluxes of original PVDF membrane and PVDF-MTCS and PVDF-FAS-C8 using DB 71 as liquid phase were studied. The results found that the ozone flux of the original PVDF membrane was reduced from $3.35 \times 10^{-3} \text{ g/m}^2\text{s}$ to $2.03 \times 10^{-3} \text{ g/m}^2\text{s}$, by 39% after 20h. Meanwhile, the ozone fluxes of PVDF-MTCS and PVDF-FAS-C8 were kept constant at the first 8h, which were $4.55 \times 10^{-3} \text{ g/m}^2\text{s}$ and $4.67 \times 10^{-3} \text{ g/m}^2\text{s}$, respectively, as shown in Figure 4.22. Then, the ozone fluxes of modified membranes were slightly reduced to $3.69 \times 10^{-3} \text{ g/m}^2\text{s}$, by 19% and $4.08 \times 10^{-3} \text{ g/m}^2\text{s}$, by 12 % for PVDF-MTCS and PVDF-FAS-C8, respectively. After 14h, the ozone fluxes of PVDF-MTCS and PVDF-FAS-C8 was kept constant. The reducing of ozone flux of original membrane was probably because membrane pores were fulfilled with water after long operating time increasing the membrane resistance. Furthermore, the reducing of ozone flux was possibly due to the increase of overall mass-transfer resistance and the changes in membrane characterization because of ozone attack [6]. The higher ozone flux of modified membranes was due to the higher hydrophobicity. In which, the WCA of original membrane was 74.7°, while that of PVDF-FAS-C8 and PVDF-MTCS membranes were 112.4° and 125.3°, respectively. As aforementioned, the membrane wettability is higher with the higher membrane porosity [72]. In this work, since membrane porosity of the original PVDF membrane was highest, the ozone flux of the original PVDF membrane was reduced rapidly by

time. In the contrary, PVDF-FAS-C8 membrane gave the highest ozone flux during the operation time although the WCA of PVDF-FAS-C8 was lower than that of PVDF-MTCS. It was implied that the stability of ozone flux was not only influenced by the hydrophobicity of membrane but also depends on the ozone resistance of the material, which can be explained by the bonding dissociation energies (BDE) of functional groups. The F long chain on PVDF-FAS-C8 has the BDE of 133.3 kcal/mol, while that of CH₃-Si is 74 kcal/mol [73]. The higher in BDE of the C-F chain makes FAS-C8 resisted the ozone attraction, while MTCS might be destroyed by ozone. Therefore, PVDF-FAS-C8 showed the higher resistance to ozone compared to PVDF-MTCS. Santos *et al.* (2015) found that PTFE membrane(-(CF₂-CF₂)-) showed the strong resistance to ozone, while structural change was observed on polydimethylsiloxane (PDMS) membrane(-(CH₃-Si-CH₃)-) [13]. Furthermore, this experiment proved the success in the membrane modification process and confirmed the theory that pores of the low hydrophobic membrane would be fulfilled by water after long operating time, reducing ozone flux.

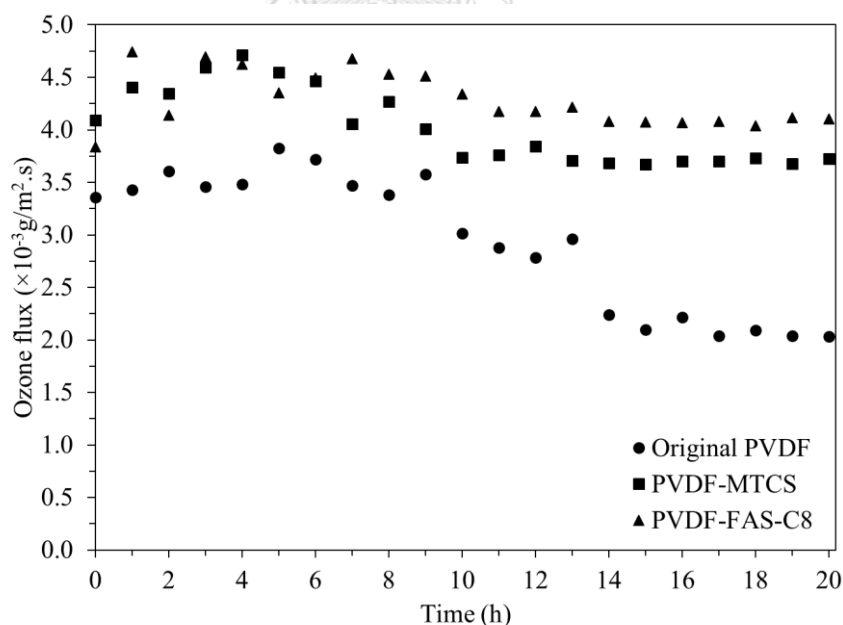


Figure 4.22 Long term ozone flux of original membrane and modified membranes using 100 mg/l DB 71 (liquid velocity: 0.46 m/s, gas velocity: 2 m/s, and ozone concentration: 40 mg/l)

4.4 Dye wastewater treatment by ozonation membrane contactor

4.4.1 Comparison of decolorization performance of modified and original membranes

The decolorization performances of DB 71 and RR 239 by ozonation membrane contactors were investigated by using different membranes, including the original PVDF, PVDF-MTCS, and PVDF-FAS-C8 membranes, as shown in Figure 4.23. The results showed that after 90 mins of ozonation time, the decolorization efficiency of DB 71 by the original membrane reached 93.0%, while that of PVDF-MTCS and PVDF-FAS-C8 were 96.6%, and 97.7%, respectively. Meanwhile, the decolorization performance of RR 239 by original PVDF, PVDF-MTCS, and PVDF-FAS-C8 membranes was 94.4%, 97.1%, and 97.6%, respectively. The decolorization efficiencies of DB 71 and RR 239 by different membranes were not significantly different. In contrast, the differences in COD removals were noticeable. After 90 mins of ozonation time, the COD removals of DB 71 using original PVDF, PVDF-MTCS and PVDF-FAS-C8 membranes were 48%, 53%, and 62.5%, respectively. Similarly, the differences in COD removal of RR 239 was shown in Figure 4.22c. The COD removal performance by PVDF-FAS-C8 gave the highest efficiency in all the treatment period. At the end of the process, the COD removal of RR 239 reached the efficiency of 32%, 59.6%, and 67.6% by the original PVDF, PVDF-MTCS, and PVDF-FAS-C8 membranes, respectively. It was clear that modified membranes gave higher decolorization performance compared to original membrane. Besides, PVDF-FAS-C8 showed the highest decolorization performances compared to other membranes. This result could be explained by the ozone consumption of each membrane as shown in Figure 4.23 (b, d). It could be seen that ozone gas in modified membranes was consumed more than original PVDF membrane almost all the time. This was possibly due to the wetting of original PVDF membrane which could reduce the mass-transfer efficiency [11]. The hydrophobicity of membrane was enhanced after modification, hence, the wetting problem could be prevented. Thereby, ozone gas, which oxidized the dye molecule by strong breaking down power, was easier to pass through the membrane pores of modified membrane into the liquid phase. This

was implied that the ozone mass-transfer was increased after membrane modification, resulting in increasing DB 71 decolorization. The results were similar to those long-term ozone fluxes as aforementioned.

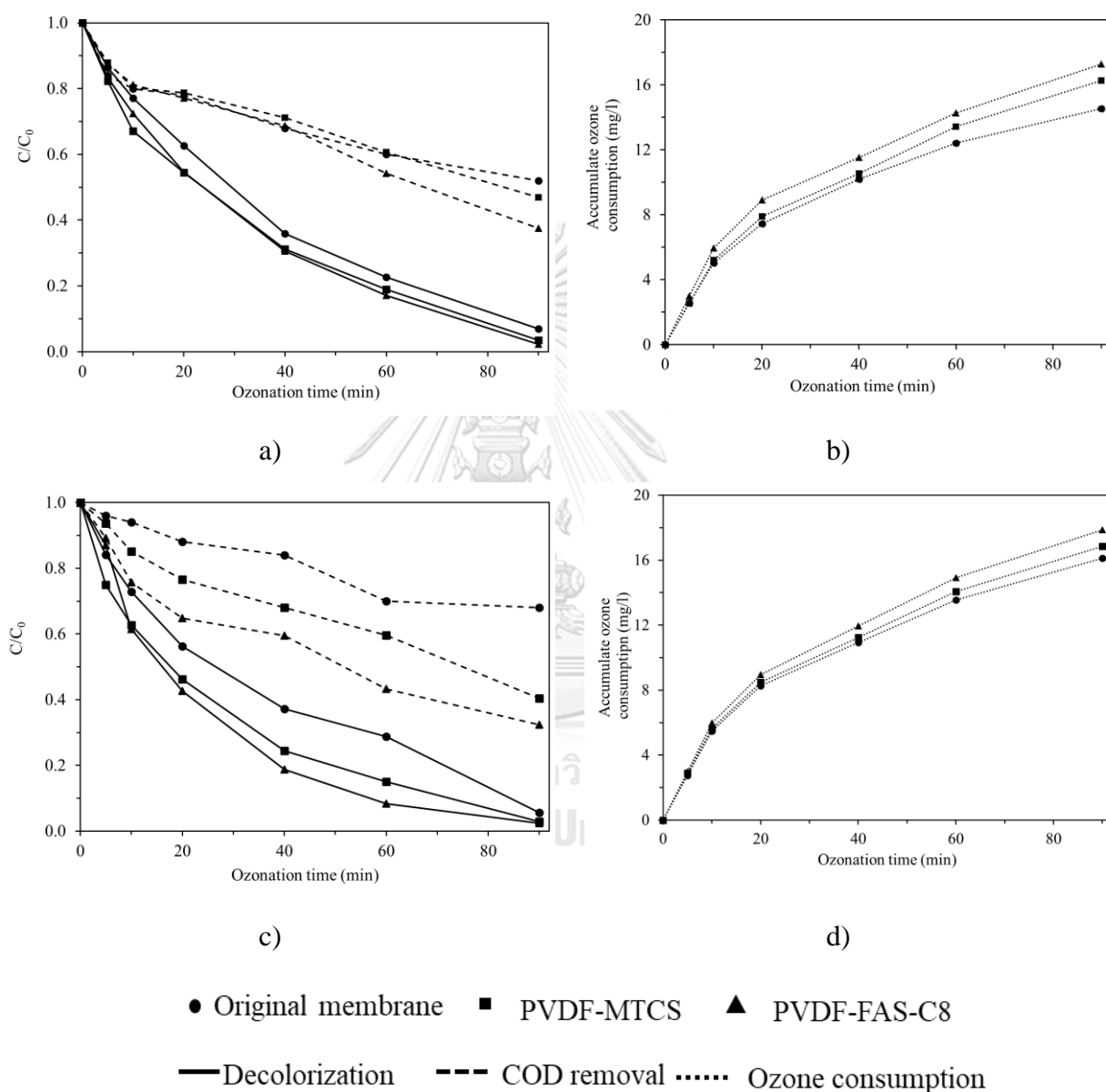


Figure 4.23 Dye wastewater treatment by membrane contacting process with ozone: a) DB 71 removal, b) ozone consumption of DB 71, c) RR 239 removal, and d) ozone consumption of RR 239, (liquid velocity: 0.46 m/s, ozone concentration: 40 mg/l)

The apparent rate constant is shown in Table 4.8. It could be seen that the decolorization rate of modified membranes was higher than that of original membrane. The apparent constant rate was 0.029 min^{-1} , 0.035 min^{-1} , and 0.039 min^{-1} for DB 71 using original PVDF membrane, PVDF-MTCS, and PVDF-FAS-C8 membranes, respectively. Similarly, the order of apparent constant rate of RR 239 by ozonation membrane contactor were 0.028 min^{-1} , 0.037 min^{-1} and 0.042 min^{-1} by original PVDF, PVDF-MTCS, and PVDF-FAS-C8 membranes, respectively. This result was because of the higher ozone flux results in a higher reaction rate between ozone and dye. This experiment proved that the success of membrane modification process results in enhancing decolorization and COD removal performances.

4.4.2 Effect of ozone concentrations

The effect of ozone concentration on DB 71 removal was investigated using original PVDF, PVDF-MTCS and PVDF-FAS-C8 membranes as shown in Figure 4.24. After 90 min of ozonation time, the DB 71 removal of the PVDF-MTCS membrane reached the efficiency from 87.7% to 98% when the ozone concentration increased from 30 mg/l to 50 mg/l. Similarly, when the ozone concentration increased from 30 mg/l to 50 mg/l, the DB 71 decolorizations were also increased from 84.8% to 98.7% and from 84.8% to 98% by PVDF-FAS-C8 and original PVDF membranes, respectively.

COD removal of DB 71 by original PVDF membrane was increased from 40.9% to 48% when the ozone concentration increased from 30 mg/l to 40 mg/l. Whereas, COD removal of DB 71 by PVDF-MTCS and PVDF-FAS-C8 membranes were improved when the ozone concentration increased from 30 mg/l to 40 mg/l, from 47.9% to 53% and from 48% to 62.5%, respectively. For the ozone concentration of 50 mg/l, the COD removal efficiency of DB 71 by ozonation membrane contactor using original PVDF, PVDF-MTCS, and PVDF-FAS-C8 membranes were 58%, 62.5%, and 67.7%, respectively.

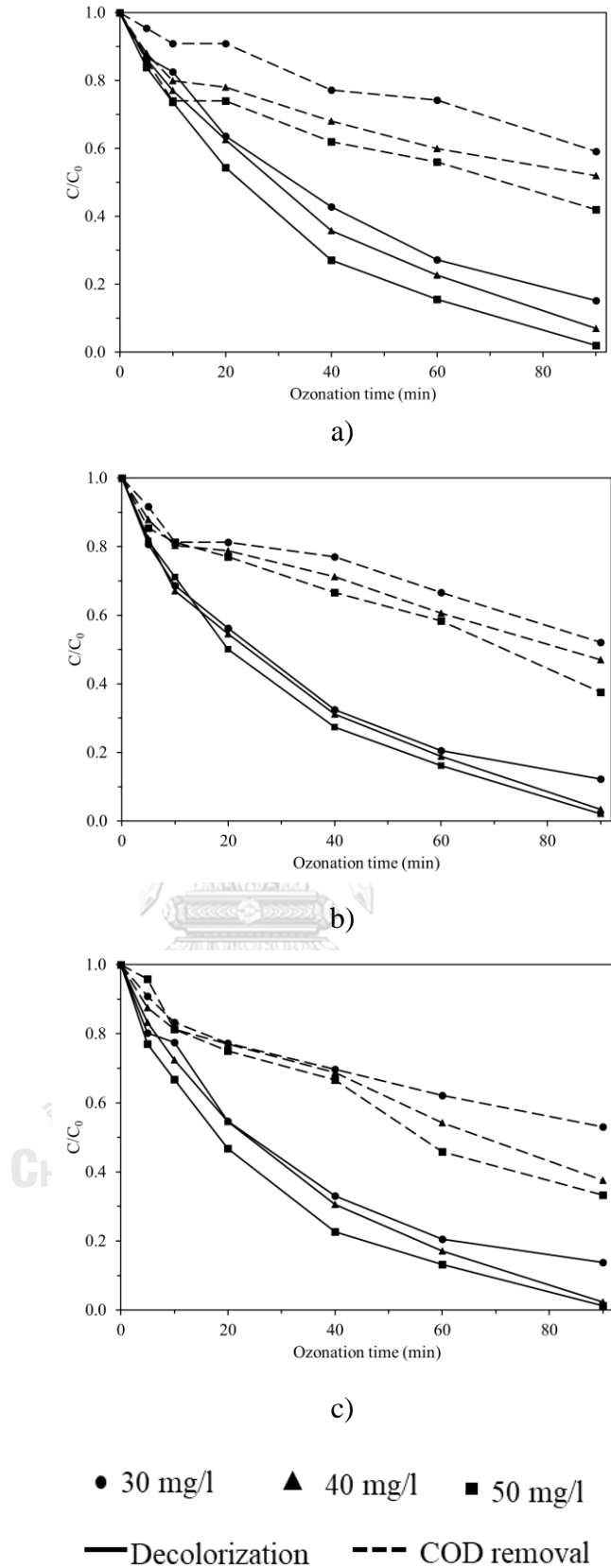


Figure 4.24 Effect of ozone concentration on DB 71 decolorization by ozonation membrane contactor of a) original PVDF, b) PVDF-MTCS, c) PVDF-FAS-C8 membranes (liquid velocity: 0.46m/s, dye concentration: 100 mg/l)

The differences on dye removal are presented by apparent rate constant (k_{app}) as shown in Table 4.6. The k_{app} increased with the increase in ozone concentration. For example, an increasing ozone concentration from 30 mg/l to 50 mg/l for PVDF-FAS-C8 membrane in membrane contactor, k_{app} increased from 0.023 min^{-1} to 0.045 min^{-1} . This result is consistent with the mass- transfer theory [74]. When the ozone concentration increased in the gas phase, the driving force for the mass transfer of ozone to the liquid phase increased, enhancing the ozone concentration in dye solution and the rate of dye degradation.

Table 4.6 Decolorization rate of DB 71 at different ozonation concentration by using different membranes

Membranes	Original PVDF			PVDF-MTCS			PVDF-FAS-C8		
Ozone concentration (mg/l)	30	40	50	30	40	50	30	40	50
k_{app} (min^{-1})	0.021	0.029	0.041	0.023	0.035	0.041	0.023	0.039	0.045
R^2	0.999	0.988	0.964	0.990	0.967	0.960	0.991	0.960	0.960
Decolorization (%)	84.8	93.0	98.0	87.7	96.6	97.9	86.3	97.7	98.7
COD removal (%)	40.9	48.0	58.0	47.9	53.0	62.5	48.0	62.5	66.7

4.4.3 Effect of dye concentration

Due to the high ozone flux and decolorization performance, PVDF-FAS-C8 membrane was then selected to study the effect of dye concentration on ozonation membrane contacting process. The decolorizations of DB 71 and RR 239 by membrane contactor using PVDF-FAS-C8 membrane at different dye concentrations were shown in Figure 4.25. At the dye concentration of 50 mg/l, DB 71 and RR 239 were completely decolorized after 40 mins of treatment time. When the dye concentration increased to 100 mg/l, the DB 71 decolonization efficiency was as high as RR 239 (97.2%-97.8%) after 90 mins of treatment time. Meanwhile, at the dye concentration of 200 mg/l, the dye removal efficiency was much lower, which were

87.3% and 91.2% for DB 71 and RR 239, respectively. In addition, the ozone consumption was increased with the increase in dye concentration (Figure 4.25b). For example, the accumulate ozone consumption of DB 71 increased from 15.77 mg/l to 24.42 mg/l as an increasing the dye concentration from 50 mg/l to 200 mg/l. This was similar to the study of Gao *et al.* (2012) that the ozone utilization efficiency increased from 42% to 86% when the dye concentration increased from 50 mg/l to 800 mg/l. Since the ozone concentration was the same for all dye concentration conditions, the higher initial dye concentration results in the lower decolorization efficiency. Besides, the increase in dye concentration causes an increase in the oxidation by-product, which competitive with dyes for ozone, leading to reducing color removal performance and raising ozone utilization efficiency [51].

Similar to the decolorization performance, the COD removals of DB 71 and RR 239 were decreased with the increasing of dye concentration. For dye concentration of 200 mg/l, after 90 mins, the COD removal efficiencies of DB 71 and RR 239 were the same, at 28%. Because the ozone concentration remained unchanged with varying dye concentrations, the lower initial dye concentration could be completely degraded, resulting in higher COD removal performance. In contrast, the large number of by-products generated from high initial dye concentration caused low COD removal [51]. This was implied that for the dye concentration <100 mg/l, the treated dye wastewater could be discharged into environment. However, the reaction time is required for the condition of 200 mg/l dye solution.

An increase in initial dye concentration from 50 mg/l to 200 mg/l, the apparent rate constant of RR 239 decolorization declined from 0.055 min^{-1} to 0.025 min^{-1} as shown in Table 4.8. This was because dye ozonation is a pseudo-first-order kinetics reaction for both ozone and dye concentration [2, 74], therefore, the apparent rate constant decreased with the increase of dye concentration. This result was similar to dye ozonation performance reported by Turhan *et al.* (2013) [74].

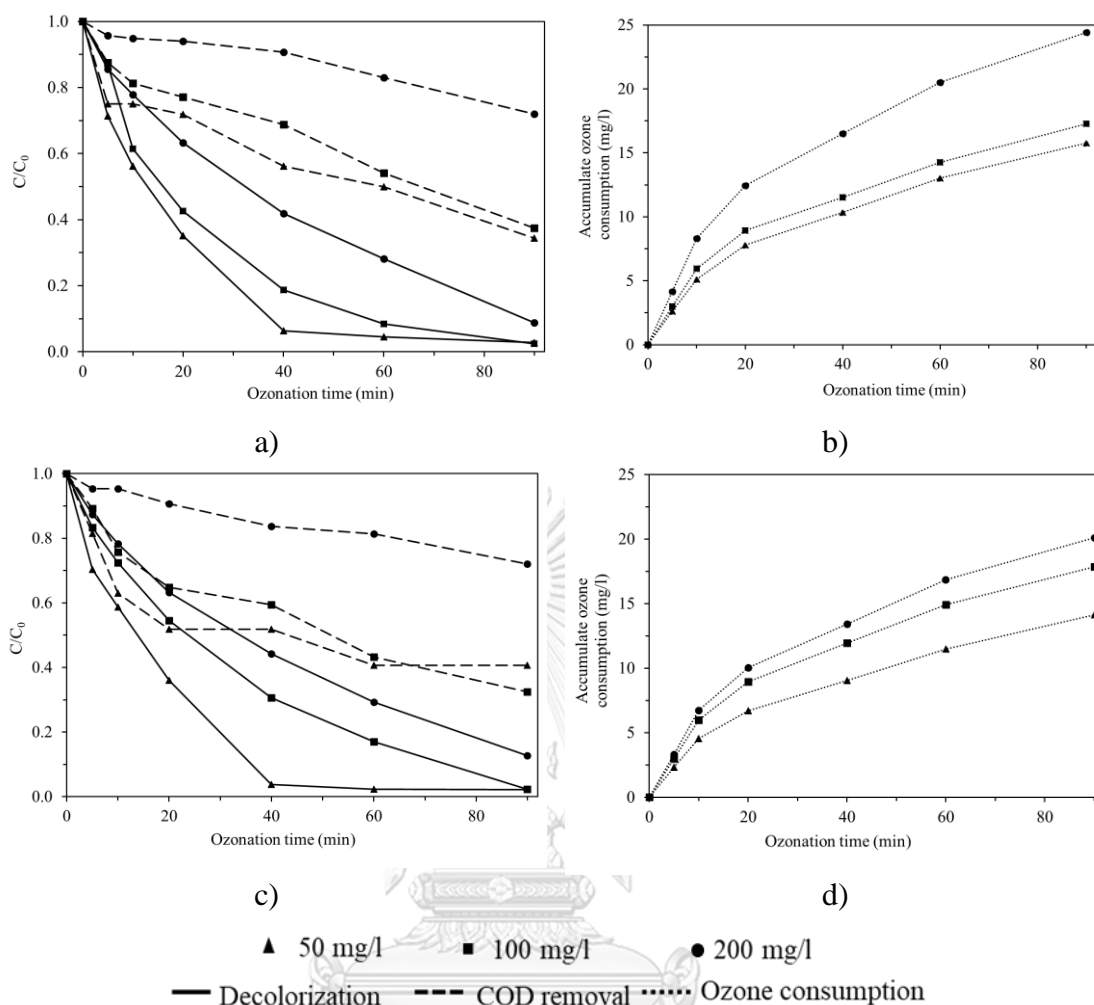


Figure 4.25 Effect of dye concentrations on dye decolorization: a) DB 71 removal, b) ozone consumption of DB 71, c) RR 239 removal, and d) ozone consumption of RR 239, (liquid velocity: 0.46 m/s, ozone concentration: 40 mg/l)

4.4.4 Effect of different dyes

PVDF-FAS-C8 membrane was selected to investigate the effect of dye solution types on decolorization performance of ozonation membrane contacting process. The results showed that the decolorization of RR 239 is faster than that of DB 71. For instance, for ozone concentration of 40 mg/l, the decolorization performance of RR 239 was 81.3% while that of DB 71 was only 69.4% after 40 mins of ozonation time. This could be explained by the reaction mechanism of ozone with the organic compound. Ozone reacts with organic compounds by direct oxidation with

ozone molecule (O_3) under low pH and by indirect oxidation with hydroxyl radical ($\bullet OH$) under high pH [49]. The pH of RR 239 and DB 71 were 5.25 and 5.61, respectively, the direct ozonation was dominated. Ozone molecules are selective and prefer to attack the unsaturated bonds of azo chromophores [6, 27], thus, the dye removal by the reaction of ozone molecules is fast. RR 239 has an azo-linked aromatic ring, while that of DB 71 is three azo bonding. Therefore, the breaking down of double bonding of RR 239 by direct ozone oxidation was faster. After 90 mins of ozonation time, pH of solution was reduced from 5.61 to 3.94 and from 5.15 to 3.98 for DB 71 and RR 239, respectively as shown in Figure 4.26b. Gunes *et al.* (2012) stated that the initial pH of dye effluent was 5.45, and after 90 minutes of ozonation it decreased to a 2.75 which was due to the formation of by-product and the production of organic and inorganic acid anions during the ozonation process [27]. On the other hand, Atchariyawut *et al.* (2009) also found that pH of Reactive Red 120 decreased from 7.44 to 3.18 during 30 min operation time by ozonation membrane contactor [8].

As can be seen in Figure 4.25, the ozone consumption by DB 71 was higher than that of RR 239. This is because the pH value of DB 71 was higher than that of RR 239. At higher pH, the indirect reaction involves radical can be occurred as followed Equation (14) [75]:



For DB 71 solution, which has a higher pH value, there is more OH^- which decay ozone into radical forms, resulting in higher gradient concentration between the gas phase and liquid phase [6]. Therefore, more ozone can be dissolved in the liquid phase resulting in a higher amount of ozone consumption.

The COD removal performance of RR 239 was also higher than that of DB 71, as shown in Figure 4.25a. After 90 mins, the COD removals of DB 71 and RR 239 by PVDF-FAS-C8 membrane was 62.5% and 67.5%, respectively.

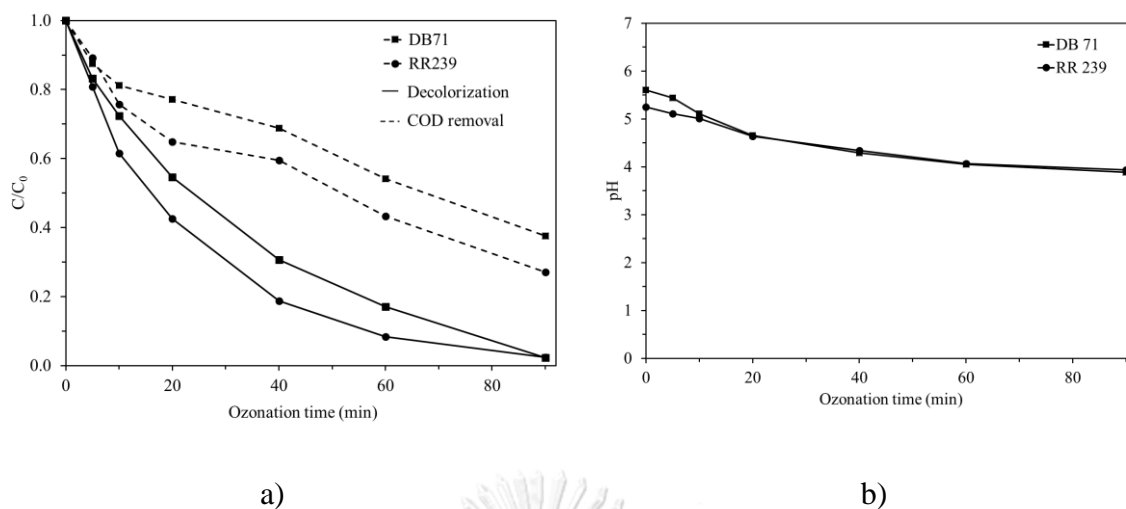


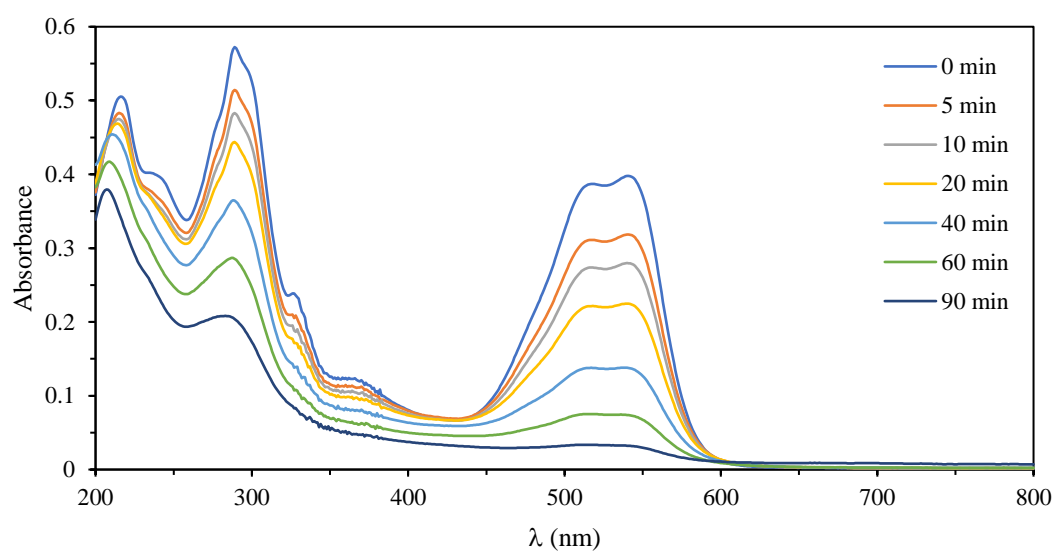
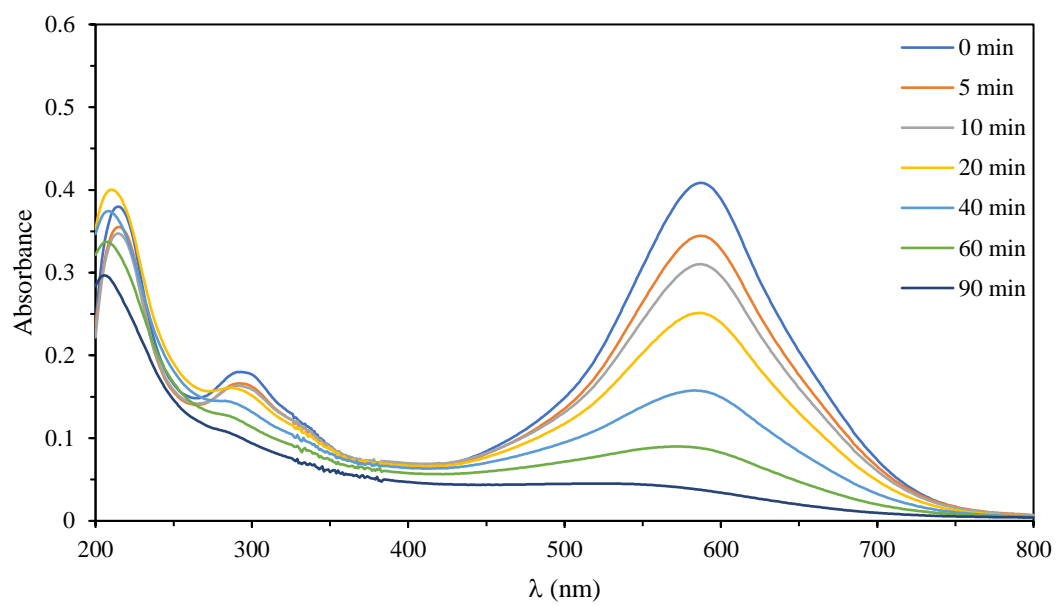
Figure 4.26 Effect of different dyes on dye decolorization by ozonation membrane contactor: a) COD removal and decolorization and b) pH changes of RR 239 and DB 71 using PVDF-FAS-C8 membrane contactor (dye concentration: 100 mg/l, ozone concentration: 40 mg/l, liquid velocity: 0.46 m/s)

Typical scanning-kinetic outputs obtained of DB 71 and RR 239 during the membrane ozonation membrane contactor process using PVDF-FAS-C8 membranes are shown in Figure 4.27. In this experiment, the process was operated under ozone concentration of 40 mg/l, liquid velocity of 0.46 m/s, and dye concentration of 100 mg/l. The maximum absorption wavelengths of DB 71 and RR 239 are at 594 and 542 nm, respectively, in the visible region. These absorption bands are corresponding to the chromophore containing azo linkage ($-N=N-$) in the azo dyes [3, 76]. The absorption peaks belong to benzene and naphthalene rings in the DB 71 are observed at 209 and 290 nm in the ultraviolet region. Besides, the peaks 328, 290 and 215 nm observed in the ultraviolet region of RR 239 can be assigned to the aromatic rings present in dye structure [77].

It could be seen that the diminution in the peak at 594 of DB 71 displays rapidly and was nearly disappeared at the end of 90 mins. This demonstrated that the decolorization of DB 71 occurred quickly because of the destruction of the $-N=N-$ bound in structure by ozone oxidation. Besides, as shown in the ultraviolet region, the peak at 290 nm exhibited a moderate decline. Moreover, the destruction of the peak at 290 nm was slow at the first 20 mins and be faster after that, while the diminish of

the peak at 594 nm was fast during the ozonation time. This was indicated that the ozone molecules firstly attack at the azo groups of DB 71. Besides, the intensity of absorption at peak 209 nm, which is attributed to benzene ring, was increased after 20 mins of ozonation time and then decreased. It was might because of the oxidative attacks the naphthalene during the ozonation process, forming benzene derivatives and naphthoquinones [78]. The similar results were reported by Stambolova *et al.* (2012) [78].

In the case of RR 239, the intensity of the absorbance peak at 542 nm was decreased sharply with the increasing time. Whereas, in the ultraviolet region, the destruction of the aromatic rings was lower. It was implied that the -N=N- structure was more destroyed than the aromatic ring. This can be explained by the RR 239 degradation mechanism by ozone conducted by Dias *et al.* (2019) as demonstrated in Figure 4.28 [3]. It indicated that ozone cleaved azo bonds (-N=N-) generated the naphthalene compounds which was degraded to phthalic acid comprised of a six-carbon benzene ring with two carboxylic acid groups (-COOH) attached. Whereas, the oxidized carbon-nitrogen bond (-C-N-) led to triazine and aromatic sulfonated compounds. At the end of the process, dye molecular was degraded to CO₂ and H₂O results in the destruction of peaks in the ultraviolet region [3].



b)

Figure 4.27 Spectral changes in the UV-vis absorption spectra of dyes during membrane ozonation process using PVDF-FAS-C8 membrane: a) DB 71 and b) RR

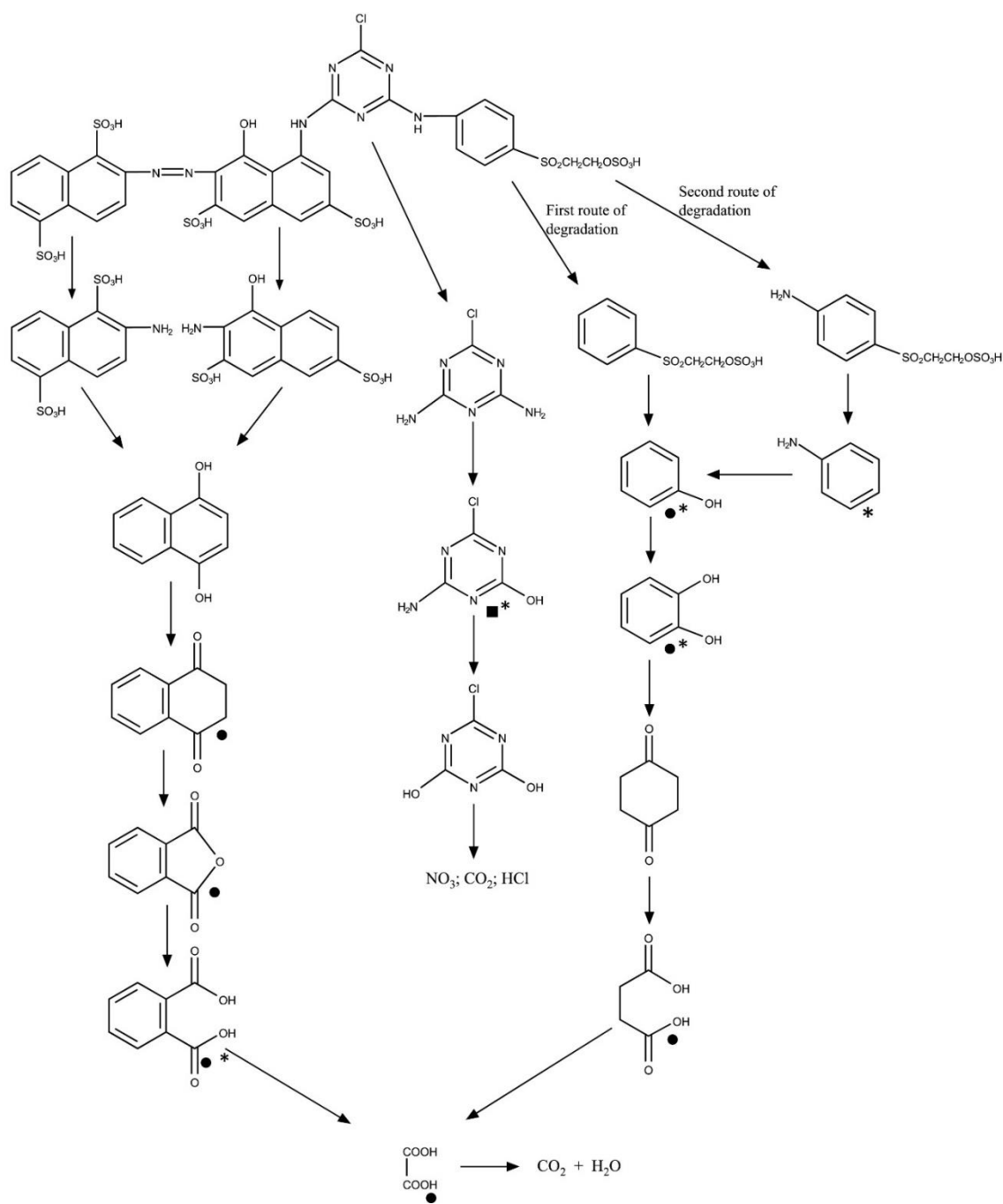


Figure 4.28 The pathway of RR 239 degradation by ozone conducted by Dias *et al.*, (2019) [3]

4.5 Comparison of hydrophobicity enhancement of PVDF membrane by plasma-activated methods and application in membrane contactors

Table 4.7 shows the comparison of hydrophobicity enhancement of PVDF membrane by plasma-based methods. The results found that there were several studies the membrane activation by the radial frequency (RF), while in this study, PICP system was used. After grafted with 0.02M FAS-C8, the WCA of modified membranes in current work was 112.4° , which was lower than that of Zheng *et al.* (2009) (155°) in which the chemical vapor grafting with 1.1M MTCS was used [16]. Besides, Sairiam *et al.* (2013) applied the direct grafting with 0.01M 1H,1H,2H,2H-perfluorodecyltriethoxysilane for 24h which perform the higher hydrophobicity (145°) [15]. However, the current work showed the higher hydrophobicity than that of Xu *et al.* (2015) and Yang *et al.* (2011) [14, 22]. Xu *et al.* (2015) studied the direct grafting method at high N-octyltriethoxysilane concentration (0.43M), while Yang *et al.* (2011) applied vapor grafting with 1H, 1H, 2H, 2H-perfluorodecyl acrylate [14, 22]. It was implied that, as the plasma RF system, the PICP system was effective in membrane activation. The modified membranes were applied for several membrane contactors such as membrane distillation [22, 79]. Sairiam *et al.* (2013) applied the modified membrane CO₂ absorption and the results found that the CO₂ absorption flux of modified membrane was higher than that of original membrane and was kept stable during 15 days operation [15]. Xu *et al.* (2015) applied the modified membrane for vacuum membrane distillation of ethanol–water mixture, which increased the permeation flux from 3.19 kg/m²h (original) to 5.39 kg/m²h [22]. In this work, modified membrane was applied for ozonation membrane contactor and the results were demonstrated that the modified membrane showed the increase decolorization performance (from 93% to 98%) and COD removal (48% to 63%) of RR 239 compared to the original PVDF membrane. In additions, the ozone flux of modified membrane was kept stable after 8h operation while that of original PVDF membrane was reduced by 40% during 20h.

Table 4.7 Comparison of different plasma-based modification methods for enhancing PVDF membrane hydrophobicity

PVDF membrane	Plasma type	Treatment conditions	WCA	Application	Modified membrane performance	References
Flat sheet	RF	Activated by O ₂ microwave plasma at 200 W for 12 mins followed by vapor grafting with 1.1M MTCS	Increased (88° to 155°)	-	-	[16]
Hollow fiber	RF	Activated by plasma followed by vapor grafting with 1H, 1H, 2H, 2H-perfluorodecylacrylate	Increased (88° to 105°)	Membrane distillation	20% flux reduction and 100% salt rejection	[14]
Hollow fiber	RF	Activated by He plasma followed by direct grafting with 0.01M 1H, 1H, 2H, 2H-perfluorodecyltriethoxysilane for 24h	Increased (68.9° to 145°)	CO ₂ absorption	CO ₂ absorption was stable for 15 days operation	[15]
Flat sheet	RF	Activated by Ar plasma at 60 Pa, 30 W, treatment time 80 s followed by direct grafting with 0.43M N-octyltriethoxysilane	Increased (70.1° to 121.0°)	Vacuum distillation	The flux increased from 3.19 kg/m ² h to 5.39 kg/m ² h	[22]
Hollow fiber	PICP	O ₂ plasma activation at 10 kV and 0.30 mbar for 2 shots followed by direct grafting with 0.02M FAS-C8 for 6h	Increased (74.7° to 112.4)	Ozonation membrane contactor	- Increase of RR 239 decolorization (from 93% to 98%) and COD removal (48% to 63%). - The ozone flux increased from 2.03×10 ⁻³ g/m ² s to 4.08×10 ⁻³ g/m ² s.	This work

4.6 Proposal of dye wastewater treatment plan using ozonation membrane contactor process

The proposal of dye wastewater treatment plan using ozonation membrane contactor process are shown in Figure 4.29. Dye wastewater from the industry is collected and firstly treated by primary treatment, including screening and settler, in order to remove the big rags and large debris. In the settler tank, settled material such as heavy solids and floating material such as oil, grease, and lighter solids are removed, and the remaining liquid then pumped to the ozonation membrane contactor system for secondary treatment. COD, color and dye contaminated are removal in this process since ozone is a strong breaking down power to degrade the dye molecules. Then, treated wastewater is discharged to the water body after ozonation membrane contactor process.

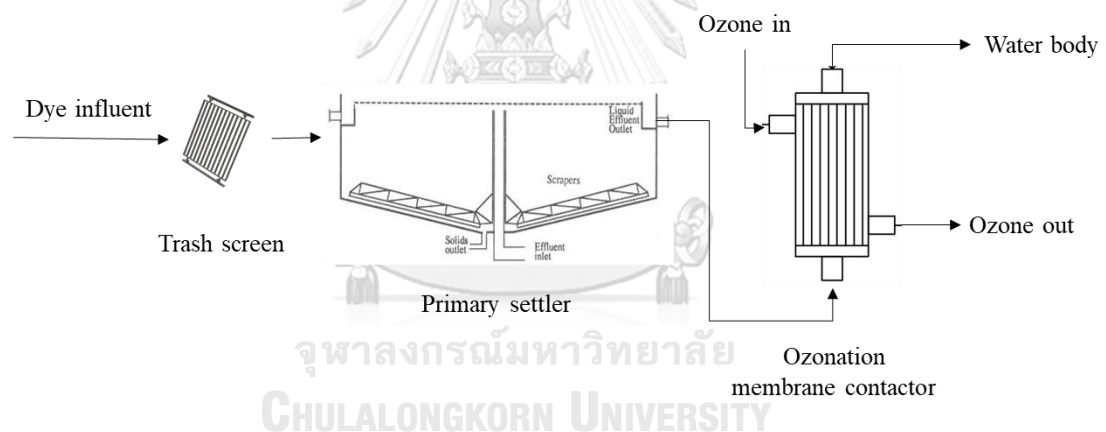


Figure 4.29 Flow diagram for proposed dye wastewater treatment plant

4.7 Energy consumption analysis of ozonation membrane contactor process

The energy consumptions of ozonation membrane contactor using original membrane and modified membrane were compared. As the results of increasing in ozone flux of modified membrane, the energy consumed would be less with modified membranes under the same ozone concentration and operating conditions compared to original membrane. Using the experimental results, the energy necessary to treat 1000 L (1 m³) wastewater until reach the condition of 10 mg/l dye concentration in the

effluent was calculated, as shown in Table 4.8. The energy consumption induced energy consumed by pump and ozone generation. The modified membranes showed higher dye decolorization efficiencies compared to original membrane, thus, requiring less treatment time, resulting in less energy consumption. For example, the energy consumed of original PVDF membrane to treat 100 mg/l DB 71 at an ozone concentration of 40 mg/l was 27 kWh/m³, while that of PVDF- MTCS and PVDF-FAS-C8 membranes were 22.4 kWh/m³ and 20.1 kWh/m³, respectively. In case of RR 239, the energy consumptions were 28.0 kWh/m³, 21.2 kWh/m³ and 18.7 kWh/m³ for original PVDF, PVDF-MTCS and PVDF-FAS-C8 membranes, respectively. This was implied that the cost for dye wastewater treatment by modified membranes was lower than that of original PVDF membrane due to low-energy consumption.

Besides, the dye wastewater contained higher dye concentration demanded more operation energy. For example, when the initial dye concentration increased from 50 mg/l to 200 mg/l, the energy consumed by ozonation membrane contacting process using PVDF-FAS-C8 membrane was increased from 8.1 kWh/m³ to 35.6 kWh/m³ and from 14.2 kWh/m³ to 31.3 kWh/m³ for DB 71 and RR 239, respectively. The energy consumption by this process was higher than that by membrane filtration process (1.75 kWh/m³), in contrast, it was lower than UV free-surface reactor process (50 kWh/m³) and electrocoagulation process (38 kWh/m³) reported in previous studies [57, 80, 81].

Table 4.8 Energy consumption for ozonation membrane contactor with different dye concentrations using original and modified membranes

Dye	Membrane	[Dye] (mg/l)	k_{app} (min^{-1})	Energy consumed during 1 cycle operation (2 L)			Energy consumed for 1m^3 of dye wastewater			
				T (min)	E_p ($\times 10^{-5}$ kWh)	E_{O_3} (kWh)	T (h)	E_p (kWh)	E_{O_3} (kWh)	Total (kWh)
DB 71	Original PVDF	100	0.029	79.4	4.59	0.057	661.7	0.023	27.0	27.0
	PVDF-MTCS	100	0.035	65.8	3.80	0.047	548.2	0.019	22.4	22.4
	PVDF-FAS-C8	100	0.039	59.0	3.41	0.042	492.0	0.017	20.1	20.1
	PVDF-FAS-C8	50	0.068	23.7	1.37	0.017	197.2	0.007	8.0	8.1
	PVDF-FAS-C8	200	0.022	136.2	7.86	0.097	1134.7	0.039	35.6	35.6
RR 239	Original PVDF	100	0.028	82.2	4.75	0.059	685.3	0.024	28.0	28.0
	PVDF-MTCS	100	0.037	62.2	3.59	0.044	518.6	0.018	21.2	21.2
	PVDF-FAS-C8	100	0.042	54.8	3.17	0.039	456.9	0.016	18.6	18.7
	PVDF-FAS-C8	50	0.055	29.3	1.69	0.021	243.9	0.008	14.2	14.2
	PVDF-FAS-C8	200	0.025	119.8	6.92	0.085	998.6	0.035	31.3	31.3

Note: Operating conditions of gas flow rate of 2 m/s, liquid flow rate: 0.46 m/s, ozone concentration: 40 mg/l.

CHAPTER 5

CONCLUSIONS AND RECOMMENDATIONS

This study aims to enhance the hydrophobicity of PVDF hollow fiber membrane by plasma activation with PICP followed by organosilanes direct grafting reaction, then apply for dye wastewater treatment using ozonation membrane contacting process. The overall results can be summarized as followed:

5.1 Hydrophobic membrane modification by PICP and follow by grafting with organosilanes

1. O₂ plasma gave higher hydrophobicity compared to Ar plasma. Under plasma operating condition of 8 kV/ 0.25 mbar/ 1 shot followed by grafting with MTCS for 2h, water contact angle (WCA) of grafted membranes activated by O₂ plasma and by Ar plasma was increased from 74.7° (original) to 119.4° and 92.0°, respectively.
2. The hydrophobicity enhancement of membrane was influenced by the plasma operating condition including applied voltage and operating pressure, plasma treatment shot. The plasma condition of O₂ plasma, 10 kV/0.30 mbar/2 shots was chosen as optimized condition.
3. WCA, EDX, SEM and surface roughness results proved that the hydrophobicity modification by MTCS and FAS-C8 was successful, while membranes grafted by TMCS and FAS-C6 were not changed. In addition, membrane grafted by MTCS after O₂ plasma activation showed the higher WCA compared to membrane grafted by FAS-C8.
4. Two condition which were membrane grafted by 0.02M MTCS for 4h (PVDF-MTCS) and membrane grafted by 0.02M FAS-C8 for 6h (PVDF-FAS-C8) at activation conditions of O₂ plasma, 10 kV/0.30 mbar/2 shots were chosen to modified membrane for dye wastewater application.

5.2 Application for dye wastewater treatment by ozonation membrane contactor

1. The long-term ozone flux showed that modified membrane gave the higher flux and more stable compared to original PVDF membrane. In addition, PVDF-FAS-C8 membrane showed the highest ozone flux.
2. For dye decolorization, the PVDF-FAS-C8 membrane showed higher performance compared to PVDF-MTCS and original PVDF membrane in ozonation membrane contactor. The results revealed that the dye removal efficiencies of ozonation membrane contactor by using modified PVDF membrane were increased compared to using original PVDF membrane.
3. The dye removal efficiencies were influenced by ozone concentrations, dye concentrations and dye solution types. The decolorization and COD removal of RR 239 was faster than that of DB 71.
4. The success of the membrane modification process results in reducing energy consumption of ozonation membrane contactor.
5. The modified hydrophobic membrane has the potential to apply for membrane contactor applications.

5.3 Recommendation

1. For plasma activation, the effect of plasma energy has been investigated. In order to understand the inside of the plasma activation process, the plasma temperature should be measured.
2. The ozone utilization efficiency in this work is still low (approximately 3.5 mg/l out of 40 mg/l O₃ inlet). It was probably because the number of fibers inside the module was not high enough. Therefore, increasing the number of hollow fibers inside the module could increase dye removal efficiency.
3. Besides increasing the number of hollow fibers inside the module, using a double ozonation membrane contactor module also can enhance the ozone utilization efficiency. The ozone outlet of the first module can be reused to be ozone inlet of the next module. With this solution, the energy consumption of

the process could be reduced since it would be less energy consumed for the ozone generator.

4. The research on recycling of end-of-life membranes can be conducted in order to extend the service life of the membrane.



REFERENCES

- [1] Khan, S. and Malik, A. Environmental and health effects of textile industry wastewater. 2013.
- [2] Carmen, Z. and Daniela, S. Textile organic dyes—characteristics, polluting effects and separation/elimination procedures from industrial effluents—a critical overview. in Organic pollutants ten years after the Stockholm convention—environmental and analytical update: InTech, 2012.
- [3] Dias, N.C., Bassin, J.P., Sant’Anna, G.L., and Dezotti, M. Ozonation of the dye Reactive Red 239 and biodegradation of ozonation products in a moving-bed biofilm reactor: Revealing reaction products and degradation pathways. International Biodeterioration & Biodegradation 144 (2019): 104742.
- [4] Jin, R., Yang, H., Zhang, A., Wang, J., and Liu, G. Bioaugmentation on decolorization of C.I. Direct Blue 71 by using genetically engineered strain *Escherichia coli* JM109 (pGEX-AZR). Journal of Hazardous Materials 163(2) (2009): 1123-1128.
- [5] Bruna, d.C.V.C. and Marin-Morales, M.A. Azo dyes: characterization and toxicity—a review. Textiles and Light Industrial Science and Technology 2(2) (2013): 85-103.
- [6] Bamperng, S., Suwannachart, T., Atchariyawut, S., and Jiratananon, R. Ozonation of dye wastewater by membrane contactor using PVDF and PTFE membranes. Separation and Purification Technology 72(2) (2010): 186-193.
- [7] Soares, O.S.G., Orfao, J.J., Portela, D., Vieira, A., and Pereira, M.F.R. Ozonation of textile effluents and dye solutions under continuous operation: Influence of operating parameters. Journal of hazardous materials 137(3) (2006): 1664-1673.
- [8] Atchariyawut, S., Phattaranawik, J., Leiknes, T., and Jiratananon, R. Application of ozonation membrane contacting system for dye wastewater treatment. Separation and purification technology 66(1) (2009): 153-158.
- [9] Pabby, A.K. and Sastre, A.M. State-of-the-art review on hollow fibre contactor technology and membrane-based extraction processes. Journal of membrane science 430 (2013): 263-303.
- [10] Matsuyama, H., Rajabzadeh, S., Karkhanechi, H., and Jeon, S. 1.7 PVDF hollow fibers membranes. in Comprehensive Membrane Science and Engineering, p. 137, 2017.
- [11] Mosadegh-Sedghi, S., Rodrigue, D., Brisson, J., and Iliuta, M.C. Wetting phenomenon in membrane contactors—causes and prevention. Journal of Membrane Science 452 (2014): 332-353.
- [12] Khaisri, S., Tontiwachwuthikul, P., and Jiratananon, R. Comparing membrane resistance and absorption performance of three different membranes in a gas absorption membrane contactor. Separation and Purification Technology 65(3) (2009): 290-297.
- [13] Santos, F.R.A.d., Borges, C.P., and Fonseca, F.V.d. Polymeric materials for membrane contactor devices applied to water treatment by ozonation. Materials Research 18(5) (2015): 1015-1022.
- [14] Yang, X., Wang, R., Shi, L., Fane, A.G., and Debowski, M. Performance improvement of PVDF hollow fiber-based membrane distillation process.

- Journal of Membrane Science 369(1-2) (2011): 437-447.
- [15] Sairiam, S., Loh, C.H., Wang, R., and Jiraratananon, R. Surface modification of PVDF hollow fiber membrane to enhance hydrophobicity using organosilanes. Journal of Applied Polymer Science 130(1) (2013): 610-621.
- [16] Zheng, Z., Gu, Z., Huo, R., and Ye, Y. Superhydrophobicity of polyvinylidene fluoride membrane fabricated by chemical vapor deposition from solution. Applied Surface Science 255(16) (2009): 7263-7267.
- [17] Hendren, Z.D., Brant, J., and Wiesner, M.R. Surface modification of nanostructured ceramic membranes for direct contact membrane distillation. Journal of Membrane Science 331(1) (2009): 1-10.
- [18] Ahmad, N., Leo, C., Ahmad, A., and Ramli, W. Membranes with great hydrophobicity: a review on preparation and characterization. Separation & Purification Reviews 44(2) (2015): 109-134.
- [19] Hashim, N.A., Liu, Y., and Li, K. Stability of PVDF hollow fibre membranes in sodium hydroxide aqueous solution. Chemical Engineering Science 66(8) (2011): 1565-1575.
- [20] Rabuni, M., Sulaiman, N.N., Aroua, M., Chee, C.Y., and Hashim, N.A. Impact of in situ physical and chemical cleaning on PVDF membrane properties and performances. Chemical Engineering Science 122 (2015): 426-435.
- [21] Wang, J., Chen, X., Reis, R., Chen, Z., Milne, N., Winther-Jensen, B., Kong, L., and Dumée, L. Plasma modification and synthesis of membrane materials—a mechanistic review. Membranes 8(3) (2018).
- [22] Xu, W.T., Zhao, Z.P., Liu, M., and Chen, K.C. Morphological and hydrophobic modifications of PVDF flat membrane with silane coupling agent grafting via plasma flow for VMD of ethanol–water mixture. Journal of Membrane Science 491 (2015): 110-120.
- [23] Prasertsung, I., Mongkolnavin, R., Kanokpanont, S., and Damrongsakkul, S. The effects of pulsed inductively coupled plasma (PICP) on physical properties and biocompatibility of crosslinked gelatin films. International journal of biological macromolecules 46(1) (2010): 72-78.
- [24] Chang, J.S. and Lin, C.Y. Decolorization kinetics of a recombinant *Escherichia coli* strain harboring azo-dye-decolorizing determinants from *Rhodococcus* sp. Biotechnology letters 23(8) (2001): 631-636.
- [25] Ulson, S.M.d.A.G., Bonilla, K.A.S., and de Souza, A.A.U. Removal of COD and color from hydrolyzed textile azo dye by combined ozonation and biological treatment. Journal of Hazardous Materials 179(1-3) (2010): 35-42.
- [26] Turhan, K. and Turgut, Z. Decolorization of direct dye in textile wastewater by ozonation in a semi-batch bubble column reactor. Desalination 242(1) (2009): 256-263.
- [27] Güneş, Y., Atav, R., and Namırtı, O. Effectiveness of ozone in decolorization of reactive dye effluents depending on the dye chromophore. Textile Research Journal 82(10) (2012): 994-1000.
- [28] Ghasemi, F., Tabandeh, F., Bambai, B., and Rao, K.R.S.S. Decolorization of different azo dyes by *Phanerochaete chrysosporium* RP78 under optimal condition. International Journal of Environmental Science & Technology 7(3) (2010): 457-464.
- [29] Arslan, S., Eyvaz, M., Gürbulak, E., and Yüksel, E. A review of state-of-the-art

- technologies in dye-containing wastewater treatment–The textile industry case. in Textile Wastewater Treatment: InTech, 2016.
- [30] Chollom, M.N., Rathilal, S., Pillay, V.L., and Alfa, D. The applicability of nanofiltration for the treatment and reuse of textile reactive dye effluent. Water SA 41(3) (2015): 398-405.
- [31] Holkar, C.R., Jadhav, A.J., Pinjari, D.V., Mahamuni, N.M., and Pandit, A.B. A critical review on textile wastewater treatments: possible approaches. Journal of environmental management 182 (2016): 351-366.
- [32] Nidheesh, P., Zhou, M., and Oturan, M.A. An overview on the removal of synthetic dyes from water by electrochemical advanced oxidation processes. Chemosphere 197 (2018): 210-227.
- [33] Portjanskaja, E. Ozone reactions with inorganic and organic compounds in water. Encyclopedia of Life Support Systems (EOLSS).–Ozone Science and Technology.–Формат доступа: <http://www.eolss.net/sample-chapters/c07/e6-192-06-00.pdf> (2010).
- [34] Zhang, Y., Li, K., Wang, J., Hou, D., and Liu, H. Ozone mass transfer behaviors on physical and chemical absorption for hollow fiber membrane contactors. Water Science and Technology 76(6) (2017): 1360-1369.
- [35] Ciardelli, G., Ciabatti, I., Ranieri, L., Capannelli, G., and Bottino, A. Membrane contactors for textile wastewater ozonation. Annals of the New York Academy of Sciences 984(1) (2003): 29-38.
- [36] Giorno, L., Drioli, E., and Strathmann, H. The principle of membrane contactors. in Drioli, E. and Giorno, L. (eds.), Encyclopedia of Membranes, pp. 1-6. Berlin, Heidelberg: Springer Berlin Heidelberg, 2016.
- [37] Gabelman, A. and Hwang, S.-T. Hollow fiber membrane contactors. Journal of Membrane Science 159(1-2) (1999): 61-106.
- [38] Law, K.Y. Definitions for hydrophilicity, hydrophobicity, and superhydrophobicity: getting the basics right. 2014, ACS Publications.
- [39] Mori, Y., Oota, T., Hashino, M., Takamura, M., and Fujii, Y. Ozone-microfiltration system. Desalination 117(1-3) (1998): 211-218.
- [40] López-García, J. Wettability analysis and water absorption studies of plasma activated polymeric materials. in Non-Thermal Plasma Technology for Polymeric Materials, pp. 261-285: Elsevier, 2019.
- [41] Liu, F., Hashim, N.A., Liu, Y., Abed, M.R.M., and Li, K. Progress in the production and modification of PVDF membranes. Journal of Membrane Science 375(1) (2011): 1-27.
- [42] Perera, M.H.J. Superhydrophobicity and structures of adsorbed silane coupling agents on silica and diatomaceous earth. Oklahoma State University, 2016.
- [43] Kujawa, J., Cerneaux, S., Kujawski, W., and Knozowska, K. Hydrophobic ceramic membranes for water desalination. Applied Sciences 7(4) (2017): 402.
- [44] Zhai, T., Zheng, Q., Cai, Z., Turng, L.S., Xia, H., and Gong, S. Poly(vinyl alcohol)/Cellulose nanofibril hybrid aerogels with an aligned microtubular porous structure and their composites with polydimethylsiloxane. ACS Applied Materials & Interfaces 7(13) (2015): 7436-7444.
- [45] Liu, Q.F., Lee, C.H., and Kim, H. Performance evaluation of alkaline treated poly (vinylidene fluoride) membranes. Separation Science and Technology 45(9) (2010): 1209-1215.

- [46] Yu, H.Y., He, X.C., Liu, L.Q., Gu, J.S., and Wei, X.W. Surface modification of poly (propylene) microporous membrane to improve its antifouling characteristics in an SMBR: O₂ plasma treatment. Plasma Processes and Polymers 5(1) (2008): 84-91.
- [47] Akashi, N. and Kuroda, S. Protein immobilization onto poly (vinylidene fluoride) microporous membranes activated by the atmospheric pressure low temperature plasma. Polymer 55(12) (2014): 2780-2791.
- [48] Lin, S.H., Tung, K.L., Chang, H.W., and Lee, K.R. Influence of fluorocarbon flat-membrane hydrophobicity on carbon dioxide recovery. Chemosphere 75(10) (2009): 1410-1416.
- [49] Balasubramanyan, S. and S, K. Ozonation of textile dyeing wastewater - A review. Vol. 2014-15, 2014.
- [50] Sevimli, M.F. and Sarikaya, H.Z. Ozone treatment of textile effluents and dyes: effect of applied ozone dose, pH and dye concentration. Journal of Chemical Technology & Biotechnology: International Research in Process, Environmental & Clean Technology 77(7) (2002): 842-850.
- [51] Gao, M., Zeng, Z., Sun, B., Zou, H., Chen, J., and Shao, L. Ozonation of azo dye Acid Red 14 in a microporous tube-in-tube microchannel reactor: Decolorization and mechanism. Chemosphere 89(2) (2012): 190-197.
- [52] Kusvuran, E., Gulnaz, O., Samil, A., and Erbil, M. Detection of double bond-ozone stoichiometry by an iodimetric method during ozonation processes. Journal of hazardous materials 175(1-3) (2010): 410-416.
- [53] Yuan, Y. and Lee, T.R. Contact angle and wetting properties. in Surface science techniques, pp. 3-34: Springer, 2013.
- [54] De Oliveira, R., Albuquerque, D., Cruz, T., Yamaji, F., and Leite, F. Measurement of the nanoscale roughness by atomic force microscopy: basic principles and applications. Atomic force microscopy-imaging, measuring and manipulating surfaces at the atomic scale (2012): 147-175.
- [55] Yan, H., Lu, X., Wu, C., Sun, X., and Tang, W. Fabrication of a super-hydrophobic polyvinylidene fluoride hollow fiber membrane using a particle coating process. Journal of Membrane Science 533 (2017): 130-140.
- [56] Wu, J. and Wang, T. Ozonation of aqueous azo dye in a semi-batch reactor. Water Research 35(4) (2001): 1093-1099.
- [57] Wang, X., Davies, S.H., and Masten, S.J. Analysis of energy costs for catalytic ozone membrane filtration. Separation and Purification Technology 186 (2017): 182-187.
- [58] Wang, H., Zhan, J., Gao, L., Yu, G., Komarneni, S., and Wang, Y. Kinetics and mechanism of thiamethoxam abatement by ozonation and ozone-based advanced oxidation processes. Journal of Hazardous Materials 390 (2020): 122180.
- [59] Correia, D.M., Nunes-Pereira, J., Alikin, D., Kholkin, A.L., Carabineiro, S.A., Rebouta, L., Rodrigues, M.S., Vaz, F., Costa, C.M., and Lanceros-Méndez, S. Surface wettability modification of poly (vinylidene fluoride) and copolymer films and membranes by plasma treatment. Polymer 169 (2019): 138-147.
- [60] Kaynak, A., Mehmood, T., Dai, X.J., Magniez, K., and Kouzani, A. Study of radio frequency plasma treatment of PVDF film using Ar, O₂ and (Ar + O₂) gases for improved polypyrrole adhesion. Materials 6(8) (2013): 3482-3493.
- [61] Sethunga, G.S.M.D.P., Rongwong, W., Wang, R., and Bae, T.-H. Optimization

- of hydrophobic modification parameters of microporous polyvinylidene fluoride hollow-fiber membrane for biogas recovery from anaerobic membrane bioreactor effluent. Journal of Membrane Science 548 (2018): 510-518.
- [62] Huang, X., Li, B., Song, X., Wang, L., Shi, Y., Hu, M., Gao, J., and Xue, H. Stretchable, electrically conductive and superhydrophobic/superoleophilic nanofibrous membrane with a hierarchical structure for efficient oil/water separation. Journal of Industrial and Engineering Chemistry 70 (2019): 243-252.
- [63] Wang, H., Huang, X., Li, B., and Gao, J. Facile preparation of superhydrophobic nanofibrous membrane for oil/water separation in a harsh environment. Journal of materials science 53(14) (2018): 10111-10121.
- [64] Yuenyao, C., Chittrakarn, T., Tirawanichakul, Y., and Nakajima, H. Low pressure dc-plasma system for the modification of polymeric membrane surfaces. Sains Malaysiana 46(5) (2017): 783-793.
- [65] Nageswaran, G., Jothi, L., and Jagannathan, S. Plasma Assisted Polymer Modifications. in Non-Thermal Plasma Technology for Polymeric Materials, pp. 95-127: Elsevier, 2019.
- [66] Kujawa, J. and Kujawski, W. Functionalization of ceramic metal oxide powders and ceramic membranes by perfluoroalkylsilanes and alkylsilanes possessing different reactive groups: Physicochemical and tribological properties. ACS applied materials & interfaces 8(11) (2016): 7509-7521.
- [67] Kujawa, J., Kujawski, W., Cyganiuk, A., Dumée, L.F., and Al-Gharabli, S. Upgrading of zirconia membrane performance in removal of hazardous VOCs from water by surface functionalization. Chemical Engineering Journal 374 (2019): 155-169.
- [68] Bystrzycka, E., Prowizor, M., Piwoński, I., Kisielewska, A., Batory, D., Jędrzejczak, A., Dudek, M., Kozłowski, W., and Cichomski, M. The effect of fluoroalkylsilanes on tribological properties and wettability of Si-DLC coatings. Materials Research Express 5(3) (2018): 036411.
- [69] Yusefi, M.G., Rahimpour, A., and Mehdipour, H. Hydrophobic modification of PVDF membranes for biodiesel purification. Biofuels 7(3) (2016): 263-270.
- [70] Kujawa, J. From nanoscale modification to separation-The role of substrate and modifiers in the transport properties of ceramic membranes in membrane distillation. Journal of membrane science 580 (2019): 296-306.
- [71] Maciejewski, H., Karasiewicz, J., Dutkiewicz, M., and Nowicki, M. Effect of the type of fluorofunctional organosilicon compounds and the method of their application onto the surface on its hydrophobic properties. RSC Advances 4(95) (2014): 52668-52675.
- [72] Gryta, M. Influence of polypropylene membrane surface porosity on the performance of membrane distillation process. Journal of Membrane Science 287(1) (2007): 67-78.
- [73] Luo, Y.R. Handbook of bond dissociation energies in organic compounds. CRC press, 2002.
- [74] Turhan, K. and Ozturkcan, S.A. Decolorization and degradation of reactive dye in aqueous solution by ozonation in a semi-batch bubble column reactor. Water, Air, & Soil Pollution 224(1) (2013): 1353.
- [75] Cuerda-Correa, E.M., Alexandre-Franco, M.F., and Fernández-González, C. Advanced oxidation processes for the removal of antibiotics from water. An

- Overview. Water 12(1) (2020): 102.
- [76] Tunç, S., Gürkan, T., and Duman, O. On-line spectrophotometric method for the determination of optimum operation parameters on the decolorization of Acid Red 66 and Direct Blue 71 from aqueous solution by Fenton process. Chemical Engineering Journal 181 (2012): 431-442.
- [77] Saggiaro, E.M., Oliveira, A.S., Pavesi, T., Maia, C.G., Ferreira, L.F.V., and Moreira, J.C. Use of titanium dioxide photocatalysis on the remediation of model textile wastewaters containing azo dyes. Molecules 16(12) (2011): 10370-10386.
- [78] Stambolova, I., Shipochka, M., Blaskov, V., Loukanov, A., and Vassilev, S. Sprayed nanostructured TiO₂ films for efficient photocatalytic degradation of textile azo dye. Journal of Photochemistry and Photobiology B: Biology 117 (2012): 19-26.
- [79] Zhang, Y., Wang, X., Cui, Z., Drioli, E., Wang, Z., and Zhao, S. Enhancing wetting resistance of poly (vinylidene fluoride) membranes for vacuum membrane distillation. Desalination 415 (2017): 58-66.
- [80] Bahadori, E., Rapf, M., Di Michele, A., and Rossetti, I. Photochemical vs. photocatalytic azo-dye removal in a pilot free-surface reactor: Is the catalyst effective? Separation and Purification Technology 237 (2020): 116320.
- [81] Bazrafshan, E. and Mahvi, A.H. Textile wastewater treatment by electrocoagulation process using aluminum electrodes. Iranian journal of health sciences 2(1) (2014): 16-29.

APPENDIXES

Appendix A. Samples calculation of energy consumption

Using 40 mg/l ozone injection concentration with original membrane under DB 71 concentration of 100 mg/l, liquid velocity of 23 ml/s, gas velocity of 2 m/s, rate constant $k = 0.029 \text{ min}^{-1}$ be an example:

Time to treat 1 m^3 dye wastewater to reach concentration of 10 mg/l:

$$T = \frac{-\ln \frac{C}{C_0} \times 1000}{k \times V \times 60} = \frac{-\ln(0.1) \times 1000}{0.029 \times 2 \times 60} = 661.7 \text{ (h)}$$

The pressure drop (ΔP) during recirculation cycle (except membrane module) was 0.01 bar, obtained from pressure drop online calculator. The pressure drop (ΔP) in the membrane module was 0.0013 bar (based on membrane length and cut-off area), so the power demand for this part was:

$$P = \frac{q \times \sum \Delta P}{\eta} = \frac{23 \times 10^{-6} \text{ (m}^3/\text{s)} \times (0.01 + 0.0013) \times 10^5 \text{ N}\cdot\text{m}^2}{75\%} = 0.00347 \text{ watt} = 3.47 \times 10^{-5} \text{ kW}$$

Energy demand during operation period for this pressure drop was:

$$P \times T = 3.47 \times 10^{-5} \text{ kW} \times 661.7 \text{ h} = 0.023 \text{ kWh}$$

Energy demand for ozone generation was:

$$E_{EO}(\text{O}_3) = \frac{-\ln \frac{C}{C_0} \times r \times [\text{O}_3] \times Q_{\text{O}_3}}{k \times V \times 1000} = \frac{-\ln(0.1) \times 10 \times 40 \times 1.7}{0.029 \times 2 \times 1000} = 27 \text{ kWh}$$

The total energy was: $E = E_p + E_{EO} = 27 + 0.023 = 27.023 \text{ kWh}$

Appendix B



Figure A1 Pulse inductive coupled plasma device



Figure A2 Capacitor controller

VITA

NAME Hanh Le Thi My

DATE OF BIRTH 15 August 1994

PLACE OF BIRTH Vietnam

INSTITUTIONS ATTENDED

BACHELOR'S DEGREE
Bachelor's degree of engineering, Thuyloi University, 2017

MASTER'S DEGREE
International program in Hazardous Waste and Environmental Management, Graduate School, Chulalongkorn University, 2020

HOME ADDRESS Dong Loc, Can Loc, Ha Tinh, Vietnam

PUBLICATION

Le, T. M. H., Mongkolnavin, R., Nuisin, R., and Sairiam, S. (2019). Enhancing hydrophobicity of PVDF hollow fiber membrane by plasma induced and grafted with chloroalkylsilanes. The 45th Congress on Science and Technology of Thailand (STT45) Conference Proceeding, (D_037_OF), 479–484.

Le, T. M. H., Mongkolnavin, R., Nuisin, R., and Sairiam, S. (2019). Plasma activated PVDF hollow fiber membrane grafted with chloroalkylsilanes improving hydrophobicity for wastewater treatment by ozonation with membrane contactor. International Conference on the “Challenges in Environmental Science and Engineering” (CESE-2019).